1983

Homo- and heteropolyatomic anions of the post-transition elements of group IV and V: Synthesis and crystal structure characterization

Susan Carol Critchlow
Iowa State University

INFORMATION TO USERS

This reproduction was made from a copy of a document sent to us for microfilming. While the most advanced technology has been used to photograph and reproduce this document, the quality of the reproduction is heavily dependent upon the quality of the material submitted.

The following explanation of techniques is provided to help clarify markings or notations which may appear on this reproduction.

1. The sign or "target" for pages apparently lacking from the document photographed is "Missing Page(s)". If it was possible to obtain the missing page(s) or section, they are spliced into the film along with adjacent pages. This may have necessitated cutting through an image and duplicating adjacent pages to assure complete continuity.

2. When an image on the film is obliterated with a round black mark, it is an indication of either blurred copy because of movement during exposure, duplicate copy, or copyrighted materials that should not have been filmed. For blurred pages, a good image of the page can be found in the adjacent frame. If copyrighted materials were deleted, a target note will appear listing the pages in the adjacent frame.

3. When a map, drawing or chart, etc., is part of the material being photographed, a definite method of "sectioning" the material has been followed. It is customary to begin filming at the upper left hand corner of a large sheet and to continue from left to right in equal sections with small overlaps. If necessary, sectioning is continued again—beginning below the first row and continuing on until complete.

4. For illustrations that cannot be satisfactorily reproduced by xerographic means, photographic prints can be purchased at additional cost and inserted into your xerographic copy. These prints are available upon request from the Dissertations Customer Services Department.

5. Some pages in any document may have indistinct print. In all cases the best available copy has been filmed.

University Microfilms International
300 N. Zeeb Road
Ann Arbor, MI 48106

Critchlow, Susan Carol

HOMO- AND HETEROPOLYATOMIC ANIONS OF THE POST-TRANSITION ELEMENTS OF GROUP IV AND V: SYNTHESIS AND CRYSTAL STRUCTURE CHARACTERIZATION

Iowa State University

PH.D. 1983

PLEASE NOTE:

In all cases this material has been filmed in the best possible way from the available copy. Problems encountered with this document have been identified here with a check mark __√__.

1. Glossy photographs or pages _____
2. Colored illustrations, paper or print _____
3. Photographs with dark background _____
4. Illustrations are poor copy _____
5. Pages with black marks, not original copy _____
6. Print shows through as there is text on both sides of page _____
7. Indistinct, broken or small print on several pages __✓__
8. Print exceeds margin requirements _____
9. Tightly bound copy with print lost in spine _____
10. Computer printout pages with indistinct print __✓__
11. Page(s) _____ lacking when material received, and not available from school or author.
12. Page(s) _____ seem to be missing in numbering only as text follows.
13. Two pages numbered _____. Text follows.
14. Curling and wrinkled pages _____
15. Other _____

Homo- and heteropolyatomic anions of the post-transition elements of group IV and V: Synthesis and crystal structure characterization

by

Susan Carol Critchlow

A Dissertation Submitted to the
Graduate Faculty in Partial Fulfillment of the
Requirements for the Degree of
DOCTOR OF PHILOSOPHY

Department: Chemistry
Major: Inorganic Chemistry

Approved:

Signature was redacted for privacy.

In Charge of Major Work

Signature was redacted for privacy.

For the Major Department

Signature was redacted for privacy.

For the Graduate College

Iowa State University
Ames, Iowa

1983

TABLE OF CONTENTS

LIST OF TABLES

LIST OF FIGURES

INTRODUCTION

About 90 years ago, Joannis first reported that lead dissolved in solutions of sodium in liquid ammonia to produce an intensely green colored solution.[1] Kraus, in 1907, demonstrated the electrolytic nature of this solution, and noted the characteristic red color of similar sodium-tin solutions.[2] In 1917, Smyth deduced a stoichiometry of about 2.25 lead atoms to one sodium atom from electrolysis measurements in liquid ammonia,[3] while Peck, in 1918, found that antimony dissolved in sodium ammonia solutions to give a deep red color up to a maximum amount of 2.33 antimony atoms per sodium.[4] Kraus and Kurtz observed that similar solutions could be prepared through the reduction of Sn, Pb, Sb or Bi halides by sodium in liquid ammonia, or through the dissolution of alkali metal-tin or alkali metal-lead alloys in ammonia.[5] These results led Kraus to propose the existence of complex anions such as $Sb^{3-}\cdot Sb_6$ and $Pb^{4-}\cdot Pb_8$ or Pb_9^{4-}.[6,7]

In the 1930s, Zintl and coworkers systematically investigated such homopolyatomic anions, by potentiometric titrations of sodium with halide or chalcogenide salts of the main group elements in liquid ammonia and/or by analysis of products after exhaustive extraction of alloys with ammonia.[8-11] For group IV and V metals, they identified the following anions: Sn_9^{4-}, Pb_7^{4-}, Pb_9^{4-}, As_3^{3-}, As_5^{3-}, As_7^{3-}, Sb_3^{3-}, Sb_7^{3-}, Bi_3^{3-}, Bi_5^{3-}, and 'Bi_7^{3-}' (actually $Bi_{5.85}^{3-} \triangleq Bi_4^{2-}$[12]). (Their attempts to produce germanium anions were not too successful, though Johnson and Wheatly in 1934 reported an intensely red solution could be prepared by

the reaction of sodium and finely divided germanium in ammonia.[13]) However, all attempts to isolate crystalline solids for structural studies failed; the $Na(NH_3)_n^+$ salts which formed on solvent evaporation were amorphous and lost ammonia to revert to known intermetallic phases plus occasionally the element itself.

Many of the binary compounds between alkali or alkaline earth metals and main group elements, which are now commonly known as Zintl phases, do contain homoatomic clusters, chains or networks. Schäfer, Eisenmann, and Müller have reviewed the structure and bonding of these Zintl phases,[14] and the various clusters are also discussed in von Schnering's review of main group cluster bonding.[15] However, in most cases complete charge transfer to form discrete anions cannot be presumed to occur, and the clusters found in Zintl phases do not generally correspond to the polyatomic anions seen in solution, especially for the heavier elements.

The key to successful isolation of polyatomic anions as stable salts have been the application of 2,2,2-crypt[16] as an alkali metal complexing agent. This octadentate ligand ($N(C_2H_4OC_2H_4OC_2H_4)_3N$) is one of a family of macrobicyclic ligands which form complexes with alkali or alkaline earth cations that are not only highly stable but can be quite selective due to differing cavity size.[17] 2,2,2-crypt in particular is ideally suited for K^+ ions. In the polyatomic anion salts, this complexation serves both to increase the solubility of the anion and to prevent the reversion to the otherwise more energetically favorable intermetallic phases.

Numerous polyatomic anions have recently been synthesized by this means and structurally characterized.[18] Table 1 lists the anions which are pertinent to this work, principally those involving group IV or V post-transition elements (the polychalcogenide anions, which generally form only simple chains, and the polyphosphide anions, which are found mostly in Zintl phases, are excluded from this discussion). These elements are rich in their ability to form a wide variety of clusters. The configurations of the anions are in basic accord with Wade's rules[29] for skeletal electrons, and there are not surprisingly many isoelectronic analogs among the homopolyatomic cations and the polyboranes.

There are examples of polyatomic anion salts which do not employ crypt cations. Kummer and coworkers isolated the compounds $(Na_4 \cdot 7en)Sn_9$, $(Na_4 \cdot 5en)Ge_9$ and $(Na_3 \cdot 4en)Sb_7$ and reported the partial crystal structure and some reaction results for the tin compound.[30,31] The Sn_9^{4-} anion found is a very distorted tricapped trigonal prism which still retains some direct interaction with two of the sodium atoms. Very recently, the Sn_9^{4-} anion has also been isolated as both the $(CH_3)_4N^+$ and the $K(HMPA)_2^+$ salts;[32] however, these compounds are of marginal stability and have only been identified by elemental analysis and ^{119}Sn solution nmr.

Recent investigations into the nature of such anions in solution by nmr have added valuable information. Rudolph and coworkers established the fluxionality of Sn_9^{4-} in solution by the observation of a single nmr resonance split by intramolecular coupling between ^{119}Sn and ^{117}Sn.[33,34] The entire $Sn_{9-x}Pb_x^{4-}$ (x = 0-9) family has been established by ^{207}Pb and

Table 1. Polyatomic anions of known structure[a]

Anion	Symmetry	Configuration	Skeletal Electrons
Homoatomic Examples			
Pb_5^{2-}	D_{3h}	trigonal bipyramid	12
Sn_5^{2-}	D_{3h}	trigonal bipyramid	12
Sn_9^{3-}	D_{3h}	tricapped trigonal prism	21
Sn_9^{4-}	C_{4v}	unicapped square antiprism	22
Ge_9^{2-}	C_{2v}	distorted tricapped trigonal prism	20
Ge_9^{4-}	C_{4v}	unicapped square antiprism	22
Bi_4^{2-}	D_{4h}	square plane	14
Sb_4^{2-}	D_{4h}	square plane	14
Sb_7^{3-}	C_{3v}	nortricyclene	24
As_{11}^{3-}	D_3	'UFOsane'	36
Heteroatomic Examples			
$Sn_2Bi_2^{2-}$	∿Td	tetrahedron	12
$Pb_2Sb_2^{2-}$	∿Td	tetrahedron	12
$Tl_2Te_2^{2-}$	C_{2v}	butterfly	12
$TlSn_8^{3-}$	C_{2v} (D_{3h}[b])	tricapped trigonal prism	20
$TlSn_9^{3-}$	C_{4v} (D_{4d}[b])	bicapped square antiprism	22

[a]Crypt-K^+ or crypt-Na^+ salts.

[b]Configuration neglecting heteroatom.

Isoelectronic Analogs	Crystal Characteristics	References
Bi_5^{3-}	ruby red chips	19
	orange-brown plates	19
-	reddish-black plates	20, this work
Bi_9^{5+} (D_{3h})	dark red rods	21
$B_9H_9^{2-}$, Sn_9^{4-}	deep red rods	22
Se_4^{2+}, Te_4^{2+}	greenish-black crystals	12
	blue-black wedges	23, this work
P_7^{3-}, As_7^{3-}, P_4S_3	brown needles, rods	23, 24, this work
P_{11}^{3-}	deep red rods	25
P_4, Sb_4	black hexagonal plates	26, this work
	black hexagonal plates	this work
-	dark brown blocks	27
$B_9H_9^{2-}$, $B_{10}H_{10}^{2-}$	deep red-brown crystals	28

^{119}Sn nmr,[33,34] and the $Sn_{9-x}Ge_x^{4-}$ family, Sn_4^{2-}, and $T\ell Sn_8^{5-}$ have similarly been identified in part by ^{119}Sn nmr.[35]

The goal of this research has been the production of new polyatomic anions. For homoatomic systems, the method has been to utilize different alkali metals or crypt ligands; hopefully changing the starting alloy or the cation size from that in previous investigations could promote the isolation of new species. For the heteroatomic systems, the expectation was that the use of elements from different groups would lead to new electronic and structural configurations. The results include the crystal structures of four new anions, Sb_4^{2-},[23] Sn_9^{3-},[20] $Sn_2Bi_2^{2-}$ [26] and $Pb_2Sb_2^{2-}$; the previously known Sb_7^{3-} anion as a new salt;[23] and two structures that are only partially solved due to disorder, the one apparently containing Ge_4^{2-} [36] and the other having the known Sn_9^{4-} anion occurring in both C_{4v} and D_{3h} configurations.

EXPERIMENTAL

Materials and Syntheses

All manipulations were performed either in an inert-atmosphere (N_2 or Ar) drybox or on a vacuum line, as both the starting reactants and the products are generally moisture and air sensitive. Sources of the elements are as follows: lithium (Fischer Scientific Co.), sodium (Fischer Scientific Co.), potassium (J. T. Baker Chemical Co., "purified"), germanium (United Mineral and Chemical, zone refined), tin (J. T. Baker Chemical Co.), lead (Fischer Scientific Co.), antimony (A. D. Mackay, Inc., 99.999%), and bismuth (Oak Ridge National Laboratory, 99.999%). Lithium must be handled in an inert atmosphere other than nitrogen as the freshly cut metal reacts rapidly and exothermically with N_2. 2,2,2-crypt ($C_{18}H_{36}N_2O_6$; 4,7,13,16,21,24-hexaoxa-1,10-diazobicyclo-(8.8.8)hexacosane) was used as obtained from Merck, as was 2,2,1-crypt ($C_{16}H_{32}N_2O_5$; 4,7,13,16,21-pentaoxa-1,10-diazobicyclo(8.8.5)tricosane) and 2,1,1-crypt ($C_{14}H_{28}N_2O_4$; 4,7,13,18-tetraoxa-1,10-diazobicyclo(8.5.5)-eicosane). Ethylenediamine (en, Fischer Scientific Co.) was first dried by refluxing over CaH_2 for 2 days, then distilled into a storage flask containing molecular sieves.

Alloy preparation

Various alloys were prepared by fusion of stoichiometric amounts of the appropriate elements in a sealed tantalum tube (heliarc welded) enclosed in an evacuated fused silica jacket. After heating to an appropriate temperature in a furnace for about two hours, most alloys

were quenched to give a more reactive microcrystalline product. Synthesis conditions are summarized in Table 2. When feasible, powder patterns (Debye-Scherrer or Guinier) were compared with calculated patterns[37] for known phases.

There are five compounds reported in the potassium-tin system: K_2Sn, KSn_2, KSn_4, KSn and K_8Sn_{46}.[38] However, only the latter two have known structures. The alloy of composition KSn_2 synthesized here was not homogeneous; the powder pattern contained elemental tin lines as well as lines presumably from a tin-poorer K-Sn alloy, not matching those calculated for KSn,[39] however.

For the Na-Ge system, NaGe[40] is the only known phase, containing Ge_4 tetrahedra.[41] The powder pattern for $NaGe_{0.8}$ matched that calculated for NaGe. (Off-stoichiometry alloys were deliberately chosen to increase reactivity.) $NaGe_{1.6}$ and $NaGe_{3.8}$ contain an unknown phase, probably of stoichiometry close to $NaGe_2$ as the $NaGe_{3.8}$ powder pattern exhibited strong Ge elemental lines as well as all the $NaGe_{1.6}$ lines.

There are many known phases in the Li-Sn system.[42,43] The Li-Sn alloys prepared here had powder patterns matching the calculated patterns very closely. Comparable data for the ternary alloys are not available. The KPbSb alloy was visibly inhomogeneous; the molten alloy solidified progressively from apparently a Sb-rich to a Pb-rich phase during quenching.

Table 2. Alloy preparation

Alloy	Temperature, °C	Conditions	Color
KSn_2[a]	975	quenched	dark gray
K_3Bi_2[b]	700	slowly cooled, annealed <442°	brown
KSnBi	975	quenched	golden
KGeSb	970	quenched	dark gray
KPbSb	970	quenched	dark gray
$NaGe_{0.8}$[a]	1000	quenched	gray
$NaGe_{1.6}$	1000	quenched	dark gray
$NaGe_{3.8}$[a]	1000	quenched	light gray
Li_7Sn_3	800	cooled, annealed 480°	silver
Li_5Sn_2	800	quenched, annealed 693°	bluish-silver
$Li_{13}Sn_5$	800	quenched, annealed 711°	purplish-silver

[a]Prepared by Mike Denney.

[b]Prepared by Al Cisar, cited in reference 12.

Synthetic and analytic methods

Reactions of alloy with crypt are generally performed as follows: 0.1 g of 2,2,2-crypt or 0.1 ml of 2,2,1- or 2,1,1-crypt and a stoichiometric or slight excess amount of alloy for all the alkali metal to be complexed are loaded into a three-armed apparatus equipped with two Teflon needle valves (there is no valve between the inner two arms).[44]

After evacuation, about 15 ml of en are added using an ice water-room temperature gradient on the vacuum line. The alloys all evolve small amounts of hydrogen gas from reduction of the solvent, and there is always some undissolved alloy residue present.

Important reaction parameters include the length of time the solution is allowed to stand over the alloy before attempting to grow crystals, whether or not the reaction is heated, whether crystals are grown from a solution in contact with or decanted from the alloy residue, and the period of time for crystal growth (this includes the time spent concentrating the solution to the saturation point). Crystals are best grown by slow removal of solvent, either by gently heating the solution arm (to $\sim 40^{\circ}C$) so that en gradually distills to the second arm, or by using the thermal gradient between room temperature (solution arm) and a Dewar filled with water ($\sim 18^{\circ}C$, for the second arm). The latter method generally produces the better crystals, especially for products soluble in en.

Some reaction products were analyzed by X-ray fluorescence, microprobe, or atomic absorption. ESR measurements were made on a Bruker ER 200D-SRC spectrometer with an Oxford ESR-900 flow-through cryostat, DTC-2 digital temperature controller and a Hewlett-Packard 5342A microwave frequency counter. Magnetic susceptibility data were measured on a Faraday balance constructed in Ames Laboratory[45] with a Cahn RH Electrobalance and a platinum resistance thermometer.

However, since reaction amounts are small and the products are often multiphase, single crystal X-ray crystallography is the most useful

method of analysis. Reaction vessels were opened in a dry box especially designed for crystal mounting. Suitable crystals were mounted into 0.3 or 0.5 mm capillaries using a small amount of vaseline to hold the crystal in place if necessary, and the capillaries were sealed temporarily with grease, then permanently with a small torch outside the dry box. Many crystals were examined with oscillation and Weissenberg photographs using a standard camera and Ni-filtered Cu radiation, though generally the best crystals were saved for diffractometer use, as many of these phases decay too rapidly when exposed to X-rays.

Unit cell dimensions alone can be very enlightening. The cell volume in these polyatomic anion-crypt structures is relatively independent of the anion and directly related to the number of crypt cations, which in turn indicates the probable anion charge.[27] 2,2,2-crypt-K^+ and 2,2,2-crypt-Na^+ salts average about 670 and 640 $Å^3$ per crypt respectively, though large bulky anions, such as As_{11}^{3-}, can increase these values up to 70 $Å^3$. The presence of en solvent molecules is usually indicated by an increase of about 30 $Å^3$ per crypt per independent en. In passing, it should be noted that the majority of 2,2,2-crypt-K^+ salts do contain solvent molecules, while none of the known Na^+ ones do, and also the Na^+ salts tend to occur in higher symmetry cells.

Also, anions with a 2- charge all occur in similar unit cells of roughly hexagonal symmetry with two axes near 12 Å, the third axis a multiple of about 11 Å, and an opposing angle near 120° or 60°. Examples include those 2- anions listed in Table 1, Te_3^{2-},[46] $HgTe_2^{2-}$,[47] and $As_2Se_6^{2-}$ [48] (some of these unit cell parameters can be compared later in

Tables 4, 6 and 8). There is also a group of similar unit cells apparently containing 3- anions, with approximate dimensions a $\approx$ 15 Å, b $\approx$ 21 Å, c $\approx$ 14 Å, $\alpha \approx 95^{o}$, $\beta \approx 103^{o}$ and $\gamma \approx 89^{o}$, though only the four found in Table 1 are of known structure. The large crypt cations evidently dominate the packing in the unit cells; unfortunately, this sometimes leads to anion disorder, either of a positional variety or indicating a lack of selectivity (two different anions disordered on the same site).

K-Sn-Bi reactions

Table 3 summarizes the conditions used for reactions with 2,2,2-crypt in the binary K-Sn and the ternary K-Sn-Bi systems. The original intent was to produce a mixed cluster such as Sn_8Bi^{3-} or $Sn_7Bi_2^{2-}$ (isoelectronic with Sn_9^{4-}), which accounts for the 7Sn:1Bi ratio used. The numbers listed under products represent a very rough guesstimate of what percent of the total product might be a particular phase, based on visual observations and oscillation photos or indexing to identify individual crystals. It is clear that reaction conditions greatly influence the products. For the ternary system it is not surprising that several different phases can be produced, but even the binary KSn_2 alloy can react to form one of three phases depending on the conditions.

When en and crypt are added to the alloys KSn_2 and K_3Bi_2, they dissolve to give red and green colors, respectively, indicating initial formation of homopolyatomic anions which evidently interact in solution (or more likely at the alloy surface) to form heteroatomic species. The

Table 3. K-Sn-Bi-2,2,2-crypt reactions

Alloys	Over alloy	Soln. color	Decant	Heated 30-40°C	Crystal growth	Products, % I	II	III	IV	V	VI
$7KSn_2 + K_3Bi_2$ (1)	1 d	red-brown	no	yes	1 mo			30			
$7KSn_2 + K_3Bi_2$ (2)	3 d	red-brown	no	3 d	2 mo	30		60			
$7KSn_2 + K_3Bi_2$ (3)	3 wk	red-brown	yes	1 d	4 d	60			30		
$KSn_2 + K_3Bi_2$	2 wk	red-green	yes	no	1 wk	10	20	60			
KSnBi	1 wk	red-brown	yes	no	1 wk	95				3	
KSn_2 (1)	3 wk	blood-red	yes	no	4 d					90	
KSn_2 (2)	4 d	blood-red	no	no	2 mo						85
KSn_2 (3)	3 d	blood-red	yes	no	3 wk					95	
KSn_2 (4)	1 d	blood-red	yes	no	2 wk				85	5	
KSn_2 (5)	3 d	blood-red	yes	no	3 wk					80	

Products

I = $Sn_2Bi_2^{2-}$ --black pseudohexagonal chunky plates, sometimes with a bluish-gold sheen.

II = Bi_4^{2-} (known) --black wedges with a purplish sheen.

III = $Sn_xBi_y^{3-}$? --black rods.

IV = $(Sn_x)^{7-}$? --black rods.

V = Sn_9^{3-} --reddish-black thin plates and rods.

VI = Sn_9^{4-} ? --brownish-black rhomboid-shaped plates.

7:1 ratio reactions produced dark reddish-brown solutions. Although heating the solution in the first reaction (and in the process slowly transferring en to a second arm) did produce crystals, the quality was not good as they grew too rapidly and redissolved too easily in any refluxing en. Slow solvent removal using the water-air temperature gradient generally produced better crystals.

The reaction $KSn_2 + K_3Bi_2$ in a 1:1 ratio gave a red-green dichroic solution similar to that described for bismuth alloy reactions.[12] In this case Bi_4^{2-} crystals (phase II) formed first, irreversibly, and as they crystallized the solution turned red-brown, at which point the other phases began growing.

The ternary alloy KSnBi initially produced a gold colored solution which darkened to a similar reddish-brown, so heteropolyatomic anions are probably present from the beginning. This reaction produced beautiful, large crystals of phase I, with the very small amount of phase V forming only when the last traces of solvent were trapped off.

The expected product for the reaction of 2,2,2-crypt with KSn_2 was $(2,2,2\text{-crypt-}K^+)_4Sn_9^{4-}$; this anion is well known as the 2,2,2-crypt-Na^+ salt, but the potassium salt would not necessarily be isostructural. The reaction gives a dark blood-red colored solution. After about 24 hours, gray material, which is presumably tin metal, begins plating slowly out on the walls of the apparatus. Phase V is easily produced by slow solvent removal, if the solution is first decanted after standing a couple of days over the alloy residue (reactions 1, 3 and 5). These

rods or long plates often grow together in an X-shaped fashion. Instead of the expected Sn_9^{4-} anion, this phase contains the new Sn_9^{3-} anion.

In the second KSn_2 reaction, where unlike the others en was initially added to alloy alone rather than to an alloy-crypt mixture, tin metal plated out immediately and in a much larger quantity. The solution was also not decanted from the alloy during attempts to grow crystals, and when the initial solvent removal gave poorly formed crystals, these were redissolved. The second time solvent was removed, phase VI formed as singly growing plates, very distinctive in habit. In the fourth KSn_2 reaction, the solution was probably decanted from the alloy before it had fully reacted (before any gray material plated out). This apparently is important, since the majority of the product is phase IV.

All six phases in this system were at least indexed on the diffractometer, giving the unit cells listed in Table 4. Phase I has been shown by single crystal work and conventional analysis to be 2,2,2-crypt-$K^+)_2Sn_2Bi_2^{2-}$·en. Analysis of the KSnBi reaction product by atomic absorption gave the following: calc: Bi, 27.0; Sn, 15.3; K, 5.06%; found: Bi, 25.2; Sn, 15.0; K, 5.47%. An examination of individual crystals including the data crystal by electron microprobe also gave mole ratios near 1:1 for Sn:Bi; however, the weight percentages were inconsistent and the potassium values were always quite high. ESR measurements on single crystals gave no evidence of unpaired spin density.

Phase II, $(2,2,2\text{-crypt-}K^+)_2Bi_4^{2-}$, was previously known.[12] Crystals of phase III, though well formed, exhibited extremely poor diffraction ability, and a crystal suitable for data collection was never found.

Table 4. Unit cells for K-Sn-Bi reaction products

	Products[a]	Å			deg.			$V, Å^3$	V/Cp	Temp. °C	Notes
		a	b	c	α	β	γ				
I	$(CpK)_2Sn_2Bi_2 \cdot en$	12.640	20.943	12.353	90	118.97	90	2861	715		-[b]
II	$(CpK)_2Bi_4$	11.604	11.796	11.096	98.12	98.02	61.37	1315	658		Ref. 12
III	$(CpK)_3Sn_xBi_y$?	15.44	20.21	14.80	94.2	109.2	89.9	4349	725		-[c]
IV	$(CpK)_7Sn_x$?	30.51	36.01	17.82	90	93.1	90	19550	698		-[c]
V	$(CpK)_3Sn_9 \cdot 1.5en$	15.050	21.983	14.106	99.43	101.61	89.64	4508	751		-[b]
		15.002	21.794	14.060	99.77	101.59	89.69	4436	739	-60	-[b]
VI	$(CpK)_4Sn_9$?	15.79	26.50	15.47	91.8	116.2	79.8	5715	714		-[c]
	For Comparison										
	$(CpK)_3 - (T\ell Sn_8 T\ell Sn_9)_{1/2} \cdot en$	15.141	22.195	14.113	98.72	101.04	89.44	4600	767		Ref. 28
	$(CpNa)_4Sn_9$	16.655	21.207	15.370	107.98	103.43	81.70	5007	626	5	Ref. 21
	$(CpNa)_2Sn_5$	11.620	11.620	22.160	90	90	120	2591	648		Ref. 19

[a]Cp = 2,2,2-crypt.
[b]From LATT.
[c]From indexing after standard selection.

No additional analytical work was done, so the anion is not necessarily a heteroatomic species. Volume considerations indicate a 3- anion, so an anion such as Sn_8Bi^{3-} is a likely possibility, but the poor diffraction quality is probably a result of intrinsic disorder in the crystal. Though the stoichiometry would seem to favor a tin-rich phase, the unknown Bi_7^{3-} anion cannot be eliminated as a possibility.

Phase IV diffracts well and good single crystals have been found but the unit cell is so large as to make data collection impractical. Oscillation and Weissenberg photographs show extinctions appropriate for the nonstandard $P2_1/a$ space group. The unique volume would therefore be 4887 $Å^3$ (z=4) and the volume per crypt would be 611, 698, or 815 $Å^3$ for 8, 7, or 6 independent crypts, respectively. The first value is much too small, and the last is 50 $Å^3$ greater than the largest value so far observed. While one cannot rule out having 6 unique crypts with some large bulky anions and several solvent molecules to produce such a large volume per crypt, the more likely possibility is 7 unique crypts (or 28 total in the cell), giving a formula of $(2,2,2\text{-crypt-}K^+)_7Sn_x^{7-}$. It is highly unlikely that one anion would have such a high charge; probably there are two unique anions such as Sn_9^{4-} and Sn_9^{3-}, or, less likely, some disordered combination of a 4- and 2- anion that gives an average 7- charge. The product of the fourth KSn_2 reaction does exhibit an ESR signal, similar to but much weaker than that exhibited by $(2,2,2\text{-crypt-}K^+)_3Sn_9^{3-}\cdot 1.5en$, so either some of this phase is also present in the product or phase IV is paramagnetic, which it must be if it actually contains a 3- tin anion.

Crystal structure analysis, ESR, and magnetic susceptibility measurements have proved phase V is $(2,2,2\text{-crypt-}K^+)_3Sn_9^{3-}\cdot 1.5en$. The product of the fifth KSn_2 reaction was analyzed by atomic absorption, giving the following weight percentages: calc: K, 4.88; Sn, 44.41%; found: K, 4.79; Sn, 43.45%. Also, X-ray fluorescence demonstrated the absence of any other element heavier than Aℓ. It is believed this product is not pure phase V, since its magnetic susceptibility is lower than that measured for the product from reaction 3; perhaps there was some decomposition. However, as the analysis indicates exactly a 3Sn:1K ratio, any contaminant cannot deviate too far from this ratio.

Phase VI is triclinic with a volume appropriate for 8 crypts in the cell. Though it is clearly not isostructural with the known $(2,2,2\text{-crypt-}Na^+)_4Sn_9^{4-}$,[21] this phase is most probably $(2,2,2\text{-crypt-}K^+)_4Sn_9^{4-}$, and since this anion is so well known, the compound was not investigated further.

KPbSb and KGeSb reactions

Table 5 lists the conditions for reactions of KPbSb or KGeSb with 2,2,2-crypt in en. All crystals were grown by slow solvent removal using the water-air temperature gradient. KPbSb reacts to form a dark reddish-brown solution. When the solution was decanted before crystal growth, phase II was the major product. It is not clear why the first and third reactions produced a different minor phase, I or III, since the conditions were essentially the same. These formed first and III deposited irreversibly. The inhomogeneity of the alloy may be a factor

Table 5. KPbSb and KGeSb-2,2,2-crypt reactions

Alloy	Over alloy	Soln. color	Decant	Crystal growth	Products, % I	II	III	IV	V
KPbSb (1)	1 wk	brown	yes	2 wk	30	70			
KPbSb (2)	5 d	brown	no	1 wk			15		70
KPbSb (3)	4 d	brown	yes	3 wk		75	20	3	
KGeSb (1)	1 wk	red-brown	yes	2 wk			20	5	
KGeSb (2)	5 d	red-brown	no	1 wk			15	50	30

Products

I = $Pb_2Sb_2^{2-}$ --black pseudohexagonal plates and chunks.

II = $Pb_xSb_y^{3-}$? --long thin black blades.

III = Sb_4^{2-} --bluish-black wedges.

IV = Sb_7^{3-} --dark red rods.

V = Sb_7^{3-} ? --dark red rods or laths.

here. The presence of alloy residue in the second reaction gave quite different results; apparently the products contain no lead.

KGeSb reactions form a more reddish colored solution. When the solution was decanted from the alloy residue before crystal growth, phase III again formed initially and irreversibly, but the major product was poorly crystalline needles and frayed blades which could not be mounted. The small amount of phase IV that formed grew in the apparatus arm where alloy residue was present. When in the second reaction the solution was not decanted from the alloy, only homopolyatomic antimony salts were produced.

Unit cell parameters are listed in Table 6. Phase I crystals are very similar in appearance to the $Sn_2Bi_2^{2-}$ salt, and the crystal structure does indeed demonstrate that this phase is the isostructural $(2,2,2\text{-crypt-}K^+)_2Pb_2Sb_2^{2-}\cdot en$ salt. Similarly, phase III greatly resembles $(2,2,2\text{-crypt-}K^+)_2Bi_4^{2-}$ crystals, being reddish-black in color, but exhibiting a bluish reflectance and sometimes a blue color when crushed (Bi_4^{2-} crystals appear green when crushed). The unit cell dimensions and crystal structure solution prove this to be the isostructural $(2,2,2\text{-crypt-}K^+)_2Sb_4^{2-}$ salt. This phase is also observed as the major product of the reaction of KAuSb with 2,2,2-crypt, occurring as diamond-shaped plates.[49]

Phase II forms as long thin blades. When a hard vacuum is applied to remove all solvent, they sometimes curl slightly, and cutting the crystals when mounting tends to damage them. A crystal good enough for data collection was not found, but the cell volume would indicate a 3-

Table 6. Unit cells for KPbSb and KGeSb reaction products

	Products[a]	Å			deg.			$V, Å^3$	V/Cp	Temp. °C	Notes
		a	b	c	α	β	γ				
I	$(CpK)_2Pb_2Sb_2 \cdot en$	12.589	20.735	12.201	90	118.97	90	2786	709	-80	-[b]
II	$(CpK)_3Pb_xSb_y$?	15.12	19.82	14.41	94.3	108.8	90.9	4074	679		-[c]
III	$(CpK)_2Sb_4$	11.555	11.795	11.067	97.60	97.80	61.24	1306	653		-[b]
IV	$(CpK)_3Sb_7 \cdot 2en$	14.589	21.753	13.872	92.46	99.63	89.12	4331	722	-80	-[b]
V	$(CpK)_3Sb_7$?	14.85	22.02	13.96	93.7	106.1	91.7	4373	729		-[c]
For Comparison											
	$(CpK)_2Sn_2Bi_2 \cdot en$	12.640	20.848	12.353	90	118.97	90	2861	715		Ref.26
	$(CpK)_2Bi_4$	11.604	11.796	11.096	98.12	98.02	61.37	1315	658		Ref.12
	$(CpNa)_3Sb_7$	23.292	13.791	25.355	90	108.56	90	7721	643		Ref.24

[a]Cp = 2,2,2-crypt.
[b]From LATT.
[c]From indexing after standard selection.

anion. The volume per crypt is noticeably smaller than most 3- anion salts which contain 1-2 en molecules, so there probably are no solvent molecules, but it may also indicate a relatively small anion (perhaps $PbSb_3^{3-}$?). A semiquantitative analysis by X-ray fluorescence of some of the product from reaction 3 indicates phase II must be quite antimony-rich, even taking into account the presence of the Sb_4^{2-} phase. The mole ratio obtained was about 9K:1Pb:21Sb.

The crystal structure solution of phase IV proves it to be $(2,2,2\text{-crypt-}K^+)_3Sb_7^{3-}\cdot 2en$. In the second KGeSb reaction, phase IV and V both formed as rod-shaped crystals, indistinguishable by eye. Several crystals of both phases were indexed; the lattice constants for the phase V crystals from this KGeSb reaction and for the larger lath-shaped crystals produced by the second KPbSb reaction were identical. Microprobe analyses of the products of these two reactions also could not distinguish between phases IV and V but did indicate little if any Ge or Pb in the products. (Again, microprobe for these compounds is at best semiquantitative, and cannot clearly distinguish Sb_4^{2-} from Sb_7^{3-}.) The unit cell dimensions for IV and V are very similar except for the β angle, and since V must contain a homopolyatomic antimony anion, the most likely possibility is another polymorph of Sb_7^{3-}.

Na-Ge and Li-Sn reactions

Table 7 summarizes the reactions attempted in these systems while pertinent unit cell dimensions are listed in Table 8. The cavity inside 2,2,2-crypt is most appropriate for K^+; the undersized Na^+ ion causes

Table 7. Na-Ge and Li-Sn-crypt reactions

Alloy	Crypt	Solution color	Reaction conditions	Time	Products
$NaGe_{0.8}$	2,2,2	yellow-orange	heated 43°	2 wk	I orange cubes
$NaGe_{1.6}$ or $NaGe_{3.8}$	2,2,2	red-orange	heated 35-40° or slow solvent removal	2 d	II red prisms and rods
$NaGe_{0.8}$	2,2,1	orange	heated 42°[a], ea[b] added	>3 yr	black oil
$NaGe_{1.6}$	2,2,1	red/green-brown	heated 50°[a], ea added	2 yr	light orange plates
$NaGe_{3.8}$	2,2,1	red/green-brown	heated 42°[a]	2½ yr	greenish-black dendritic crystals
$NaGe_{3.8}$ + $NaGe_{0.8}$	2,2,1	orange-red	no heating	1½ yr	III dark red plates and rods
$NaGe_{0.8}$	2,1,1	orange	no heating	>1 yr	orange oil
Li_7Sn_3	2,1,1	ruby red	heated 37°[a]	1½ yr	IV reddish black, pseudohexagonal gems

[a]Heating was halted after 1-3 weeks when no crystal formation was observed.

[b]ea = ethylamine.

Table 8. Unit cells for Na-Ge and Li-Sn reaction products

Products[a]	Å			deg.			V, Å^3	V/Cp	Notes
	a	b	c	α	β	γ			
I $(222Cp\text{-}Na^+)_2Ge_4^{2-}$	11.431	11.431	11.056	90	90	120	1251	626	-[b]
II $(222Cp\text{-}Na^+)_3$ - $(Ge_9^{2-}Ge_9^{4-})_{½}$?	23.31	14.71	24.73	90	107.6	90	8083	674	-[c]
III $(221Cp\text{-}Na^+)_3$ - Ge_9^{3-} ?	14.09	19.23	13.43	96.6	99.9	88.6	3559	593	-[d]
IV $(211Cp\text{-}Li^+)_4Sn_9^{4-}$	15.367	33.914	15.334	90	90.14	90	7992	500	-[b]
For Comparison									
$(222B\text{-}Cp^e\text{-}K^+)_3$ - $(Ge_9^{2-}Ge_9^{4-})_{½}$?	21.424	24.503	16.589	90	91.32	90	8706	726	Ref. 50
$(222Cp\text{-}K^+)_6$ - $Ge_9^{2-}Ge_9^{4-}\cdot 1.5en$	20.037	28.944	14.546	99.36	94.08	87.60	8313	693	Ref. 22
$(222Cp\text{-}Na^+)_2Sn_5^{2-}$	11.620	11.620	22.160	90	90	120	2591	648	Ref. 19
$(222Cp\text{-}Na^+)_3Sb_7^{3-}$	23.292	13.791	25.355	90	108.56	90	7721	643	Ref. 24
$(222Cp\text{-}K^+)_3Sn_9^{3-}\cdot 1.5en$	15.050	21.983	14.106	99.43	101.61	89.64	4508	751	Ref. 20

[a]Cp = crypt.
[b]From LATT.
[c]From Weissenberg and oscillation photographs.
[d]From indexing after standard selection.
[e]2,2,2-benzocrypt.

evident strain in the crypt. Therefore, reactions using 2,2,1-crypt and 2,1,1-crypt were also tried, as these are most effective in complexing Na^+ and Li^+, respectively. It was hoped that different sized cations could promote the isolation of new or different anions.

Crystals are easily produced by reaction of Na-Ge alloys with 2,2,2-crypt, though in general the solutions produced are relatively dilute and much alloy remains undissolved. $NaGe_{0.8}$ reacts with en alone to give a deep blue (free-electron colored) solution, producing a relatively large amount of hydrogen gas because of the excess sodium present; when 2,2,2-crypt is added the solution initially turns clear, then a light orange color develops after several days. Phase I crystals grow slowly (1-2 weeks) and singly on the walls of the apparatus above the meniscus. Crystals will not form unless alloy residue is present. Once formed, this phase is insoluble in en and in fact is relatively air-stable. Single-crystal X-ray results are examined later.

In general, $NaGe_{1.6}$ and $NaGe_{3.8}$ react identically, giving a red-orange solution. Phase II crystals grow rapidly and irreversibly at the meniscus or on the surface of the alloy residue, with many crystals growing from a single point. This intergrowth made it very difficult to separate a single crystal. Oscillation and Weissenberg photographs give the listed unit cell parameters and exhibit $P2_1/n$ space group symmetry. The volume would indicate the general formula $(2,2,2\text{-crypt-}Na^+)_3Ge_x^{3-}$ with z=4. Note the similarity of the unit cell parameters to the $(2,2,2\text{-crypt-}Na^+)_3Sb_7^{3-}$ values (also $P2_1/n$); the crypt cations are probably in similar positions. Since all polyatomic anions have had an even

number of electrons except for Sn_9^{3-}, a disorder of Ge_9^{4-} and Ge_9^{2-} on the same anion site, giving an average 3- charge, seems the most likely possibility. This disorder apparently exists in the 2,2,2B-crypt-K^+ salt listed; also, this compound and the known $(2,2,2\text{-crypt-}K^+)_6Ge_9^{2-}$-$Ge_9^{4-}\cdot 2.5en$ salt (which has independent anion sites) are both similar in color to phase II. However, since the recent discovery of the Sn_9^{3-} anion, one cannot completely rule out an actual 3- germanium cluster; ESR measurements should be made to be certain.

Reactions of these alloys with 2,2,1- and 2,1,1-crypt unfortunately do not readily produce crystals, perhaps because these crypts are viscous liquids so simply removing solvent leaves oils rather than solids. Also, unlike germanium salts with 2,2,2-crypt, the phases which do form are very soluble in en. Many attempts were made to encourage crystal growth: heating up to 50°C, freezing, removing all en, or slowly adding ethylamine (ea). When crystals were produced in some of these reactions, it was only after the solution, with most of the en trapped into another apparatus arm, was allowed to sit for upwards of six months, and crystal growth occurred extremely slowly, requiring three months or more to reach a suitable size. Such long reaction times probably prohibits the isolation of anything but the most stable anions. Also, the solvent tends to polymerize with time, combining with excess crypt to leave crystals coated with a sticky, nonvolatile substance which makes mounting difficult.

Reactions of $NaGe_{1.6}$ or $NaGe_{3.8}$ with 2,2,1-crypt produce unusual results. The solution initially is ruby red in color. After heating a

couple of days, the solution turns to a muddy greenish-brown color. If the heating is stopped, the solution will either return slowly to red or remain greenish-brown depending on whether alloy residue is present or not, and a solution can be cycled between the two colors several times before ultimately remaining greenish-brown. Apparently, an equilibrium exists between different germanium anions, which is greatly influenced by the presence of alloy.

When ethylamine was slowly added to one such greenish-brown solution ($NaGe_{1.6}$ + 2,2,1-crypt), black material precipitated out, and several months later a few light orange, thin plates formed, the color being very reminiscent of phase I. Unfortunately, it proved impossible to isolate these crystals. Another similar reaction ($NaGe_{3.8}$ + 2,2,1-crypt) eventually produced many greenish-black dendritic crystals out of a green-brown oil from which most of the solution was removed. These crystals have yet to be investigated.

The reaction of $NaGe_{3.8}$ + $NaGe_{0.8}$ + 2,2,1-crypt used about a 3:1 ratio of $NaGe_{3.8}$ to $NaGe_{0.8}$, but the $NaGe_{0.8}$ alloy was initially reserved in the third arm and added at a much later time, so it may not have contributed much to the reaction. This solution was not heated so it remained red and during the actual crystal growth period (the last four months) the solution was decanted from the alloy. The crystals finally produced (phase III) were again badly intergrown. One crystal was indexed, giving the unit cell parameters listed. These are somewhat similar to the $(2,2,2\text{-crypt-}K^+)_3Sn_9^{3-}\cdot 1.5en$ values, especially taking into account the volume decrease expected for the 2,2,1-crypt-Na^+ cation. The

general formula should be $(2,2,1\text{-crypt-}Na^+)_3Ge_x^{3-}$ with z=2 and the same conclusions apply here as for phase II. However, phase III crystals are much darker in color than those of phase II and more importantly, they do exhibit a strong ESR signal at room temperature (essentially two g values, $g_\perp = 2.043$ and $g_{||} = 1.992$) which is quite similar to that observed for the Sn_9^{3-} compound. Therefore, this phase may indeed contain the analogous paramagnetic Ge_9^{3-} anion, and it should certainly be further investigated.

The reaction of Li_7Sn_3 with 2,1,1-crypt produces an intense red solution. The hexagonally-shaped gems which finally formed grew singly from a reddish-black oil. Single crystal X-ray results are reported later.

Data Collection and Structure Solution

Single crystal X-ray diffraction methods

When a suitable crystal was found, data were collected using Mo Kα radiation monochromatized with a graphite crystal either on the four-circle automated diffractometer designed and built in the Ames Laboratory[51,52] or on the Syntex $P2_1$ diffractometer. Low temperatures were achieved by resistively heating liquid nitrogen to produce a reasonably steady stream of cold nitrogen gas flowing onto the capillary.

Standard reflections were monitored, usually every 75 reflections, to check for decay and crystal alignment. Data were corrected for decay based on either a linear or third order polynomial fit as appropriate to the sum of the integrated intensities of these standards. Absorption

corrections used the ϕ-scan method (one reflection with χ near 90° was measured every ten degrees in ϕ from 0° to 350°) and the program ABSN.[53] Reflections were considered observed if $I>3\sigma(I)$ and $F>3\sigma(F)$. Precise unit cell parameters were obtained with the program LATT[54] by a least-squares fit to the 2θ values of reflections tuned at the same temperature on both Friedel-related peaks ($\pm 2\theta$) to eliminate any instrument or centering errors.

Structure factor calculations and least-squares refinements were carried out using the block diagonal-full matrix program ALLS[55] and Fourier series calculations were done with the program FOUR.[56] Anisotropic thermal parameters of the form $\exp[-\frac{1}{4}(B_{11}h^2a^{*2}+B_{22}k^2b^{*2}+B_{33}\ell^2c^{*2}+2B_{12}hka^*b^*+2B_{13}h\ell a^*c^*+2B_{23}k\ell b^*c^*)]$ were used. The neutral atom scattering factors[57] included corrections for the real and imaginary parts of anomalous dispersion for the heavier elements (sodium or greater). All drawings of the structures were produced using the program ORTEP,[58] with thermal ellipsoids drawn at the 50% probability level unless otherwise indicated.

$(2,2,2\text{-crypt-}K^+)_2Sn_2Bi_2^{2-}\cdot en$

Preliminary oscillation and Weissenberg photographs indicated monoclinic symmetry with the extinction 0k0, k = 2n+1. Using a crystal of dimensions 0.62 x 0.52 x 0.13 mm, a total of 5639 reflections with $2\theta<50°$ in the two octants HKL and $\bar{H}\bar{K}L$ were measured at room temperature on the Ames Laboratory diffractometer (λ=0.71034 Å). The three standard reflections showed a 16% decay during data collection. As the crystal

was both large and relatively thin, an absorption correction was very necessary (μ=68.9 cm^{-1}, transmission coefficients ranged from 0.98 to 0.17). The data were corrected for absorption, decay (by a third-order polynomial), Lorentz and polarization effects to yield 2963 observed and 2944 independent reflections after averaging in $P2_1$. The final unit cell parameters, obtained by a least-squares fit to the 2θ values of 18 reflections with $27^o<2\theta<35^o$, are a = 12.640 (3) Å, b = 20.943 (5) Å, c = 12.353 (3) Å, β = 118.97 (2)^o, and V = 2861 (1) $Å^3$, with Z = 2, d(calc) = 1.80 g/cm^3, and fw = 1547. This unit cell and volume suggested the presence in the cell of four 2,2,2-crypt-K^+ cations, two 2- anions, and probably two solvent molecules.

Analysis of a conventional Patterson map clearly indicated the presence of two four-atom clusters of tetrahedral geometry in the cell related only by a 2_1 screw axis, which restricted the choice of space group to acentric $P2_1$. Even though a mixed Sn-Bi anion was anticipated, the fact that both electron densities and bond distances in the cluster were essentially equal suggested (incorrectly) a model wherein all four atoms were tin. A Sn_4^{2-} anion would not have been unprecedented; there is evidence of its existence in solution by NMR[35] and a prediction of a fluxional, nearly tetrahedral geometry.[59] Therefore, the structure was initially solved as (2,2,2-crypt-K^+)$_2Sn_4^{2-}$•en.[36]

Successive least-squares refinement and electron density maps located the 54 atoms of the two independent crypts. Refining all atoms with isotropic temperature factors led to R = 0.142 = $\Sigma||F_o|-|F_c||/\Sigma|F_o|$. Introduction of anisotropic temperature factors for the tin and potassium

atoms reduced R to 0.103. At this point, both electron density and difference maps showed the presence of an ethylenediamine solvent molecule, though it was not well defined. Refinements using several different sets of initial solvent atom positions converged to the same set, and the en molecule was chosen to have a cis-type geometry as this gave the most rational bond distances. Full matrix refinement of all 62 atoms converged at R = 0.094 and R_w = 0.115 = $[\Sigma w(|F_o|-|F_c|)^2/\Sigma w|F_o|^2]^{\frac{1}{2}}$, where $w = \sigma(F)^{-2}$. A difference map at this point was essentially flat to ± 1.1 e/Å^3.

It was at this point that the reaction of the ternary alloy KSnBi produced relatively large quantities of the phase in an essentially pure form, so it was possible to have a bulk analysis by atomic absorption performed. This proved bismuth was present in the crystals, and the approximately 1:1 Sn:Bi mole ratio found could only be rationalized by a diamagnetic $Sn_2Bi_2^{2-}$ anion rather than Sn_4^{2-}. Therefore, the anion was concluded to be $Sn_2Bi_2^{2-}$, but with completely disordered heavy atoms since the structural results indicated the four positions were substantially equivalent. Using this model, full matrix least-squares refinement of all atoms converged at R = 0.088 and R_w = 0.107, which are significantly lower. The data set was reweighted in 40 groups sorted on F_o, as a dependence of $\Sigma w(|F_o|-|F_c|)^2$ on the magnitude of F_o was observed. This did not change the residuals, but it did slightly improve the standard deviations of the atom parameters. The final difference map was flat to ± 1.5 e/Å^3.

Since the structure is in the acentric space group $P2_1$, a refinement of the enantiomorphic image was also performed, but this converged at much higher residuals; R = 0.099 and R_w = 0.121. Any attempt to partially or completely order the tin and bismuth atoms also caused a sharp increase in the residuals. There is no reason the Sn and Bi percentages must be exactly 50% at each atom position; in fact, the slight inequality of the bond distances suggests this may not be the case, though it could also arise from the effect of the local environment. However, a refinement in which multiplicities were allowed to vary demonstrated that any deviation from 50:50 Sn:Bi is insignificant. The occupancies found ranged from 0.968 (9) to 1.009 (9) of the ideal 50:50 atoms. The 80 hydrogen atoms in the asymmetric unit have not been located or estimated in the structure factor calculations; these represent 10.7% of the total electron density. The disordered cluster atoms were treated as if they had an atomic number of 66.5, with scattering factor tables which represent the average of those for Sn and Bi.

It is sobering to realize that X-ray crystallography alone is not always sufficient for an analysis of a new phase, even when there are no apparent problems in the structural refinement or results. In the present instance, either Sn_4^{2-} or $Sn_2Bi_2^{2-}$ (disordered) produced a very satisfactory solution, with convergence at R = 0.094 and R_w = 0.115 for the former and R = 0.088 and R_w = 0.107 for the latter. Though the latter is of course significantly lower, a large part of this improvement arose from a better fit of the anomalous dispersion correction. Compared with other polyatomic anions and crypt structures, the agreement

factors were better than average for either model. The final difference map, normally used as a concluding test for discrepancies in the final solution, was if anything cleaner for Sn_4^{2-} than for $Sn_2Bi_2^{2-}$.

The only crystallographic indication that the former model was incorrect is the fact that the thermal parameters for the crypt atoms (average B = 10.8 $Å^2$) were much larger than those found for the heavier anion atoms (8.2 $Å^2$). On the other hand, the values were relatively close, 8.3 $Å^2$ and 8.7 $Å^2$, respectively, for the disordered $Sn_2Bi_2^{2-}$ model. Since the heavy atoms for the most part determine the structure, the mistake of assigning too small of a scattering factor for the anion atoms in the Sn_4^{2-} model was in effect simply compensated for by a decrease in the overall scale factor and an increase in light atom thermal parameters. Thus, the error in the heavy atoms showed up only in the light atoms. Of course, the problem is moot in this case as a conventional analysis was performed, but sometimes this is not possible when reactions produce very small quantities and multiphase products.

$\underline{(2,2,2\text{-crypt-}K^+)_2Pb_2Sb_2^{2-}\cdot en}$

Oscillation and Weissenberg photographs confirmed that this phase is isostructural with the $Sn_2Bi_2^{2-}$ salt, with monoclinic symmetry and the extinction 0k0, k = 2n+1. It should be noted that because of the very nearly hexagonal lattice parameters for these phases, it is very easy to mistakenly obtain the alternative monoclinic cell ($\vec{a}' = -\vec{a}$, $\vec{b}' = \vec{a} + \vec{b}$, $\vec{c}' = -\vec{c}$) when indexing photographs or on the diffractometer;

the lattice parameters are almost indistinguishable but the diffraction intensities are of course very different.

Data were collected on a plate-shaped crystal of dimensions 0.56 x 0.45 x 0.16 mm, using the Syntex P2 diffractometer at -80°C (λ=0.71007 Å). A ω-scan was used, with a minimum and maximum scan rate of 5.86 and 29.30 deg/min, respectively. A total of 5458 reflections with $2\theta<50^{\circ}$ in the two octants HKL and $\bar{H}\bar{K}L$ were collected. Data were corrected for decay (18% based on three standard reflections measured every 60 reflections), absorption (μ=71.0 cm^{-1}, transmission coefficients ranged from 1.00 to 0.35), Lorentz and polarization effects. 3011 reflections were classified as observed, and averaging in the space group $P2_1$ gave a final data set of 3000 reflections. The monoclinic cell dimensions, obtained from 27 tuned reflections with $25^{\circ}<2\theta<32^{\circ}$, are a = 12.589 (2) Å, b = 20.735 (2) Å, c = 12.201 (2) Å, β = 118.97 (1)°, and V = 2786.4 (6) $Å^3$, with Z = 2, d(calc) = 1.84 g/cm^3 and fw = 1547.

Since the data indicated the crystal was isostructural with $(2,2,2\text{-crypt-}K^+)_2Sn_2Bi_2^{2-}\cdot$en, refinement was begun by assuming four analogous 50:50 Pb:Sb positions for an approximately tetrahedral $Pb_2Sb_2^{2-}$ anion, yielding R = 0.225. Subsequent electron density maps and least-squares refinement located the potassium and crypt atoms of the two independent cations, which are indeed in similar positions to those in the $Sn_2Bi_2^{2-}$ salt. At this point, since the space group $P2_1$ is acentric, the inverted image was refined (all x,y,z's were changed to 1-x, 1-y, 1-z's). R dropped significantly from 0.091 to 0.082, so further refinements used these inverted positions. The atoms of the ethylenediamine

solvent molecule could then be located on an electron density map, somewhat better defined than in the $Sn_2Bi_2^{2-}$ structure, and with more of a trans-type configuration.

Full matrix least-squares refinement of all 62 atoms, with the K and 50:50 Pb:Sb atoms having anisotropic thermal parameters, yielded $R = 0.079$ and $R_w = 0.089$. Since the Pb and Sb percentages are not required by symmetry to be exactly 50% at each site, the multiplicities were allowed to vary in several refinements, and indeed the four atom sites differ significantly as shown in Table 9.

Table 9. Pb and Sb percentages for $Pb_2Sb_2^{2-}$

Atom	Multiplicity when Z=66.5	Final percentages % Pb	% Sb	Average Z
PbSb1	1.023 (12)	65.7	34.3	71.4
PbSb2	0.907 (10)	40.2	59.8	63.5
PbSb3	0.849 (10)	27.0	73.0	59.4
PbSb4	1.027 (12)	67.1	32.9	71.8

The four multipliers did not total 4.00 as they ought, but this was not considered significant since these values are dependent on several factors such as the size of the thermal parameters. Therefore, the multipliers were scaled up to total 4.00, and converted to Pb and Sb percentages, giving new average scattering factor tables for each atom.

This process was repeated once, because changing the scattering factor tables changes the multiplicities slightly, to give the final percentages and average atomic numbers listed in the table.

The final full matrix refinement, using these percentages with multiplicities set at 1.00, converges at significantly lower residuals, $R = 0.072$ and $R_w = 0.079$. A final difference map was flat to ± 2 e/Å^3 near the heavy atoms and ± 1 e/Å^3 elsewhere. The 80 independent hydrogen were not located, representing 10.7% of the total electron density.

$\underline{(2,2,2\text{-crypt-}K^+)_2Sb_4^{2-}}$

A strongly diffracting crystal of dimensions 0.62 x 0.30 x 0.17 mm was examined on the Ames Laboratory diffractometer (λ=0.71034 Å). A total of 5371 reflections were collected at room temperature for the four octants HKL, $\bar{H}\bar{K}L$, $\bar{H}K\bar{L}$ and $H\bar{K}\bar{L}$ of the indicated triclinic cell with $2\theta < 50^\circ$. Three standard reflections measured every 75 reflections showed only a 7% decay in intensity during data collection (in sharp contrast to the isostructural Bi_4^{2-} salt[12] which decayed so rapidly at room temperature that two crystals were necessary to obtain a complete data set). The data were corrected for decay (by a linear fit), absorption (μ=22.8 cm^{-1}, transmission coefficients ranged from 0.99 to 0.75), Lorentz and polarization effects, giving 4591 observed reflections. After averaging in $P\bar{1}$ ($R_{ave} = 0.035$), the final data set contained 3909 independent reflections.

Precise lattice dimensions of a = 11.555 (1) Å, b = 11.795 Å, c = 11.067 Å, α = 97.60 (1)$^\circ$, β = 97.80 (1)$^\circ$, γ = 61.24 (1)$^\circ$, and V = 1306.1 Å^3 with Z = 1, d(calc) = 1.68 g/cm^3 and fw = 1318 were obtained using the 2θ values of 24 reflections in the range $36^\circ < 2\theta < 42^\circ$.

Since the unit cell parameters indicated the compound is isostructural with the Bi_4^{2-} salt, the least-squares refinement was begun by using the Bi atom coordinates for the two Sb positions, which immediately gave an agreement factor R = 0.305. Further full matrix least-squares refinement and electron density maps located all the crypt atoms (in essentially the same positions as in the Bi_4^{2-} structure) giving R = 0.080 when all 29 atoms were allowed to have anisotropic thermal parameters. At this point, both electron density and difference maps indicated a disorder in the crypt carbons α and β to the nitrogen nearest the Sb_4^{2-} anion, similar to that found in the Bi_4^{2-} structure. In particular, C1, C2, C11, C12 and C22 were resolvable into pairs (a and b), with separations of 0.7 to 1.0 Å. The 'thermal' ellipsoid for C21 is also considerably elongated but not enough to make resolution feasible. With isotropic thermal parameters and a multiplicity of 0.50 for these carbon atoms (from which they do not vary significantly) the residuals were essentially unchanged at R = 0.081 and R_w = 0.113. This disordered model is clearly preferred in terms of chemical sensibility; otherwise the N-C and C-C bond distances would be much too short. The 72 hydrogen atoms have not been located or estimated in the structure factor calculations, representing 11.0% of the total electron density. The final difference map was essentially flat to ± 2 e/Å^3 near the antimony atoms and less than ± 1 e/Å^3 in the rest of the map.

$(2,2,2\text{-crypt-}K^+)_3Sb_7^{3-}\cdot 2en$

Data were collected using a crystal of dimensions 0.42 x 0.13 x 0.04 mm at low temperature (-80°C) on the Ames Laboratory diffractometer. The crystal was not a strong diffractor but did give very sharp peaks. A total of 12,049 reflections with $2\theta<44^\circ$ in the four octants HKL, $\bar{H}\bar{K}L$, $\bar{H}K\bar{L}$, and $H\bar{K}\bar{L}$ were measured. The data were corrected for decay (according to a 22% linear decrease in the integrated intensities of three standard reflections), absorption (μ=23.8 cm^{-1}, transmission coefficients ranged from 0.99 to 0.73), Lorentz and polarization effects, yielding 8276 observed reflections. The final data set contained 7281 independent reflections after averaging in the space group $P\bar{1}$ (R_{ave} = 0.033).

Precise unit cell dimensions are a = 14.589 (2) Å, b = 21.753 (3) Å, c = 13.857 (2) Å, α = 92.46 (1)°, β = 99.63 (2)°, γ = 89.12 (2)°, and V = 4331 (1) $Å^3$ with Z = 2, d(calc) = 1.70 g/cm^3, and fw = 2219, obtained as before from 24 reflections with $25^\circ<2\theta<34^\circ$.

Analysis of a conventional Patterson map clearly showed a seven-atom cluster with bond distances and configuration indicative of Sb_7^{3-} (as in the known crypt-Na^+ salt[24]). Least-squares refinement of the seven Sb and three K positions obtained from the Patterson map immediately yielded R = 0.223. The crypt atoms and two independent en solvent molecules were located on an electron density map, and subsequent refinement of all 96 atoms with isotropic thermal parameters gave R = 0.104 and R_w = 0.131. Final block diagonal least-squares refinement allowing the Sb, K, O and crypt N atoms to have anisotropic thermal parameters converged at R = 0.075 and R_w = 0.093. The final difference map was flat to ±2 $e/Å^3$ near

the antimony atoms and less than ±1 e/Å^3 in the rest of the map. The 124 hydrogen atoms have not been located or estimated in the structure factor calculations; these represent 11.3% of the total electron density.

$\underline{(2,2,2\text{-crypt-}K^+)_3Sn_9^{3-}\cdot 1.5en}$

Preliminary oscillation and Weissenberg photographs of this phase indicated a unit cell nearly identical with that for $(2,2,2\text{-crypt-}K^+)_3$ - $(TlSn_8^{3-}TlSn_9^{3-})_{½}\cdot en$,[28] except that the volume was about 100 Å^3 smaller and some intensity differences were observed. The $TlSn_8^{3-}/TlSn_9^{3-}$ salt contains the two anions disordered 50:50 on a single anion site with seven coinciding atoms. By analogy, this phase was expected to contain the Sn_9^{4-} and Sn_{10}^{2-} anions disordered on the same site (the latter ion is so far unknown).

Data were collected at -60°C on the Ames Laboratory diffractometer (λ=0.70964 Å) using a crystal of dimensions 0.40 x 0.39 x 0.38 mm. A total of 13,229 reflections with $2\theta<45^\circ$ in four octants (HKL, $\bar{H}\bar{K}L$, $\bar{H}K\bar{L}$ and $H\bar{K}\bar{L}$) were measured. Three standard reflections measured every 75 reflections showed a linear intensity loss totalling 66% during data collection. A normal decay correction based on these standards was not completely satisfactory (leading to R_{ave} = 0.048 with 31 reflections eliminated) because the decay was also very dependent on 2θ; low angle reflections lost very little intensity while higher angle reflections decayed more than the 66% rate. (This is normally the case, but it only becomes significant when the decay is so large.) So, a better decay correction was made using a function of both 2θ (second order polynomial)

and reflection number (linear), determined from data collected more than once either as identical or Friedel-related pairs (hk0, h0ℓ and 0kℓ reflections).

The data were also corrected for absorption (μ=27.0 cm^{-1}, transmission coefficients ranged from 1.00 to 0.85), Lorentz and polarization effects, yielding 10,472 observed reflections. Averaging in $P\bar{1}$ gave 9293 independent reflections (R_{ave} = 0.034, with four reflections eliminated at the 6σ cutoff). Precise triclinic unit cell dimensions, obtained by using the 2θ values of 26 reflections in the range $30^{o}<2\theta<35^{o}$, are a = 15.002 (1) Å, b = 21.794 (2) Å, c = 14.060 (1) Å, α = 99.770 $(10)^{o}$, β = 101.595 $(9)^{o}$, γ = 89.694 $(10)^{o}$, and V = 4435.9 (7) $Å^3$, with Z = 2, d(calc) = 1.80 g/cm^3, and fw = 2405.

The compound was assumed to be nearly isostructural with the $TlSn_8^{3-}/TlSn_9^{3-}$ salt, so refinement was begun using the eight average tin-only positions from that structure, giving an initial agreement factor of about 0.40. However, the electron density map showed only a ninth tin atom (at the Tℓ position of $TlSn_8^{3-}$), with absolutely no sign of a tenth cluster atom at what would be the Tℓ position of the $TlSn_9^{3-}$ anion; hence, this rules out the Sn_9^{4-}/Sn_{10}^{2-} model.

The three independent crypts and one en solvent molecule were located by successive least-squares refinement and electron density maps; their positions are essentially the same as in the thallium-tin salt. A difference map at this point showed what appeared to be an additional en molecule sitting on the center of symmetry at 0,0,1/2. The final difference map for the thallium-tin structure also had positive electron

density at this position, though somewhat weaker. In that structure, this en would be fairly close to the Tℓ of the $Tℓ Sn_9^{3-}$ anion (∿3.8 Å), so perhaps it is present only when the anion is $Tℓ Sn_8^{3-}$.

In this structure, neither en molecule is well defined but this is typical. Final block diagonal refinement of all 96 nonhydrogen atoms, with anisotropic thermal parameters for the nine tin and three potassium atoms, converged at R = 0.085 and R_w = 0.125. A final difference map was flat to less than ±2.5 e/Å^3 near the tin atoms (within about 1.0 Å) and ±1.0 e/Å^3 elsewhere. The 120 independent hydrogen atoms have not been located or estimated in the structure factor calculations; these represent 10.2% of the total electron density.

$\underline{(2,2,2\text{-crypt-}Na^+)_2Ge_4^{2-}}$ - a partial structure solution

Data for this compound were actually measured three times, but the best data were obtained using a large crystal of dimensions 0.62 x 0.62 x 0.20 mm on the Ames Laboratory diffractometer at room temperature. 5176 reflections in four octants (HKL, $\bar{H}$KL, H$\bar{K}$L and HK$\bar{L}$) with $2\theta<50^o$ were collected (λ=0.71002). Though the absorption coefficient is small, a correction was nevertheless very necessary (μ=26.0 cm^{-1}, transmission coefficients ranged from 0.99 to 0.44). Decay in the beam was negligible. After corrections for absorption, Lorentz and polarization effects, 3549 reflections were considered observed, and averaging in $P\bar{3}$ gave 1124 independent reflections (R_{ave} = 0.034).

The trigonal unit cell parameters are a = 11.431 (2) Å, c = 11.056 (2) Å, and V = 1251.1 (4) Å^3 (Z = 1, fw = 1089, d(calc) = 1.45 g/cm^3),

using 20 reflections with $30^{o}<2\theta<40^{o}$. Since the structure solved poorly, long exposure oscillation and Weissenberg photographs were examined; there is no indication of any larger cell or alternate symmetry.

The Patterson map was unusual in that the strongest peak represented a 2.0 Å distance, much too short for a Ge-Ge bond. The only model which seems to fit the Patterson is two disordered Ge_4 tetrahedra each at 50% occupancy, with one the inverted image of the other (an inversion center occurs at the center of the tetrahedron). The strong Patterson peak would then represent a Ge-Ge vector between two different disordered Ge_4 clusters rather than an actual chemical bond.

With this germanium cluster centered at 0,0,0 and the two inversion related crypt cations in the cell located on the three-fold axes at 1/3, 2/3,z and 2/3,1/3,-z, a Ge_4^{2-} anion is implied. Refinement of this model with all 13 independent atoms considered anisotropic yielded poor agreement factors at R = 0.170 and R_w = 0.248. There seems to be no obvious reason why the residuals should be so high. All attempts to refine the structure in lower symmetry space groups were not successful. Though all the thermal parameters are reasonably small and spherical, those for the germanium atoms have noticeably larger values than do the crypt atoms ($\sim$11 $Å^2$ vs $\sim$5 $Å^2$ for isotropic B's), which is sometimes symptomatic of assigning incorrect scattering power to heavy atoms, but it may simply be due to the disorder. If the multipliers for the germanium atoms are allowed to vary, both these and the thermal parameters increase.

A detailed final difference map was very clean except in the vicinity of the germaniums, where peaks up to 2 $e/Å^3$ were seen; these are not necessarily ignorable since the 50% occupancy Ge atoms only show peak heights of $\sim$14 $e/Å^3$ on a normal map. It appears the Ge atoms simply are poorly ordered on their sites, with tetrahedrally shaped electron densities which cannot be completely accounted for by the standard ellipsoidal 'thermal' parameters; i.e., the left over electron density on the difference map occurs in four areas around each Ge atom, between it and each of the three adjacent Ge atoms (of the alternative cluster) and about 0.8 Å out from each Ge on a line from the center of symmetry. If partial Ge atoms are placed at such positions, it is possible to decrease the residuals to reasonable values at R = 0.122 and R_w = 0.178, but such a complicated solution is not very satisfactory.

$\underline{(2,1,1\text{-crypt-}Li^+)_4Sn_9^{4-}}$ - another problem structure

Crystals of this phase diffract well and give sharp spots, but the intensity drops quite rapidly at higher 2θ values. Oscillation and Weissenberg photographs indicated a unit cell of approximate dimensions a = 15.4 Å, b = 33.9 Å and c = 15.4 Å, assuming angles near 90°. The oscillation axis showed no mirror symmetry, but the zero-level Weissenberg exhibited mirror symmetry with odd reflections extinct along both axes (b^* and c^*) and very nearly a k = 4n condition for the 33.9 Å axis. From this evidence two space groups were possible, monoclinic $P2_1/n$ and tetragonal $P4_2/n$; the former proved to be the correct choice.

A crystal of dimensions 0.36 x 0.43 x 0.20 mm was used for data collection at approximately -100°C on the Syntex diffractometer (λ=0.71007 Å). Precise monoclinic unit cell parameters of a = 15.367 (3) Å, b = 33.914 (3) Å, c = 15.334 (4) Å, β = 90.14 (1)° and V = 7992 (3) Å^3 (Z = 4, d(calc) = 1.87 g/cm^3, and fw = 2249) were obtained using 24 reflections with $19^\circ<2\theta<30^\circ$. A total of 10,058 reflections with $2\theta<43^\circ$ in the two octants HKL and $\bar{H}\bar{K}L$ were measured, of which 244 were symmetry extinct (0k0, k=2n+1 and h0ℓ, h+ℓ=2n+1). The maximum and minimum scan rates were 29.3 and 3.5 deg/min, respectively. One standard reflection monitored every 50 reflections lost 43% of its original intensity. Data were corrected for decay, absorption (μ=28.4 cm^{-1}, transmission coefficients ranged from 0.98 to 0.65), Lorentz and polarization effects, yielding 5248 observed reflections.

The data averaged very poorly in $P2_1/n$; with a 6σ cutoff, R_{ave} = 0.092 and 54 reflections were eliminated, many of which were very strong reflections. The problem is not in the space group choice; rather, it is that the last third or so of the data was simply not compatible with the first two thirds, perhaps due to inconsistent decay, crystal misalignment, temperature changes or some other crystal change for which no account has been made. For instance, the 00ℓ reflections were measured once at the beginning and once at the end of data collection, and these averaged to R_{ave} = 0.13. Nothing can be done to correct this problem, but to avoid having so many strong reflections eliminated, the reflections in the last third of the data which would have been averaged were deleted so the final data set contained 4820 independent reflections.

MULTAN[60] indicated the presence of a nine-atom tin cluster, for which least-squares refinement yielded R = 0.31. Subsequent block-diagonal refinements and electron density maps located all 84 atoms of the four independent crypt cations, including the lithium atoms. With isotropic thermal parameters for all atoms R equaled 0.239, while allowing the tin atoms to have anisotropic thermal parameters gave R = 0.142 and R_w = 0.171.

The structure therefore appears to be $(2,1,1\text{-crypt-}Li^+)_4Sn_9^{4-}$, but the cluster does not have the normal C_{4v} configuration for Sn_9^{4-}.[21] Both bond distances and dihedral angles indicate the cluster is midway between a C_{4v} and a D_{3h} type configuration. Also, six of the nine tin atoms have greatly elongated thermal ellipsoids; these six atoms can be resolved into two components A and B, giving an approximately C_{4v} and D_{3h} cluster, respectively. With isotropic thermal parameters for these resolved atoms, the residuals actually increase to R = 0.151 and R_w = 0.182. The multiplicities were allowed to vary from 0.50, and showed a trend to about 60% A (C_{4v}) and 40% B (D_{3h}), but the agreement factors did not change. With the 50:50 model, the residuals dropped to R = 0.131 and R_w = 0.159 when the resolved tin atoms were allowed to have anisotropic thermal parameters. However, while the thermal ellipsoids for cluster A (C_{4v}) remained reasonably well-behaved, several atoms in cluster B (D_{3h}) became quite elongated again.

Unfortunately, this disorder and the poor quality of the data limit the success of this structure solution. The large unit cell and the very long b axis would tend to hinder collection of a good data set,

and it is not known if the disorder observed here is inherent in all the crystals. The Sn_9^{4-} anion is well known in the C_{4v} configuration, so this structure is not very important unless the presence of the D_{3h}-type configuration is provable.

RESULTS AND DISCUSSION

The $Sn_2Bi_2^{2-}$ and $Pb_2Sb_2^{2-}$ Structures

The final positional and thermal parameters for $(2,2,2\text{-crypt-}K^+)_2 - Sn_2Bi_2^{2-}\cdot en$ and $(2,2,2\text{-crypt-}K^+)_2Pb_2Sb_2^{2-}\cdot en$ are listed in Table 10 and 11, respectively. All bond distances and angles for the $Sn_2Bi_2^{2-}$ and $Pb_2Sb_2^{2-}$ anions are given later in Table 12. Remaining distances and angles in the crypt cations and en molecules appear in Appendix A. Observed and calculated structure factors for the $Sn_2Bi_2^{2-}$ salt have been deposited in reference 26; those for the $Pb_2Sb_2^{2-}$ compound are listed in Appendix B.

As previously noted, these two compounds are isostructural, though the $Pb_2Sb_2^{2-}$ salt occurs here in the inverted image as is evident in Figure 1 and 2. The general improvement in thermal parameters due to the low temperature data collection for $Pb_2Sb_2^{2-}$ is also obvious. The unit cell in both cases contains two anions, four potassium-crypt cations and two en molecules, with the disposition of these species exhibiting a marked pseudohexagonal character. Of course, the a and c axes are nearly equal and β is very close to 120^o, but also the anion and two crypt cations each have approximate three-fold axes and are located at translations in x and z of about 1/3,2/3 and 2/3,1/3 from the anion axis. Since the anion is positioned off the b axis, and 2_1 screw symmetry creates a zig-zag channel containing the anions, with an en molecule filling the empty space directly above each anion. However, there is no significant interaction between the anions and the solvent molecules. In the

Table 10. Positional and thermal parameters for (2,2,2-crypt-K)$_2$Sn$_2$Bi$_2$·en

Atom	x	y	z	B11	B22	B33	B12	B13	B23
SnBi1[a]	0.0413(2)	0.0	0.8771(2)	8.1(1)	15.2(3)	7.0(1)	0.3(2)	1.30(9)	-3.8(2)
SnBi2	0.1202(2)	0.0015(3)	0.1453(2)	10.3(1)	9.8(2)	8.1(1)	-0.7(2)	6.0(1)	-0.5(1)
SnBi3	0.3001(2)	0.0035(3)	0.0574(2)	6.24(8)	8.8(1)	7.67(9)	1.3(1)	3.28(7)	1.1(1)
SnBi4	0.1469(2)	0.1175(3)	0.0226(2)	8.5(1)	7.9(1)	7.3(1)	1.6(1)	3.31(9)	0.7(1)
K1	0.8351(6)	0.2057(5)	0.3704(6)	5.6(3)	7.5(5)	4.9(3)	0.4(4)	2.6(3)	0.5(4)
K2	0.5030(6)	0.1823(5)	0.6949(6)	5.0(3)	6.9(5)	4.7(3)	-0.3(3)	2.2(3)	-0.5(3)

Atom	x	y	z	B	Atom	x	y	z	B
N10[b]	0.808(3)	0.064(2)	0.375(3)	7.8(7)	C42	0.323(4)	0.070(3)	0.742(4)	8.7(11)
C11	0.888(4)	0.033(3)	0.332(5)	10.3(13)	O43	0.305(2)	0.129(1)	0.703(2)	7.1(6)
C12	0.017(4)	0.066(3)	0.384(4)	8.3(10)	C44	0.241(4)	0.172(3)	0.754(4)	8.8(11)
O13	0.998(2)	0.129(1)	0.347(2)	7.5(6)	C45	0.226(3)	0.237(2)	0.711(4)	7.2(9)
C14	0.110(3)	0.148(2)	0.366(4)	7.4(9)	O46	0.345(3)	0.261(2)	0.744(3)	9.0(7)
C15	0.098(3)	0.218(2)	0.315(3)	6.4(8)	C47	0.330(5)	0.325(3)	0.703(5)	10.6(14)
O16	0.047(2)	0.259(1)	0.374(2)	6.6(5)	C48	0.452(6)	0.355(3)	0.725(6)	13.3(17)
C17	0.036(4)	0.323(2)	0.336(4)	7.9(10)	N49	0.511(3)	0.320(2)	0.668(3)	8.7(9)
C18	0.980(4)	0.364(3)	0.397(4)	9.8(12)	C51	0.569(4)	0.021(3)	0.844(4)	9.5(11)
N19	0.857(2)	0.348(2)	0.365(3)	6.7(7)	C52	0.697(3)	0.055(2)	0.892(4)	8.0(10)
C21	0.685(4)	0.044(3)	0.295(5)	10.2(13)	O53	0.690(2)	0.121(1)	0.911(2)	6.6(5)
C22	0.627(5)	0.086(3)	0.168(5)	10.7(14)	C54	0.807(3)	0.151(2)	0.967(3)	6.1(8)
O23	0.622(2)	0.148(2)	0.197(2)	7.5(6)	C55	0.792(4)	0.217(3)	0.979(4)	8.4(10)
C24	0.540(4)	0.183(2)	0.089(4)	7.9(9)	O56	0.723(2)	0.245(1)	0.852(2)	7.3(6)

[a] 50:50 distribution of Sn and Bi.

[b] The first digit identifies the chain (1, 2, and 3, crypt 1; 4, 5, and 6, crypt 2), and the second indicates the position along the chain.

Table 10. Continued

Atom	x	y	z	B	Atom	x	y	z	B
C25	0.536(3)	0.248(2)	0.113(3)	6.9(8)	C57	0.718(4)	0.314(2)	0.850(4)	7.6(10)
O26	0.655(2)	0.279(1)	0.170(2)	7.2(6)	C58	0.645(4)	0.338(3)	0.733(5)	10.2(12)
C27	0.647(3)	0.342(2)	0.288(3)	6.9(8)	C61	0.532(5)	0.006(4)	0.634(5)	11.4(13)
C28	0.776(4)	0.369(3)	0.238(4)	9.0(11)	C62	0.452(4)	0.037(2)	0.495(4)	8.4(10)
C31	0.839(4)	0.042(3)	0.496(5)	10.3(14)	O63	0.490(2)	0.103(1)	0.502(2)	6.5(5)
C32	0.804(4)	0.089(3)	0.595(4)	8.8(11)	C64	0.425(3)	0.136(2)	0.374(3)	6.1(8)
O33	0.848(3)	0.146(2)	0.577(3)	9.3(8)	C65	0.466(4)	0.196(2)	0.386(4)	8.1(10)
C34	0.831(4)	0.187(2)	0.661(4)	8.2(10)	O66	0.449(2)	0.236(1)	0.463(2)	7.2(6)
C35	0.893(3)	0.243(2)	0.684(4)	7.4(9)	C67	0.485(5)	0.296(3)	0.455(5)	10.6(15)
O36	0.839(2)	0.279(2)	0.566(2)	7.3(6)	C68	0.451(5)	0.338(3)	0.532(5)	11.4(14)
C37	0.890(4)	0.339(2)	0.582(4)	7.9(10)	NEN1	0.209(15)	0.363(10)	0.103(15)	39.(8)
C38	0.826(4)	0.377(3)	0.457(4)	9.0(11)	CEN1	0.217(14)	0.306(9)	0.116(15)	25.(6)
N40	0.494(3)	0.042(2)	0.714(3)	8.1(8)	CEN2	0.169(12)	0.333(9)	0.950(13)	26.(5)
C41	0.365(4)	0.025(3)	0.681(4)	10.2(13)	NEN2	0.187(10)	0.392(7)	0.918(11)	29.(4)

Table 11. Positional and thermal parameters for $(2,2,2\text{-crypt-K})_2Pb_2Sb_2 \cdot en$

Atom	x	y	z	B11	B22	B33	B12	B13	B23
PbSb1[a]	0.9664(2)	1.0000	0.1276(2)	4.71(8)	12.12(18)	4.59(8)	1.09(13)	0.01(7)	-3.13(13)
PbSb2	0.8892(2)	0.9972(2)	0.8592(2)	6.08(10)	6.16(13)	5.59(9)	-0.35(12)	4.05(8)	-0.20(13)
PbSb3	0.7082(2)	0.9951(2)	0.9434(2)	3.32(7)	5.61(12)	4.50(9)	1.04(10)	1.84(7)	0.78(12)
PbSb4	0.8588(2)	0.8790(2)	0.9791(2)	4.76(8)	5.30(10)	4.90(8)	1.49(9)	2.08(7)	1.00(9)
K1	0.1676(6)	0.7931(4)	0.6294(6)	2.7(3)	4.5(4)	2.4(3)	0.3(3)	1.1(2)	0.3(3)
K2	0.4973(6)	0.8157(4)	0.3025(6)	2.6(3)	3.8(4)	2.7(3)	0.2(3)	1.0(2)	0.2(3)

Atom	x	y	z	B	Atom	x	y	z	B
N10[b]	0.201(2)	0.937(2)	0.630(3)	4.5(7)	C31	0.171(4)	0.961(2)	0.506(4)	6.8(11)
O13	0.006(2)	0.875(1)	0.656(2)	3.9(4)	C32	0.209(3)	0.910(2)	0.437(4)	5.0(8)
O16	0.955(2)	0.741(1)	0.627(2)	3.6(4)	C34	0.173(3)	0.812(2)	0.334(3)	3.5(7)
N19	0.137(2)	0.650(1)	0.631(2)	3.5(5)	C35	0.109(3)	0.751(2)	0.315(3)	3.9(7)
O23	0.385(2)	0.847(1)	0.806(2)	3.7(5)	C37	0.108(3)	0.654(2)	0.411(3)	4.9(8)
O26	0.348(2)	0.717(1)	0.834(2)	2.5(4)	C38	0.163(3)	0.617(2)	0.540(3)	3.6(7)
O33	0.157(2)	0.852(1)	0.418(2)	4.7(5)	C41	0.639(3)	0.973(2)	0.316(3)	4.4(8)
O36	0.160(2)	0.715(1)	0.429(2)	3.5(4)	C42	0.687(3)	0.931(2)	0.252(3)	4.1(7)
N40	0.513(3)	0.957(1)	0.284(3)	4.5(7)	C44	0.759(3)	0.822(2)	0.242(3)	4.3(8)
O43	0.700(2)	0.865(1)	0.292(2)	3.5(4)	C45	0.776(3)	0.756(2)	0.289(3)	5.0(8)
O46	0.651(2)	0.732(1)	0.253(2)	3.8(5)	C47	0.660(3)	0.670(2)	0.288(4)	5.1(9)
N49	0.485(3)	0.675(2)	0.323(3)	5.2(7)	C48	0.538(4)	0.640(2)	0.269(4)	6.7(11)
O53	0.313(2)	0.879(1)	0.087(2)	3.3(4)	C51	0.432(3)	0.980(2)	0.156(3)	4.9(8)
O56	0.278(2)	0.754(1)	0.142(2)	3.6(4)	C52	0.304(3)	0.946(2)	0.102(3)	5.0(8)

[a] Pb and Sb percentages as listed in Table 9. PbSb1 through PbSb4 have average atomic numbers of 71.4, 63.5, 59.4 and 71.8 respectively.

[b] The first digit identifies the chain (1, 2, and 3, crypt 1; 4, 5, and 6, crypt 2), and the second, the position along the chain.

Table 11. Continued

Atom	x	y	z	B	Atom	x	y	z	B
O63	0.516(2)	0.896(1)	0.502(2)	3.8(5)	C54	0.197(3)	0.850(2)	0.031(3)	3.8(7)
O66	0.551(2)	0.764(1)	0.541(2)	4.3(5)	C55	0.208(3)	0.781(2)	0.017(3)	4.4(8)
C11	0.127(3)	0.968(2)	0.672(3)	5.3(9)	C57	0.280(3)	0.683(2)	0.135(3)	4.1(7)
C12	0 996(3)	0.940(2)	0.618(4)	5.5(9)	C58	0.355(3)	0.657(2)	0.274(3)	5.4(9)
C14	0.885(3)	0.849(2)	0.627(3)	3.8(7)	C61	0.480(3)	0.989(2)	0.365(3)	4.9(7)
C15	0 908(3)	0.786(2)	0.687(3)	3.9(7)	C62	0.545(3)	0.964(2)	0.505(3)	4.9(9)
C17	0 958(3)	0.675(2)	0.662(3)	4.8(8)	C64	0.580(3)	0.867(2)	0.632(3)	4.6(8)
C18	0.007(3)	0.634(2)	0.594(3)	3.3(6)	C65	0.531(3)	0.802(2)	0.623(4)	5.1(9)
C21	0.327(4)	0.955(2)	0.712(4)	6.6(11)	C67	0.513(4)	0.697(2)	0.540(4)	6.5(11)
C22	0.386(4)	0.909(2)	0.834(4)	5.4(9)	C68	0.544(3)	0.656(2)	0.466(3)	4.9(8)
C24	0.463(3)	0.810(2)	0.916(3)	4.1(7)	NEN1	0.216(7)	0.119(4)	0.160(7)	18.(3)
C25	0.469(3)	0.743(2)	0.889(3)	3.7(7)	CEN2	0.169(9)	0.179(6)	0.090(10)	20.(4)
C27	0.348(3)	0.652(2)	0.818(3)	3.1(6)	CEN3	0.201(9)	0.170(6)	-0.010(10)	19.(3)
C28	0.217(2)	0.624(2)	0.758(3)	3.0(6)	NEN4	0.160(4)	0.118(3)	0.906(4)	11.(1)

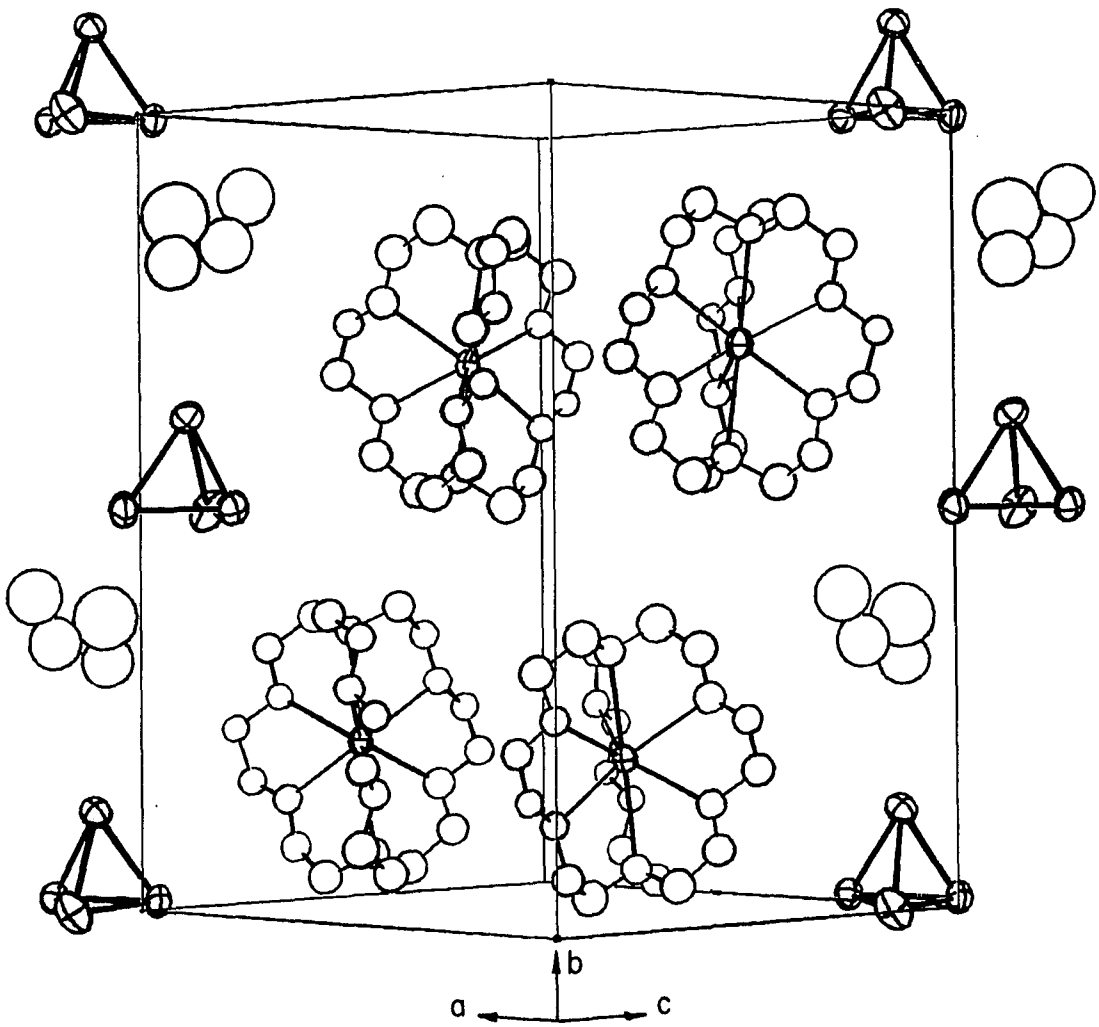

Figure 1. Approximate [101] view of the unit cell of $(2,2,2\text{-crypt-}K^+)_2$ - $Sn_2Bi_2^{2-}\cdot$en. For clarity, the anions and en molecules along the (0,y,0) and (1,y,1) axes are not included. Thermal ellipsoids are drawn at the 30% probability level

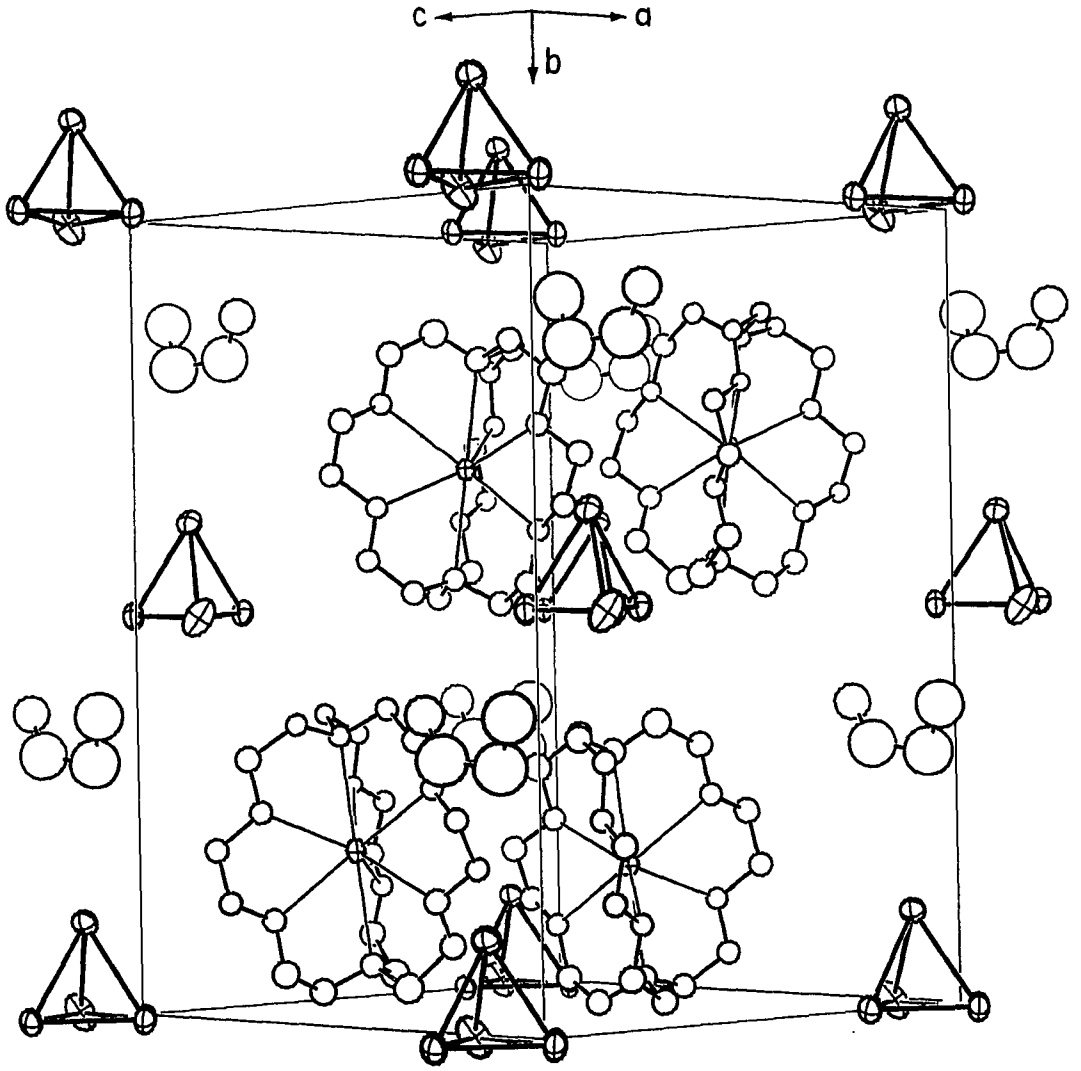

Figure 2. Approximate [101] view of the unit cell of $(2,2,2\text{-crypt-}K^{+})_2$ - $Pb_2Sb_2^{2-}\cdot en$. (Note the origin position relative to Figure 1.) Thermal ellipsoids are drawn at the 30% probability level

$Sn_2Bi_2^{2-}$ structure, the shortest contact is for SnBi4-CEN1 at 4.1 (2) Å, and there are perhaps shorter distances to crypt carbon atoms such as SnBi2-C12 at 3.99 (4) Å. In the $Pb_2Sb_2^{2-}$ structure the shortest distance is PbSb1-NEN1 at 3.87 (8) Å, but this is not significantly shorter than distances to crypt carbons such as PbSb2-C12 at 3.96 (4) Å, where hydrogen may also be important. The 2,2,2-crypt-K^+ cations in both structures have conformations comparable to those in other crypt structures, with the potassium atoms more or less centrally located along the N-N axes.

The interesting features of the two structures are the ditindibismuthide(2-) and dileaddiantimonide(2-) anions, shown in Figure 3. Since the atoms within $Sn_2Bi_2^{2-}$ are disordered 50:50, the observed cluster geometry represents merely a mean configuration; each bond distance should be an average of one Sn-Sn, one Bi-Bi and four Sn-Bi distances. The cluster found is substantially tetrahedral with bond distances ranging from 2.934 (3) to 2.971 (6) Å, with an average of 2.957 Å, and bond angles which vary from 59.3 (4)° to 60.6 (1)° (see Table 12). The SnBi1-SnBi3 distance of 2.934 (3) Å is significantly shorter than the other five, possibly implying greater than average Sn-Sn character. In spite of the positional disorder, the thermal parameters of the atoms are quite normal for this type of structure except for SnBi1 which is elongated in a direction approximately tangent to the sphere of the cluster; presumably this arises from poor overlap of the positionally disordered atoms on this site.

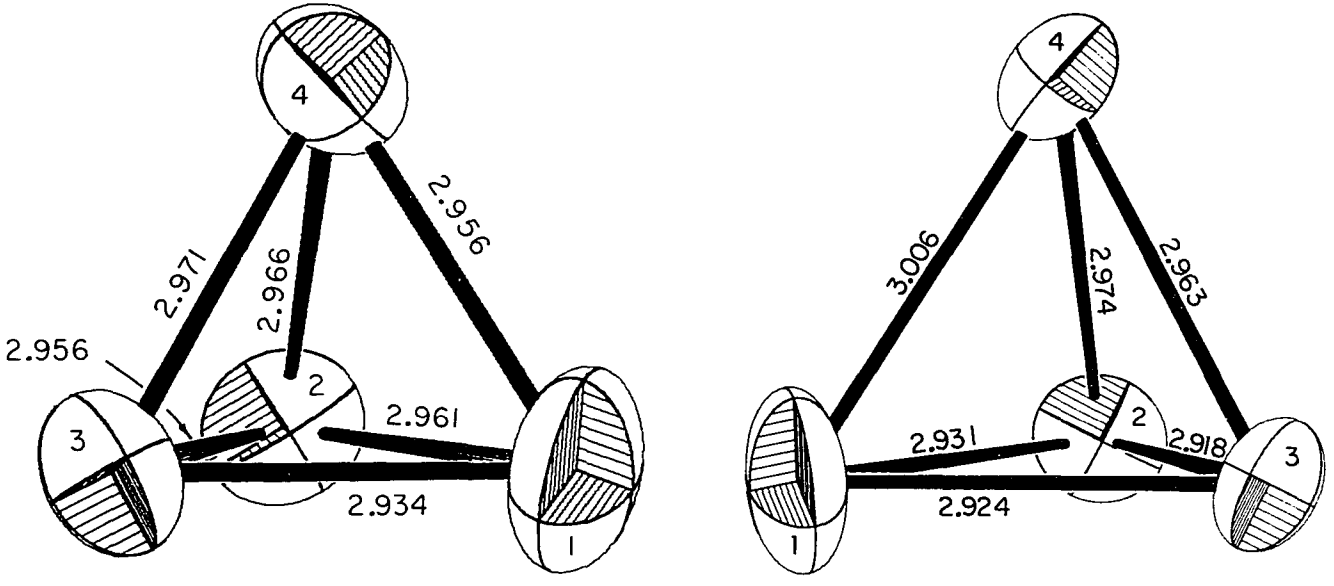

Figure 3. The $Sn_2Bi_2^{2-}$ (left) and $Pb_2Sb_2^{2-}$ (right) anions, with b approximately vertical

Table 12. Distances and angles in $Sn_2Bi_2^{2-}$ and $Pb_2Sb_2^{2-}$

Distances, Å		
Atoms	$Sn_2Bi_2^{2-}$	$Pb_2Sb_2^{2-}$
1 - 2	2.961 (3)	2.931 (3)
1 - 3	2.934 (3)	2.924 (2)
1 - 4	2.956 (5)	3.006 (4)
2 - 3	2.956 (3)	2.918 (3)
2 - 4	2.966 (6)	2.974 (5)
3 - 4	2.971 (6)	2.963 (5)

Angles, deg		
Atoms	$Sn_2Bi_2^{2-}$	$Pb_2Sb_2^{2-}$
2 - 1 - 3	60.20 (7)	59.79 (6)
2 - 1 - 4	60.17 (12)	60.10 (10)
3 - 1 - 4	60.58 (12)	59.95 (10)
1 - 2 - 3	59.45 (7)	59.98 (6)
1 - 2 - 4	59.84 (9)	61.20 (7)
3 - 2 - 4	60.22 (13)	60.39 (11)
1 - 3 - 2	60.35 (7)	60.23 (6)
1 - 3 - 4	60.08 (8)	61.41 (7)
2 - 3 - 4	60.06 (13)	60.74 (11)
1 - 4 - 2	59.99 (12)	58.70 (9)
1 - 4 - 3	59.34 (12)	58.65 (9)
2 - 4 - 3	59.72 (13)	58.88 (10)

The average bond length of 2.957 Å for $Sn_2Bi_2^{2-}$ compares well with what one would expect for a Sn-Bi bond. The only known bismuth polyanion is Bi_4^{2-} [12] with an average distance of 2.938 Å, but since the Bi-Bi bond order is 1.25 this is not directly comparable. The cationic species Bi_9^{5+} [61] has an average bond length of 3.14 Å but all atoms exhibit higher connectivity. A reasonable value of 2.972 Å for a Bi-Bi single bond can be obtained by estimating the average bond length for a hypothetical "Bi_7^{3-}" anion based on the known values for Bi_4^{2-}, Sb_4^{2-} (2.750 Å),[23] and Sb_7^{3-} (2.782 Å).[24] For a Sn-Sn bond, several polytin reference anions are known, including Sn_9^{4-} with an average bond length of 3.02 Å[21] and "Sn_4^{4-}" (isolated tetrahedra in the intermetallic phase KSn) with a distance of 2.98 Å.[39] The average distance of 2.942 Å for Sn_5^{2-} [19] is probably the better estimate as this anion is more similar to $Sn_2Bi_2^{2-}$. This would imply that the Bi-Bi and Sn-Sn bond distances are nearly identical, which is in part borne out by the observed positional disorder, but these values are somewhat deceptive. Using only the average distance in the base of the "Bi_7^{3-}" anion (3.053 Å) and only the axial-equatorial distance in Sn_5^{2-} (2.866 Å) probably gives the best estimates for Bi-Bi and Sn-Sn bonds in the $Sn_2Bi_2^{2-}$ cluster, as these distances involve constrained triply-bonded atoms. In either case, the Sn-Bi bond is estimated at 2.96 Å, which agrees very well with observation.

It is interesting that the $Pb_2Sb_2^{2-}$ anion does show some preference in orientation, and the cluster correspondingly exhibits a wider range of bond distances and angles. PbSb1-PbSb4 is significantly longer than the others, as expected for the bond length with the most Pb-Pb character

according to occupation refinement. The bond with the most Sb-Sb character (PbSb2-PbSb3) is the shortest, but not significantly. This $Pb_2Sb_2^{2-}$ anion does remarkably resemble $Sn_2Bi_2^{2-}$; both anions have longer distances in general to atom 4 and a very similar elongation of the thermal ellipsoid of atom 1. It is probable that these effects arise from the crystal packing of the crypt cations.

Bond lengths for Pb-Pb and Sb-Sb in this cluster can be estimated from the Pb_5^{2-} [19] and Sb_7^{3-} [24] anions as before. Using the average of all distances, the values are 3.081 Å and 2.782 Å, while using the axial-equatorial lengths from Pb_5^{2-} and the basal distances from Sb_7^{3-} gives 3.002 Å and 2.858 Å, respectively. Either way, a Pb-Sb bond is estimated to be 2.93 Å, which compares well with the average distance of 2.953 Å observed for $Pb_2Sb_2^{2-}$.

The $Sn_2Bi_2^{2-}$ and $Pb_2Sb_2^{2-}$ anions, though ideally C_{2v} clusters, are the first heteroatomic members of the 20-electron tetrahedral family which includes P_4, As_4, Sb_4, Ge_4^{4-}, Sn_4^{4-}, and Pb_4^{4-}.[15] (The latter three occur as isolated tetrahedra in intermetallic Zintl phases, but the formal 4- charge is derived only for complete electron transfer from the alkali metal to the cluster, which is not entirely plausible.) MO treatments and rationalizations of the bonding for such 20-electron tetrahedra are well known.[62,15,29] In contrast, the isoelectronic $Tl_2Te_2^{2-}$ has a butterfly or folded diamond configuration with Tl atoms at the fold and is derived most easily from a D_{2h} square planar geometry. This is energetically more favorable than a tetrahedral configuration which would formally partition the charge to give positive and large

negative charges on Te and Tℓ, respectively.[27] The $Sn_2Bi_2^{2-}$ or $Pb_2Sb_2^{2-}$ anions by comparison can be credibly represented by a localized valence bond cluster with negative formal charges on the tin or lead atoms. A similar folded diamond shape for $Sn_2Bi_2^{2-}$ or $Pb_2Sb_2^{2-}$ would be less favorable energetically as it would reduce the number of bonds and not allow the considerable delocalization of charge that the tetrahedral geometry does.

Wilson reports that an appropriate ^{119}Sn solution NMR signal for $Sn_2Bi_2^{2-}$ is observed upon reaction of LiSnBi or NaSnBi with ethylenediamine or reaction of KSn_2 and K_3Bi_2 with 2,2,2-crypt in ethylenediamine.[63] He has similarly "identified" the Sn_8Bi^{3-} and Sn_8Sb^{3-} anions[63] (although at least in the latter case the relative intensities may as easily be indicative of nine tin atoms[33]), but both the charge assignment and number of Bi or Sb atoms are speculative. Our investigations also indicate the possibility of other new heteroatomic anions from group IV and V elements; it is not unlikely that they may also represent new configurations.

The Sb_4^{2-} and Sb_7^{3-} Structures

The final positional and thermal parameters for all atoms in $(2,2,2\text{-crypt-}K^+)_2Sb_4^{2-}$ and $(2,2,2\text{-crypt-}K^+)_3Sb_7^{3-}\cdot 2en$ are listed in Tables 13 and 14, respectively. Characteristic distances and angles for the Sb_4^{2-} anion are given later in Table 15, while those for the Sb_7^{3-} anion together with comparable values from the crypt-Na^+ salt are given later in Table 16. Remaining distances and angles for the crypt cations and en molecules are listed in Appendix A. The observed and

Table 13. Positional and thermal parameters for (2,2,2-crypt-K)$_2$Sb$_4$

Atom	x	y	z	B11	B22	B33	B12	B13	B23
Sb1	0.18408(6)	0.86645(7)	0.00182(6)	5.16(3)	6.52(4)	6.60(4)	-1.64(3)	0.41(3)	1.39(3)
Sb2	0.02067(6)	0.06419(6)	0.85552(6)	6.32(4)	6.50(4)	5.37(4)	-2.67(3)	0.47(2)	1.40(3)
K	0.3232(2)	0.3242(1)	0.4082(1)	5.16(7)	4.08(7)	3.58(6)	-2.11(6)	1.06(5)	-0.09(5)
O3[a]	0.0967(8)	0.3211(10)	0.2767(6)	7.9(4)	12.9(6)	4.4(3)	-6.3(4)	0.9(3)	-1.6(3)
O13	0.3303(8)	0.5186(6)	0.2866(5)	12.7(5)	5.8(3)	3.6(2)	-4.9(3)	0.9(3)	0.8(2)
O23	0.5212(8)	0.1058(6)	0.2865(5)	8.2(4)	6.1(3)	4.4(3)	-1.7(3)	2.8(3)	-1.2(2)
O6	0.1732(5)	0.2568(6)	0.5262(5)	3.9(2)	5.7(3)	6.3(3)	-2.2(2)	0.6(2)	0.8(2)
O16	0.5644(5)	0.1774(5)	0.5371(5)	4.7(2)	3.7(2)	5.6(3)	-1.4(2)	1.2(2)	-0.1(2)
O26	0.2691(5)	0.5615(5)	0.5343(5)	5.5(2)	4.4(2)	4.5(2)	-2.7(2)	1.0(2)	0.2(2)
N0	0.3026(9)	0.3043(8)	0.1372(6)	9.2(5)	6.7(4)	4.1(3)	-4.6(4)	1.2(3)	-0.2(3)
N9	0.3426(6)	0.3463(6)	0.6817(5)	5.4(3)	4.1(3)	4.0(3)	-1.9(2)	1.4(2)	0.3(2)
C21	0.4102(18)	0.1831(16)	0.0937(11)	13.6(11)	10.3(9)	4.7(5)	0.4(8)	1.5(6)	-1.8(5)
C4	0.0814(11)	0.2242(13)	0.3294(13)	6.4(5)	8.2(7)	9.8(8)	-2.7(5)	-1.3(5)	-2.6(6)
C14	0.2399(9)	0.6413(9)	0.3395(9)	6.3(4)	5.9(4)	6.9(5)	-2.8(4)	0.2(4)	2.3(4)
C24	0.6455(13)	0.0857(11)	0.3401(11)	9.0(7)	7.9(6)	7.4(6)	-4.5(5)	4.9(5)	-2.8(5)
C5	0.0567(10)	0.2590(13)	0.4544(11)	6.4(5)	11.2(8)	8.1(6)	-5.8(5)	-2.7(4)	4.4(6)
C15	0.2846(10)	0.6500(7)	0.4728(8)	7.5(5)	3.7(3)	6.3(4)	-2.7(3)	2.3(4)	0.2(3)
C25	0.6544(9)	0.0627(9)	0.4697(10)	5.0(4)	4.5(4)	8.5(6)	-0.5(3)	1.0(4)	-1.3(4)
C7	0.1467(9)	0.3058(10)	0.6514(8)	5.7(4)	6.8(5)	5.3(4)	-3.0(4)	1.4(3)	0.5(3)
C17	0.3088(9)	0.5695(8)	0.6609(8)	6.6(4)	5.0(4)	4.6(4)	-2.6(3)	1.5(3)	-1.0(3)
C27	0.5702(8)	0.1587(8)	0.6606(8)	5.4(4)	4.1(3)	6.1(4)	-1.3(3)	0.3(3)	0.5(3)
C8	0.2802(9)	0.2755(9)	0.7219(7)	6.8(4)	6.4(4)	4.3(3)	-3.7(4)	1.1(3)	0.9(3)
C18	0.2741(9)	0.4856(8)	0.7250(7)	6.7(4)	4.8(4)	4.3(3)	-2.4(3)	2.0(3)	-0.8(3)
C28	0.4835(8)	0.2890(8)	0.7293(7)	5.1(4)	5.7(4)	4.2(3)	-2.1(3)	0.1(3)	0.0(3)

[a] The last digit identifies the position along the crypt chain, the first digit (O (missing), 1 or 2) identifies the chain.

Table 13. Continued

Atom	x	y	z	B	Atom	x	y	z	B
C1a[b]	0.200(2)	0.278(2)	0.086(2)	5.7(4)	C2b	0.113(2)	0.257(3)	0.155(2)	8.0(5)
C1b	0.156(3)	0.343(3)	0.097(2)	7.5(5)	C12a	0.358(2)	0.490(2)	0.154(2)	6.6(4)
C11a	0.282(2)	0.425(2)	0.093(2)	5.2(3)	C12b	0.262(2)	0.533(2)	0.158(2)	6.9(4)
C11b	0.357(3)	0.386(2)	0.101(2)	7.0(4)	C22a	0.482(2)	0.094(2)	0.148(2)	7.1(4)
C2a	0.075(2)	0.350(2)	0.145(2)	7.2(4)	C22b	0.542(2)	0.123(2)	0.167(2)	6.8(4)

[b] a and b denote the disordered pairs of carbon atoms at 0.50 occupancy.

Table 14. Positional and thermal parameters for $(2,2,2\text{-crypt-K})_3Sb_7 \cdot 2en$

Atom	x	y	z	B11	B22	B33	B12	B13	B23
Sb1	0.31262(9)	0.15894(6)	0.79123(9)	2.85(6)	2.91(6)	3.88(6)	0.12(5)	0.48(5)	-0.29(5)
Sb2	0.36995(9)	0.24997(7)	0.66639(10)	2.90(6)	4.69(7)	3.72(6)	-0.69(5)	0.82(5)	-0.17(5)
Sb3	0.20155(9)	0.18220(6)	0.60189(9)	3.59(6)	3.25(6)	3.20(6)	-0.67(5)	0.44(5)	-0.97(5)
Sb4	0.23242(10)	0.22837(6)	0.92250(9)	4.14(7)	3.60(7)	3.28(6)	-0.14(5)	0.74(5)	-0.10(5)
Sb5	0.31312(10)	0.35957(7)	0.74188(10)	4.00(7)	3.56(7)	4.57(7)	-1.47(6)	0.06(5)	-0.25(5)
Sb6	0.05935(9)	0.25747(6)	0.63954(10)	2.66(6)	3.19(6)	4.36(7)	-0.56(5)	0.08(5)	0.06(5)
Sb7	0.15470(9)	0.32173(6)	0.80308(10)	3.63(6)	2.95(6)	3.75(6)	-0.16(5)	0.71(5)	-0.45(5)
K1	0.8189(3)	0.0255(2)	0.8112(3)	3.3(2)	2.2(2)	2.8(2)	-0.3(1)	0.2(1)	0.0(1)
K2	0.2790(3)	0.4783(2)	0.3173(3)	3.8(2)	2.6(2)	3.0(2)	-0.3(2)	1.0(1)	-0.1(1)
K3	0.7745(3)	0.3084(2)	0.0782(3)	2.6(2)	2.5(2)	2.9(2)	-0.3(1)	0.3(1)	-0.3(1)
N100[a]	0.0264(10)	0.9632(7)	0.3033(11)	3.1(8)	4.2(9)	4.0(8)	-0.6(6)	-0.4(6)	1.1(7)
N109	0.3386(11)	0.9871(7)	0.0726(11)	4.2(8)	3.6(8)	4.0(8)	1.9(7)	0.9(6)	0.4(6)
O103	0.1003(8)	0.0851(6)	0.2630(8)	3.6(6)	3.4(6)	3.0(6)	-0.3(5)	1.2(5)	-0.5(5)
O106	0.2660(9)	0.0891(5)	0.1811(9)	4.2(6)	2.7(6)	3.8(6)	-0.8(5)	0.7(5)	-0.2(5)
O112	0.0231(10)	0.9144(6)	0.0985(9)	6.6(8)	4.6(7)	3.4(6)	-3.1(7)	-1.9(6)	1.3(6)
O115	0.1575(12)	0.9402(6)	0.9807(10)	9.2(11)	2.9(7)	4.5(7)	-1.8(7)	-0.5(7)	-0.4(6)
O120	0.2097(8)	0.9100(5)	0.3680(8)	2.9(6)	3.3(6)	3.5(6)	-0.1(5)	0.7(5)	0.5(5)
O123	0.3424(8)	0.9028(6)	0.2396(8)	3.0(6)	3.7(6)	2.9(6)	0.2(5)	1.2(4)	0.7(5)
N200	0.3506(10)	0.3742(6)	0.2053(10)	3.4(7)	2.1(7)	3.8(7)	-0.5(6)	0.9(6)	-0.9(6)
N209	0.2120(15)	0.5829(8)	0.4348(12)	9.3(13)	3.3(9)	4.2(9)	0.1(9)	1.9(9)	-0.5(7)
O203	0.2280(9)	0.3566(6)	0.3519(8)	4.3(6)	3.2(6)	2.9(6)	-1.4(5)	0.1(5)	-0.1(5)
O206	0.1979(10)	0.4558(6)	0.4782(9)	6.7(8)	3.4(6)	3.0(6)	-0.8(6)	1.9(6)	-0.3(5)
O212	0.2218(8)	0.4684(6)	0.1116(8)	3.5(6)	4.1(7)	3.0(6)	-0.4(5)	-0.1(5)	0.7(5)
O215	0.1289(10)	0.5496(7)	0.2278(11)	5.9(8)	5.2(8)	6.4(9)	3.0(7)	1.9(7)	1.9(7)
O220	0.4749(9)	0.4679(6)	0.3160(10)	3.5(7)	4.5(7)	5.7(8)	-2.3(6)	0.9(6)	0.2(6)

[a] The first digit refers to the crypt, the latter two to the position within the crypt.

Table 14. Continued

Atom	x	y	z	B11	B22	B33	B12	B13	B23
O223	0.4036(12)	0.5779(6)	0.3874(11)	9.6(11)	3.2(7)	6.9(9)	-3.3(7)	3.3(8)	-2.7(6)
N300	0.0484(9)	0.6845(7)	0.7874(10)	2.2(6)	3.6(8)	2.7(7)	-0.2(6)	0.0(5)	0.2(6)
N309	0.3976(10)	0.6990(7)	0.0565(10)	2.3(7)	3.5(8)	3.4(7)	-0.1(6)	-0.1(5)	0.2(6)
O303	0.1581(8)	0.5741(5)	0.8464(8)	3.1(6)	3.0(6)	3.1(6)	-0.4(5)	-0.1(4)	-1.5(5)
O306	0.3475(8)	0.5874(6)	0.9286(8)	3.9(6)	3.2(6)	3.1(6)	0.1(5)	0.1(5)	-0.1(5)
O312	0.2092(8)	0.7480(6)	0.7374(9)	3.5(6)	4.2(7)	3.5(6)	-0.9(5)	0.7(5)	0.5(5)
O315	0.3570(9)	0.7797(6)	0.8900(9)	4.1(7)	3.9(7)	4.2(7)	-0.8(5)	1.0(5)	0.5(5)
O320	0.0637(8)	0.7410(5)	0.9851(8)	3.0(6)	1.9(5)	3.3(6)	-0.8(4)	0.8(4)	-0.1(4)
O323	0.2219(7)	0.7182(5)	0.1254(8)	2.9(5)	2.2(5)	2.5(5)	-0.3(4)	0.5(4)	-0.6(4)

Atom	x	y	z	B	Atom	x	y	z	B
C101	0.980(1)	0.0247(10)	0.309(2)	4.8(5)	C219	0.504(2)	0.4275(11)	0.242(2)	5.5(5)
C102	0.050(1)	0.0762(10)	0.340(2)	4.5(4)	C221	0.521(2)	0.5256(10)	0.316(2)	4.9(5)
C104	0.168(1)	0.1338(9)	0.288(1)	3.4(4)	C222	0.500(2)	0.5660(11)	0.399(2)	5.5(5)
C105	0.214(1)	0.1427(9)	0.200(1)	3.6(4)	C224	0.380(2)	0.6176(15)	0.466(2)	8.5(8)
C107	0.316(1)	0.0988(10)	0.103(1)	4.5(4)	C225	0.278(2)	0.6344(14)	0.437(2)	8.3(8)
C108	0.385(2)	0.0472(11)	0.102(2)	5.9(5)	C301	0.010(1)	0.6233(8)	0.791(1)	3.0(4)
C110	0.957(1)	0.9182(10)	0.248(1)	4.4(4)	C302	0.080(1)	0.5704(10)	0.769(1)	4.2(4)
C111	0.938(2)	0.9266(12)	0.137(2)	5.9(6)	C304	0.228(1)	0.5312(9)	0.822(1)	4.0(4)
C113	0.005(2)	0.9068(12)	0.993(2)	6.6(6)	C305	0.304(1)	0.5292(9)	0.911(1)	4.1(4)
C114	0.087(2)	0.8938(12)	0.957(2)	6.2(6)	C307	0.421(1)	0.5861(9)	0.012(1)	3.8(4)
C116	0.242(2)	0.9319(11)	0.935(2)	5.5(5)	C308	0.464(1)	0.6505(9)	0.030(1)	3.4(4)
C117	0.306(2)	0.9840(11)	0.968(2)	5.2(5)	C310	0.060(1)	0.6990(10)	0.685(1)	4.2(4)
C118	0.061(1)	0.9424(10)	0.403(1)	4.2(4)	C311	0.116(1)	0.7584(10)	0.683(1)	4.4(4)
C119	0.128(1)	0.8897(9)	0.402(1)	4.1(4)	C313	0.265(1)	0.8007(10)	0.735(1)	4.3(4)
C121	0.278(1)	0.8637(9)	0.375(1)	3.4(4)	C314	0.363(1)	0.7905(10)	0.791(2)	4.6(5)
C122	0.363(1)	0.8877(10)	0.340(1)	4.4(4)	C316	0.447(1)	0.7774(9)	0.948(1)	3.9(4)
C124	0.426(1)	0.9261(10)	0.209(2)	4.6(5)	C317	0.441(1)	0.7598(9)	0.052(1)	3.3(4)

Table 14. Continued

Atom	x	y	z	B	Atom	x	y	z	B
C125	0.404(2)	0.9344(10)	0.099(2)	5.0(5)	C318	0.983(1)	0.7317(8)	0.821(1)	3.2(4)
C201	0.302(1)	0.3175(9)	0.221(1)	4.2(4)	C319	0.975(1)	0.7270(9)	0.929(1)	3.4(4)
C202	0.292(1)	0.3099(9)	0.329(1)	4.1(4)	C321	0.058(1)	0.7401(9)	0.088(1)	3.5(4)
C204	0.214(2)	0.3478(11)	0.452(2)	5.1(5)	C322	0.150(1)	0.7592(8)	0.149(1)	3.1(4)
C205	0.151(2)	0.3992(11)	0.481(2)	5.6(5)	C324	0.308(1)	0.7319(9)	0.186(1)	3.5(4)
C207	0.155(2)	0.5026(12)	0.532(2)	6.2(6)	C325	0.381(1)	0.6909(9)	0.157(1)	3.5(4)
C208	0.219(2)	0.5607(12)	0.536(2)	5.9(6)	NEN1	0.300(2)	0.0356(12)	0.482(2)	8.9(6)
C210	0.331(1)	0.3871(9)	0.099(1)	3.6(4)	CEN1	0.366(2)	0.0184(14)	0.571(2)	7.6(7)
C211	0.234(1)	0.4080(10)	0.065(2)	4.6(5)	CEN2	0.303(2)	0.9778(13)	0.633(2)	7.3(7)
C213	0.129(1)	0.4925(10)	0.076(2)	4.6(5)	NEN2	0.366(2)	0.9657(11)	0.725(2)	7.5(6)
C214	0.120(2)	0.5555(11)	0.128(2)	5.1(5)	NEN3	0.434(2)	0.0859(11)	0.353(2)	7.6(6)
C216	0.113(2)	0.6086(13)	0.275(2)	7.3(7)	NEN4	0.529(2)	0.2354(11)	0.453(2)	8.3(6)
C217	0.119(2)	0.5994(13)	0.388(2)	7.3(7)	CEN3	0.441(3)	0.168(2)	0.371(3)	11.2(10)
C218	0.449(1)	0.3669(10)	0.240(2)	4.5(5)	CEN4	0.517(3)	0.157(2)	0.423(3)	14.0(13)

calculated structure factors for the two compounds have been deposited in reference 23.

The Sb_4^{2-} salt is indeed isostructural with $(2,2,2\text{-crypt-}K^+)_2Bi_4^{2-}$.[12] The drawing of the unit cell presented in Figure 4 demonstrates the pseudohexagonal close-packing of the ions. It is amazing how similar the disorder of the α- and β-carbon atoms is in the two compounds, in spite of the smaller size of the Sb_4^{2-} anion, supporting the conclusion that the disorder is real and correctly treated. This disorder represents a choice of whether the conformations of the N-Cα-Cβ fragments at the two ends of each crypt chain are placed in an essentially eclipsed (a) or crossed (b) manner when viewed down the N-K-N axis, the latter being the normal configuration for 2,2,2-crypt-K^+ salts. The disordered end of the crypt does have the closer interactions with the anion, which undoubtedly influences this behavior.

The most interesting aspect of the structure is the tetra-antimonide(2-) anion, Sb_4^{2-}. It is truly square planar (D_{4h}), Figure 5 and Table 15, although the point symmetry is only required to be C_i. As with Bi_4^{2-} and Te_4^{2+}, the MO diagram implies a bond order of 1.25, with four bonding levels (a_{1g}, b_{2g}, e_u, a_{2u}) and one nonbonding (actually slightly antibonding) level (e_g) accommodating the 14 skeletal electrons.[12] The average Sb-Sb bond distance of 2.750 Å is significantly shorter than that in Sb_7^{3-}, 2.797 Å.

It is odd that the Sb_4^{2-} anion was never found in earlier studies of Na-Sb binary alloy reactions with crypt, in spite of the fact that alloy compositions ranging from NaSb to $NaSb_3$ were investigated; rather

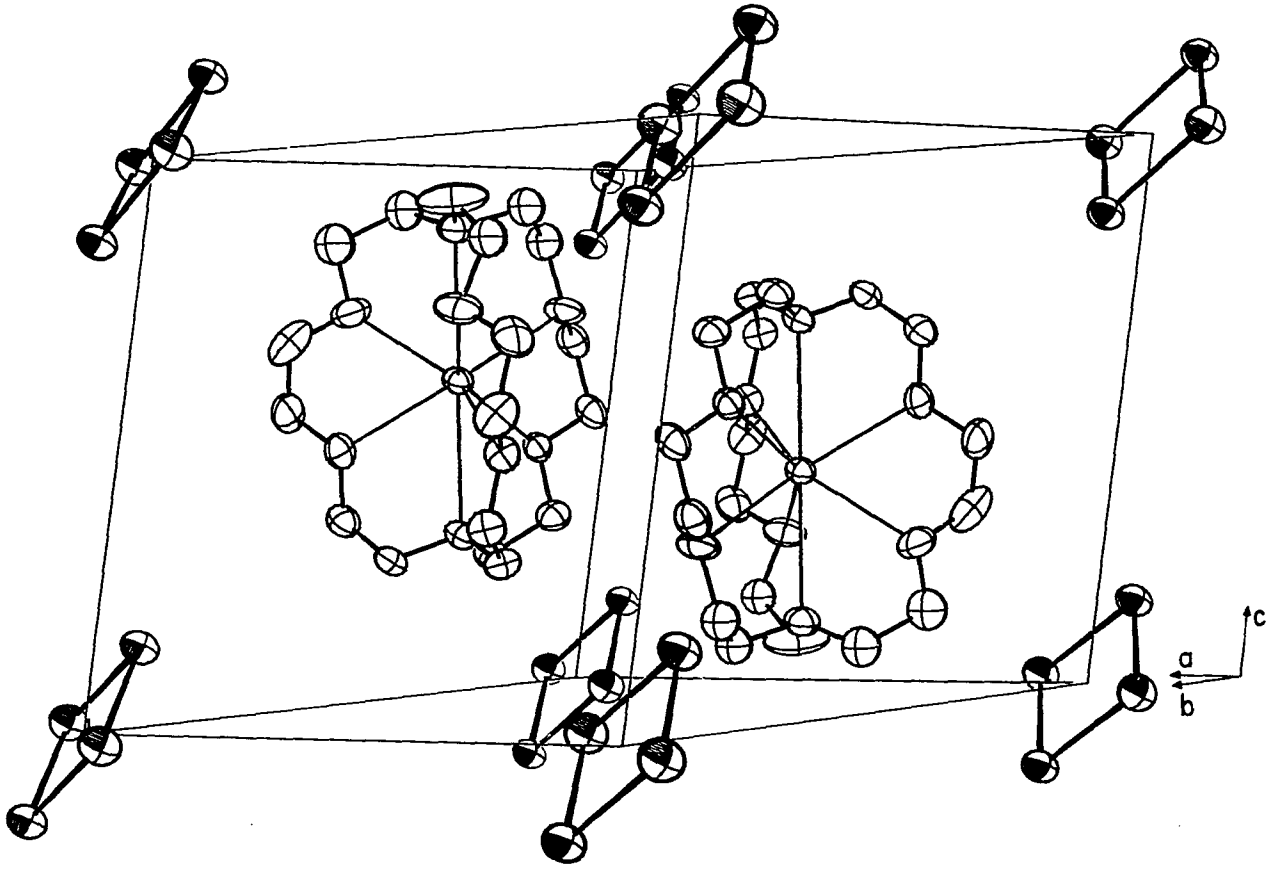

Figure 4. Approximate $[1\bar{1}0]$ view of the unit cell of $(2,2,2\text{-crypt-}K^+)_2Sb_4^{2-}$ with thermal ellipsoids at the 30% probability level. For clarity, only one consistent set (b) of the disordered carbon atoms is shown

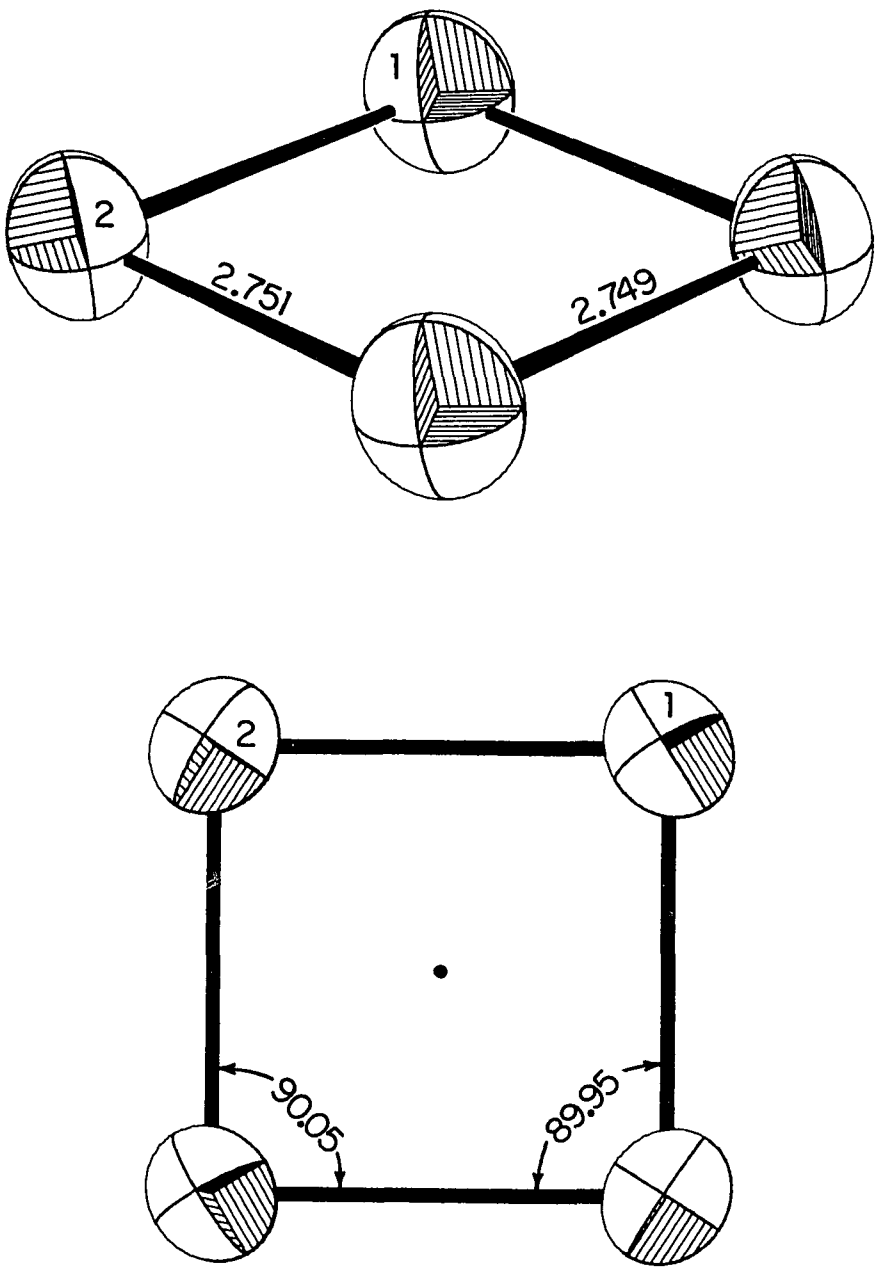

Figure 5. Two views of the Sb_4^{2-} anion

Table 15. Distances and angles for Sb_4^{2-}

Atom 1	Atom 2	d, Å	Atoms	Angle, deg
Sb1	Sb2	2.749 (1)	1-2-1'	89.95 (3)
Sb1	Sb2'	2.751 (1)	2-1-2'	90.05 (3)
Sb1	Sb1'	3.888 (1)		
Sb2	Sb2'	3.891 (1)		

$(2,2,2\text{-crypt-}Na^+)_3Sb_7^{3-}$ was the only product.[24] However, all the ternary alloys KGeSb, KAuSb, and KPbSb demonstrate facile formation of Sb_4^{2-}. Although binary K-Sb alloys have not been investigated, presumably Sb_4^{2-} could be readily produced from these as well unless the ternary alloys serve in some unusual way as reducing agents. There is a cell volume decrease expected on switching from crypt-K^+ to crypt-Na^+ cations (approximately 30 $Å^3$ per crypt) which may destabilize the smaller anion. More likely, the growth conditions used for the Na-Sb reactions, namely solvent evaporation after a few days, may have been inadequate for formation of Sb_4^{2-} crystals which spontaneously precipitate over longer periods.

The unit cell for $(2,2,2\text{-crypt-}K^+)_3Sb_7^{3-}\cdot 2en$ bears no obvious resemblance to that of the previously known $(2,2,2\text{-crypt-}Na^+)_3Sb_7^{3-}$ salt.[24] Instead, the present phase's large volume (722 $Å^3$/crypt) and close similarity in dimensions to other cells containing six crypt-K^+ ions such as $(2,2,2\text{-crypt-}K^+)_3(T\ell Sn_8^{3-}T\ell Sn_9^{3-})_{½}\cdot en$[28] led to an expectation

of a nine-atom cluster. The packing of the ions in the unit cell is indeed similar (compare Figure 6 with later Figure 8), with the center of the anion and the three independent potassium atoms in essentially the same positions as in the Tℓ/Sn salt although the N-K-N axes of the cations are oriented in different directions. The extra solvent molecule compensates for the smaller Sb_7^{3-} anion. The 2,2,2-crypt-K^+ cations in this structure have normal conformations, with the potassium centrally located along the N-N axis. However, crypt 3 is unusually symmetrical, with somewhat shorter than normal K-N bonds (∿2.90 Å compared to ∿3.00 Å in the other two crypts) and with a very narrow range of K-O bond lengths.

This structure is very well behaved, with small thermal parameters originating from both the low temperature of the data collection and the good quality of the crystal; even the en solvent molecules show none of the usual disorder and have well-defined z-shaped conformations. Consequently, the standard deviations for the bond distances are generally about half those observed for the crypt-Na^+ salt (see Table 16). The hepta-antimonide(3-) anion depicted in Figure 7 has an approximate C_{3v} configuration, analogous to the isoelectronic P_7^{3-} [64], As_7^{3-} [65] and P_4S_3 [66] species which all exhibit a similar variance in distances for the three types of bond lengths.[67] It is interesting that the anion chooses to be distorted somewhat from C_{3v} symmetry in that the Sb2-Sb3 bond distance is significantly shorter than Sb1-Sb2 and Sb2-Sb3 in the triangular base, and Sb5-Sb7 is shorter than Sb4-Sb7 and Sb6-Sb7 to the trigonal apex. There is one fairly short contact to a crypt carbon, Sb5-C221 at 3.71 Å, which may be pertinent to the latter difference.

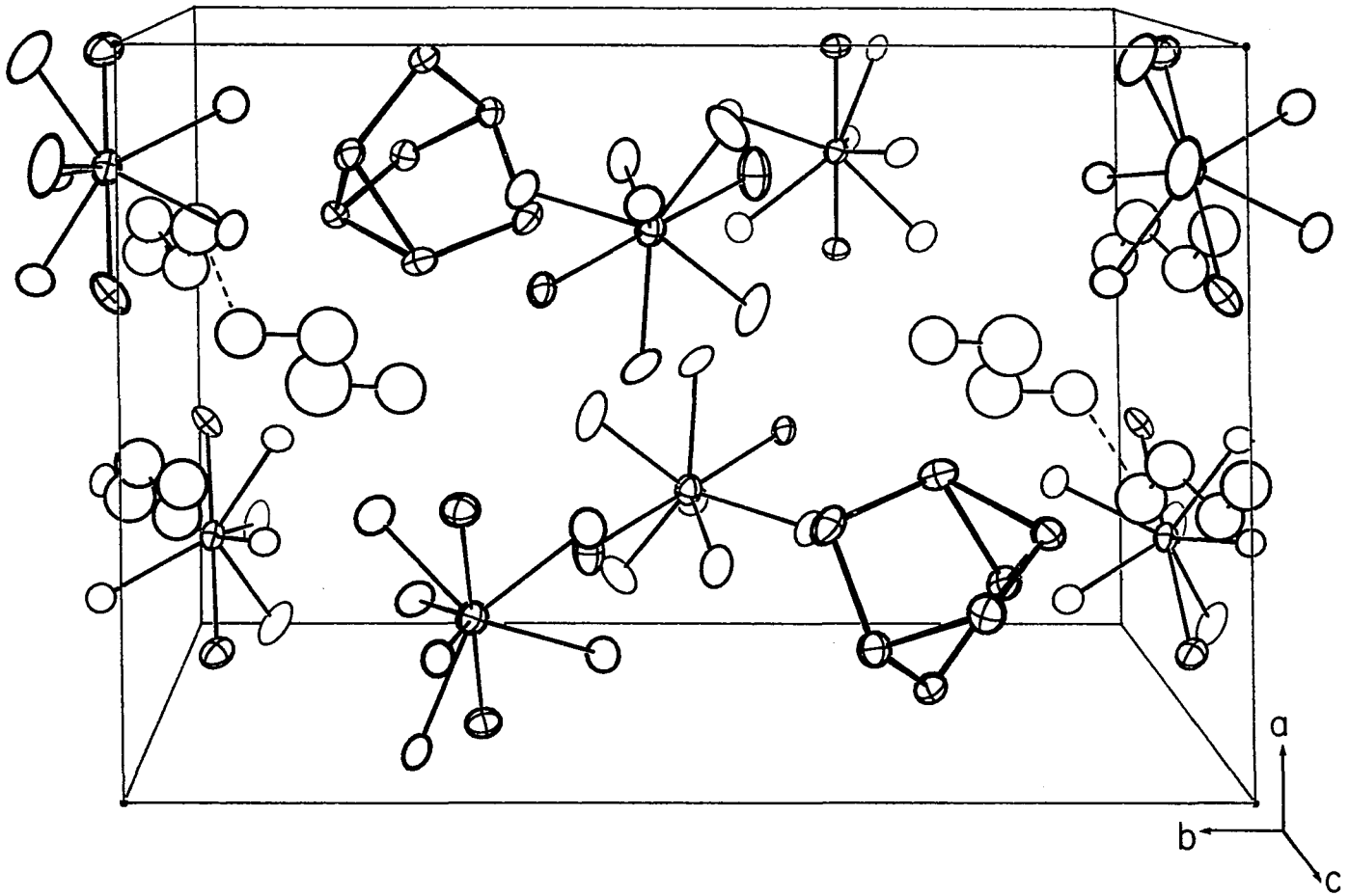

Figure 6. Approximate [00$\bar{1}$] view of the unit cell of (2,2,2-crypt-K^+)$_3Sb_7^{3-}$•2en. For clarity, crypt carbon atoms are not included, and the N-K-N axes are differentiated. The dashed lines indicate H-bonding

Table 16. Comparative distances and angles for Sb_7^{3-} anions in $(2,2,2\text{-crypt-}K^+)_3Sb_7^{3-}\cdot 2en$ and $(2,2,2\text{-crypt-}Na^+)_3Sb_7^{3-}$

Distances, Å					
Sb atoms	K^+ salt[a]	Na^+ salt[b]	Sb atoms	K^+ salt	Na^+ salt
1-2	2.906 (2)	2.856 (4)	6-7	2.785 (2)	2.776 (4)
1-3	2.904 (2)	2.880 (4)	1-7	4.207 (2)	4.210 (4)
2-3	2.876 (2)	2.838 (3)	2-7	4.180 (2)	4.159 (4)
1-4	2.717 (2)	2.693 (4)	3-7	4.159 (2)	4.209 (4)
2-5	2.735 (2)	2.706 (4)	4-5	4.183 (2)	4.313 (4)
3-6	2.728 (2)	2.711 (4)	4-6	4.359 (2)	4.253 (4)
4-7	2.782 (2)	2.824 (4)	5-6	4.345 (2)	4.397 (4)
5-7	2.741 (2)	2.755 (4)			

Angles, deg					
Sb atoms	K^+ salt	Na^+ salt	Sb atoms	K^+ salt	Na^+ salt
2-1-3	59.35 (5)	59.3 (1)	2-3-6	106.30 (6)	106.0 (1)
1-2-3	60.29 (5)	60.8 (1)	1-4-7	99.83 (6)	99.5 (1)
1-3-2	60.36 (5)	59.9 (1)	2-5-7	99.51 (6)	99.2 (1)
2-1-4	103.08 (6)	105.2 (1)	3-6-7	97.95 (6)	100.2 (1)
3-1-4	105.06 (6)	105.4 (1)	4-7-5	98.48 (6)	101.3 (1)
1-2-5	104.02 (6)	106.1 (1)	4-7-6	103.07 (6)	96.9 (1)
3-2-5	104.88 (6)	106.1 (1)	5-7-6	103.66 (6)	103.4 (1)
1-3-6	105.88 (6)	102.6 (1)			

[a]This work.
[b]Reference 24 (atom numbering has been changed to be comparable).

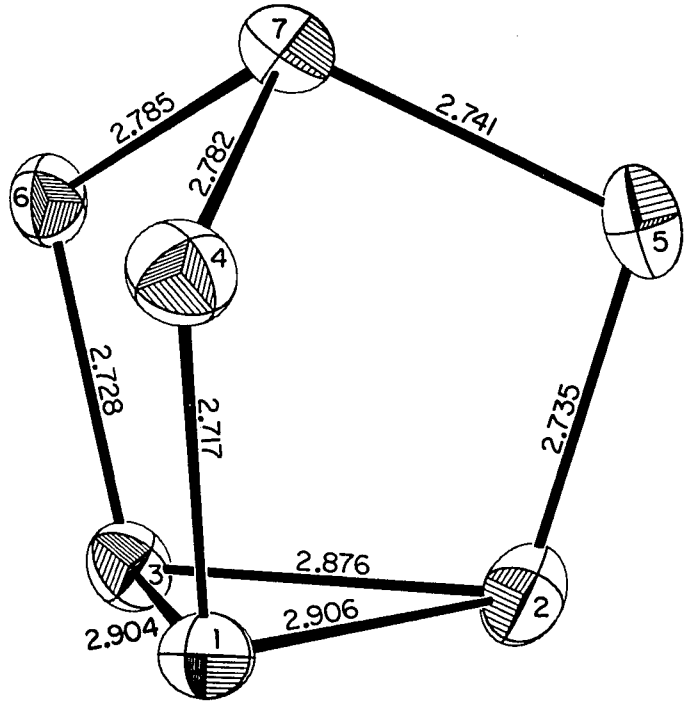

Figure 7. The Sb_7^{3-} anion, with approximate C_{3v} axis vertical

The shortest distance to an en atom is Sb3-NEN1 at 3.90 (3) Å, which is much too long to contemplate any hydrogen bond type interaction. However, there does appear to be hydrogen bonding between the two en molecules, with a NEN1-NEN3 distance of 3.10 (3) Å; the average observed distance for common N-H•••N hydrogen bonds is 3.1 Å.[68] These two nitrogen atoms are also surprisingly close to two crypt oxygens; the distances are NEN3-O106 at 3.12 (2) Å and NEN1-O120 at 3.27 (3) Å. The distortions in the Sb_7^{3-} anion found in the crypt-Na^+ salt are qualitatively somewhat similar but there are also major differences, e.g., in Sb4-Sb7. In general, comparable distances in the two clusters differ by 2 to 10σ, changes in the crystal packing of the surrounding crypt cations undoubtedly being the prime factor here. However, it is surprising that the result of the crypt-K^+ structure solution at -80° actually has the longer average Sb-Sb bond distances, 2.797 Å compared with the room temperature results for crypt-Na^+ salt of 2.782 Å.

It is clear that the presence of alloy residue during crystal growth greatly enhances the production of the homopolyatomic anions, especially for the more soluble elements. In the KPbSb reaction which produces Sb_4^{2-} and phase V (see Table 5), only small amounts of Pb are found in the products, while the heteroatomic $Pb_2Sb_2^{2-}$ anion is easily obtained from solutions decanted from the same alloy after three days. Rudolph and coworkers[34] also observed during NMR investigations of similar ternary alloy systems dissolved in en that equilibrium between anions in solution is very slow and occurs principally at the surface of the solid alloys. In the KGeSb reactions, the amount of germanium present in solution may

be insufficient to begin with; certainly when crystals were grown in the presence of alloy, no significant amount of germanium in the products was observed. A much more germanium-rich alloy is probably required in order to produce Ge-Sb heteropolyatomic anions, since Ge homoatomic anions like Ge_9^{4-} and Ge_9^{2-} [22] and perhaps any mixed anions as well are much less soluble than the polyantimony anions.

It is interesting to speculate whether the unknown Bi_7^{3-} ion can be produced. Zintl and Dullenkopf[10] reported a Bi_7^{3-} species from exhaustive extraction of bismuth-rich sodium alloys, but their analytical data are much more appropriate to the composition Bi_4^{2-}.[12] It should be noted that they also saw no evidence for Sb_4^{2-}, only Sb_3^{3-} and Sb_7^{3-}.[8,10] Reactions of various K-Bi alloys with crypt in en have produced only the Bi_4^{2-} salt, though various colored solutions have been noted in the course of the reaction.[12,44] Perhaps the use of Na-Bi alloys or an appropriate ternary composition may facilitate the isolation of a Bi_7^{3-} anion analogous to Sb_7^{3-}.

The Structure and Properties of Sn_9^{3-}

Table 17 lists the final positional and thermal parameters for $(2,2,2\text{-crypt-}K^+)_3Sn_9^{3-}\cdot 1.5en$. Distances, bond angles, and dihedral angles for the Sn_9^{3-} cluster are given in Table 18 while remaining distances and angles for the cations and en molecules are listed in Appendix A. Observed and calculated structure factors have been deposited in reference 20. The unit cell is drawn in Figure 8 and two views of the Sn_9^{3-} anion are shown in Figure 9.

Table 17. Positional and thermal parameters for $(2,2,2\text{-crypt-K})_3Sn_9 \cdot 1.5en$

Atom	x	y	z	B11	B22	B33	B12	B13	B23
Sn1	0.35928(8)	0.25828(6)	0.70553(9)	2.69(5)	5.48(7)	3.31(5)	0.12(5)	1.00(4)	0.77(5)
Sn2	0.17619(8)	0.34118(6)	0.68732(9)	3.22(5)	4.60(6)	3.30(5)	0.18(5)	0.16(4)	1.53(5)
Sn3	0.15948(9)	0.33082(7)	0.89735(9)	3.56(6)	5.60(7)	3.50(6)	0.81(5)	1.23(4)	0.71(5)
Sn4	0.34338(8)	0.24559(6)	0.91709(9)	2.87(5)	5.61(7)	3.02(5)	0.60(5)	-0.19(4)	0.87(5)
Sn5	0.18405(9)	0.21611(7)	0.57515(9)	4.17(6)	6.13(8)	3.28(6)	0.06(5)	-0.24(5)	0.35(5)
Sn6	0.06435(8)	0.23462(7)	0.72219(10)	2.64(5)	6.27(8)	4.58(6)	-0.92(5)	-0.21(4)	1.99(6)
Sn7	0.15952(9)	0.19656(7)	0.90614(10)	3.51(6)	6.62(8)	5.09(7)	0.75(5)	1.58(5)	2.90(6)
Sn8	0.24932(10)	0.15000(6)	0.74071(10)	4.99(7)	4.21(6)	4.27(6)	-0.17(5)	0.91(5)	0.50(5)
Sn9	0.33468(8)	0.36678(6)	0.85305(10)	3.19(5)	4.85(7)	4.24(6)	-0.48(5)	-0.01(5)	0.33(5)
K1	0.6831(3)	0.0134(2)	0.7295(3)	4.4(2)	3.7(2)	4.6(2)	-0.1(1)	0.8(2)	1.0(2)
K2	0.2913(2)	0.4875(2)	0.3358(3)	3.0(2)	4.6(2)	2.9(2)	0.1(1)	0.3(1)	1.1(1)
K3	0.8249(2)	0.3046(2)	0.2000(3)	2.6(1)	4.8(2)	3.0(2)	0.4(1)	0.5(1)	0.6(1)

Atom	x	y	z	B	Atom	x	y	z	B
N11[a]	0.6447(11)	0.8891(8)	0.7791(12)	4.9(3)	C21	0.154(2)	0.3406(13)	0.259(2)	8.0(7)
N12	0.7163(16)	0.1398(11)	0.6815(18)	8.6(6)	C22	0.102(2)	0.3813(12)	0.200(2)	6.8(6)
O11	0.5537(11)	0.0018(7)	0.8548(11)	6.5(3)	C23	0.063(2)	0.4886(12)	0.192(2)	7.3(6)
O12	0.5772(12)	0.1143(8)	0.7933(13)	7.3(4)	C24	0.065(2)	0.5470(12)	0.253(2)	7.0(6)
O13	0.8278(9)	0.9495(6)	0.8262(10)	5.3(3)	C25	0.164(2)	0.6315(10)	0.345(2)	5.6(5)
O14	0.8548(12)	0.0736(8)	0.8083(13)	7.4(4)	C26	0.256(1)	0.6613(10)	0.350(1)	5.0(4)
O15	0.6094(10)	0.9160(7)	0.5734(11)	6.1(3)	C27	0.307(2)	0.3167(12)	0.354(2)	6.8(6)
O16	0.6700(12)	0.0273(8)	0.5345(12)	7.2(4)	C28	0.301(2)	0.3483(15)	0.457(2)	9.5(8)
N21	0.2552(12)	0.3507(8)	0.2756(13)	5.4(4)	C29	0.340(2)	0.4365(10)	0.573(2)	5.6(5)
N22	0.3319(10)	0.6248(7)	0.4021(11)	4.2(3)	C210	0.394(1)	0.4954(10)	0.599(2)	5.1(4)
O21	0.1103(10)	0.4453(7)	0.2493(11)	5.9(3)	C211	0.394(2)	0.5956(11)	0.568(2)	6.3(5)
O22	0.1570(9)	0.5736(6)	0.2781(9)	4.6(3)	C212	0.336(2)	0.6416(11)	0.510(2)	5.8(5)
O23	0.3509(9)	0.4075(6)	0.4746(9)	4.9(3)	C213	0.290(2)	0.3293(11)	0.185(2)	6.2(5)

[a] The first digit refers to the crypt cation.

Table 17. Continued

Atom	x	y	z	B	Atom	x	y	z	B
O24	0.3484(8)	0.5376(5)	0.5366(9)	4.1(2)	C214	0.380(2)	0.3572(11)	0.184(2)	5.9(5)
O25	0.3713(9)	0.4219(6)	0.1881(10)	5.1(3)	C215	0.443(1)	0.4484(9)	0.156(1)	4.9(4)
O26	0.4228(8)	0.5452(6)	0.2618(9)	4.2(2)	C216	0.427(1)	0.5162(9)	0.165(1)	4.4(4)
N31	0.9026(11)	0.2233(7)	0.3470(11)	4.5(3)	C217	0.424(1)	0.6105(9)	0.269(1)	4.4(4)
N32	0.7456(9)	0.3879(7)	0.0541(10)	3.6(3)	C218	0.419(1)	0.6399(10)	0.372(2)	5.4(4)
O31	0.7133(9)	0.2159(6)	0.2465(9)	4.7(3)	C31	0.837(1)	0.1741(10)	0.349(2)	5.3(4)
O32	0.6342(8)	0.3020(6)	0.1302(9)	4.5(3)	C32	0.739(1)	0.1945(10)	0.339(2)	5.1(4)
O33	0.9058(9)	0.3603(6)	0.3992(9)	4.9(3)	C33	0.618(2)	0.2264(11)	0.225(2)	6.0(5)
O34	0.8537(9)	0.4337(6)	0.2516(10)	5.1(3)	C34	0.595(1)	0.2419(10)	0.122(1)	5.0(4)
O35	0 9583(8)	0.2196(6)	0.1551(9)	4.6(3)	C35	0.607(1)	0.3235(9)	0.037(1)	4.8(4)
O36	0.8649(8)	0.2848(6)	0.0089(9)	4.5(3)	C36	0.647(1)	0.3869(9)	0.046(1)	4.8(4)
C11	0.594(2)	0.8969(10)	0.861(2)	5.8(5)	C37	0.925(1)	0.2626(9)	0.445(1)	4.2(4)
C12	0.514(2)	0.9402(11)	0.846(2)	6.6(5)	C38	0.971(1)	0.3223(10)	0.451(2)	5.3(4)
C13	0.487(2)	0.0477(12)	0.851(2)	6.9(6)	C39	0.939(1)	0.4214(10)	0.406(2)	5.4(4)
C14	0.531(2)	0.1075(13)	0.868(2)	8.0(7)	C310	0.868(1)	0.4576(10)	0.355(2)	5.1(4)
C15	0.612(2)	0.1759(14)	0.803(2)	8.7(7)	C311	0.793(2)	0.4754(11)	0.196(2)	5.7(5)
C16	0.639(2)	0.1793(15)	0.701(2)	9.1(8)	C312	0.785(1)	0.4512(10)	0.092(2)	5.6(5)
C17	0.731(2)	0.8601(11)	0.808(2)	6.3(5)	C313	0.989(2)	0.1967(10)	0.319(2)	5.6(5)
C18	0.801(2)	0.9058(12)	0.884(2)	6.9(6)	C314	0.977(2)	0.1695(11)	0.207(2)	6.1(5)
C19	0.904(2)	0.9870(13)	0.882(2)	7.5(6)	C315	0.947(1)	0.1970(10)	0.050(2)	5.1(4)
C110	0.929(2)	0.0335(13)	0.821(2)	7.6(6)	C316	0.948(1)	0.2523(9)	-0.002(1)	4.8(4)
C111	0.880(2)	0.1182(13)	0.756(2)	7.5(6)	C317	0.861(1)	0.3399(9)	0.963(1)	4.9(4)
C112	0.802(2)	0.1660(15)	0.753(2)	9.0(8)	C318	0.768(1)	0.3651(10)	0.954(1)	5.0(4)
C113	0.588(2)	0.8533(11)	0.692(2)	5.8(5)	NEN1	0.742(6)	0.063(4)	0.053(7)	36. (4)
C114	0.623(2)	0.8552(12)	0.596(2)	7.3(6)	CEN1	0.730(6)	0.034(4)	0.108(6)	25. (3)
C115	0.640(2)	0.9198(12)	0.486(2)	7.3(6)	CEN2	0.816(3)	0.010(2)	0.152(3)	12. (1)
C116	0.621(2)	0.9800(13)	0.460(2)	7.7(6)	NEN2	0.773(5)	0.020(4)	0.265(5)	30. (3)
C117	0.648(2)	0.0890(14)	0.513(2)	8.5(7)	CEN3	0.058(7)	0.018(5)	0.500(9)	36. (5)
C118	0.728(2)	0.130(2)	0.575(3)	10.7(9)	NEN3	-0.023(7)	0.048(4)	0.492(7)	36. (4)

Table 18. Distances, bond angles, and dihedral angles in the Sn_9^{3-} anion

Distances, Å					
Atoms	d	Atoms	d	Atoms	d
1-2	3.270 (2)	3-6	3.060 (2)	8-7	2.949 (2)
3-4	3.309 (2)	1-5	2.938 (2)	1-9	2.943 (2)
6-8	3.315 (2)	2-5	2.923 (2)	2-9	2.956 (2)
1-4	3.090 (2)	6-5	2.977 (2)	3-9	2.959 (2)
1-8	3.050 (2)	8-5	2.943 (2)	4-9	2.926 (2)
4-8	3.058 (2)	3-7	2.949 (2)	5-7	4.831 (2)
2-3	3.059 (2)	4-7	2.929 (2)	5-9	4.830 (2)
2-6	3.034 (2)	6-7	2.940 (2)	7-9	4.802 (2)

Bond angles, deg					
Atoms	Angle	Atoms	Angle	Atoms	Angle
2-1-4	89.42 (4)	4-1-9	57.96 (4)	3-4-7	56.03 (4)
2-1-8	89.46 (5)	5-1-8	58.84 (4)	3-4-9	56.26 (4)
1-2-3	91.30 (5)	3-2-9	58.90 (4)	5-6-8	55.46 (4)
1-2-6	91.38 (5)	5-2-6	59.93 (5)	7-6-8	55.88 (4)
2-3-4	89.23 (4)	2-3-9	58.82 (4)	5-8-6	56.44 (4)
4-3-6	89.86 (5)	6-3-7	58.56 (5)	6-8-7	55.62 (4)
1-4-3	90.03 (4)	1-4-9	58.51 (4)	1-5-8	62.47 (5)
3-4-8	90.24 (5)	7-4-8	58.98 (5)	2-5-6	61.89 (5)
2-6-8	88.90 (5)	2-6-5	58.18 (4)	3-7-6	62.60 (5)
3-6-8	90.10 (5)	3-6-7	58.84 (5)	4-7-8	62.70 (5)
1-8-6	90.26 (5)	1-8-5	58.69 (4)	1-9-4	63.53 (4)
4-8-6	89.79 (5)	4-8-7	58.32 (4)	2-9-3	62.28 (4)
4-1-8	59.75 (4)	2-1-5	55.86 (4)	1-5-2	67.83 (5)
3-2-6	60.29 (4)	2-1-9	56.52 (4)	6-5-8	68.10 (5)
2-3-6	59.46 (4)	1-2-5	56.31 (4)	3-7-4	68.52 (5)
1-4-8	59.48 (4)	1-2-9	56.14 (4)	6-7-8	68.50 (5)
2-6-3	60.26 (4)	4-3-7	55.45 (4)	1-9-2	67.33 (4)
1-8-4	60.77 (4)	4-3-9	55.31 (4)	3-9-4	68.43 (5)

Table 18. Continued

Dihedral angles[a], deg					
Plane 1	Plane 2	Angle	Plane 1	Plane 2	Angle
(1-4-8)	(2-3-6)	179.1	(1-2-5)	(3-4-7)	42.4
(1-4-8)	(5-7-9)	179.6	(1-2-9)	(6-8-7)	42.2
(2-3-6)	(5-7-9)	179.2	(3-4-9)	(6-8-5)	42.5
(1-2-5)	(1-2-9)	17.5	(1-2-3-4)	(3-4-8-6)	59.5
(3-4-7)	(3-4-9)	18.1	(1-2-3-4)	(1-2-6-8)	60.0
(6-8-5)	(6-8-7)	17.4	(1-2-6-8)	(3-4-8-6)	60.5
(1-4-8)	(1-4-9)	40.4	(1-4-8)	(1-2-3-4)	89.4
(1-4-8)	(1-8-5)	40.9	(1-4-8)	(1-2-6-8)	90.7
(1-4-8)	(4-8-7)	41.0	(1-4-8)	(3-4-8-6)	91.1
(2-3-6)	(2-3-9)	40.8	(2-3-6)	(1-2-3-4)	90.0
(2-3-6)	(2-6-5)	40.2	(2-3-6)	(1-2-6-8)	89.6
(2-3-6)	(3-6-7)	42.4	(2-3-6)	(3-4-8-6)	89.8

[a]For planes (1-2-3-4), (1-2-6-8) and (3-4-8-6) the atoms are within 0.008, 0.0004, and 0.007 Å of their respective, best least-squares plane.

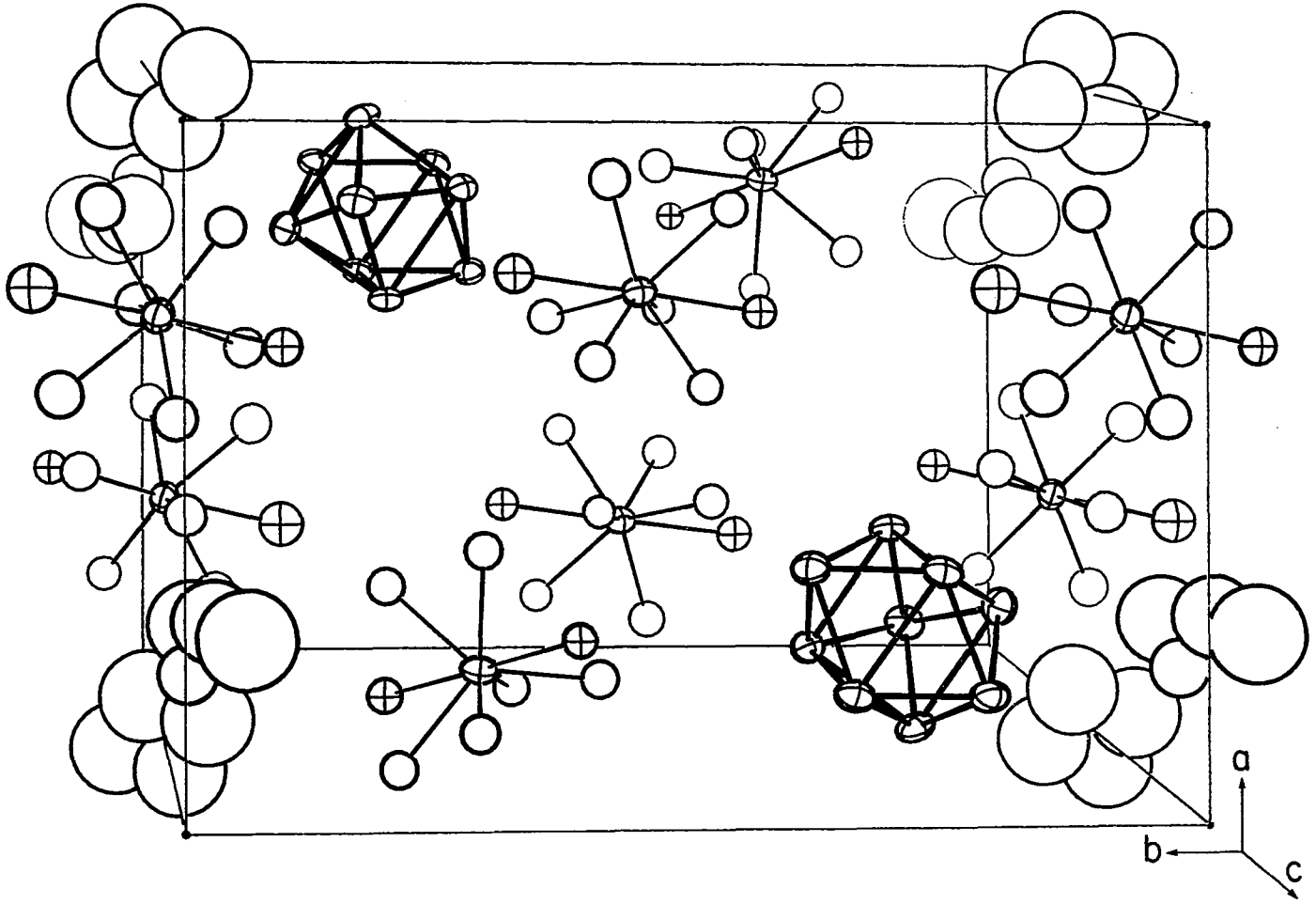

Figure 8. Approximate [00$\bar{1}$] view of the unit cell of (2,2,2-crypt-K^+)$_3Sn_9^{3-}$•1.5en. For clarity, crypt carbon atoms are not included, and the N-K-N axes are differentiated

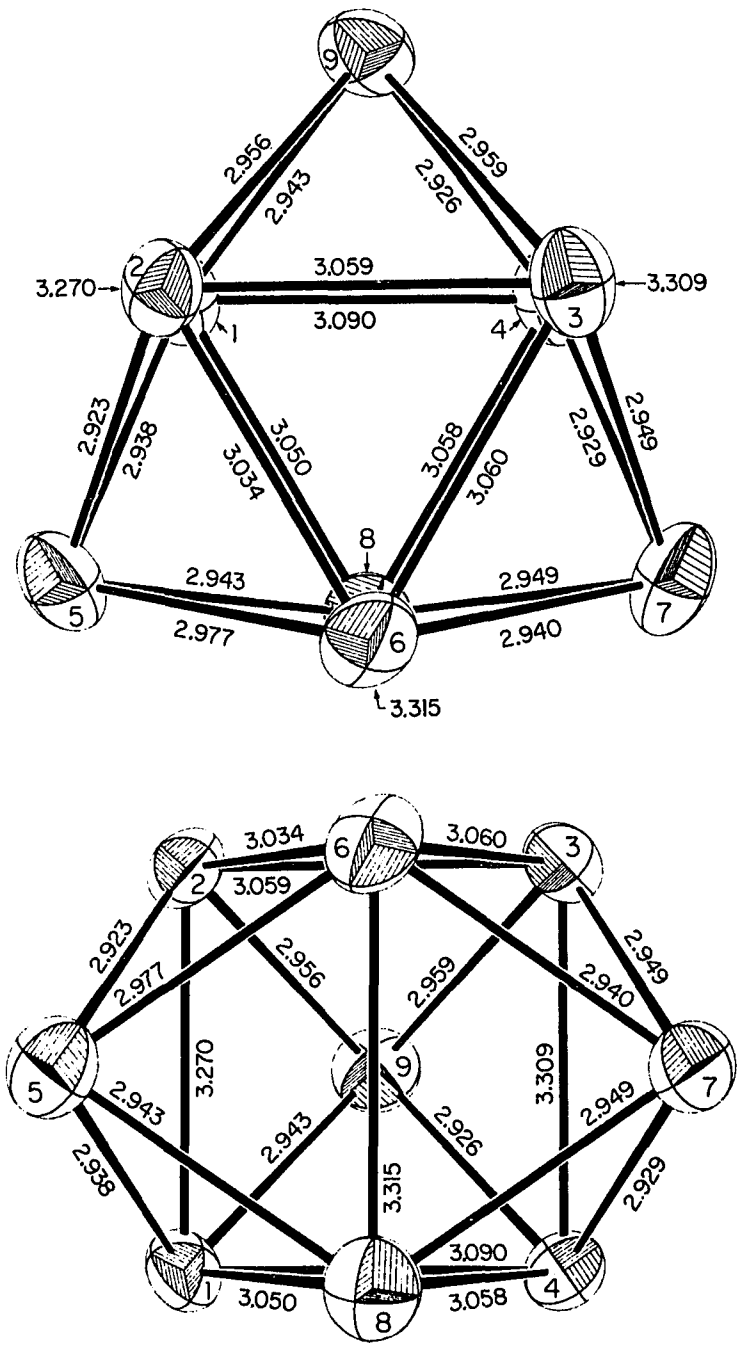

Figure 9. Two views of the Sn_9^{3-} anion

The unit cell contains six crypt-K^+ cations, two Sn_9^{3-} anions, and three ethylenediamine molecules (one sits on an inversion center) as seen in Figure 8. Except for the difference in anions, this salt is isostructural with (2,2,2-crypt-K^+)$_3$($Tl Sn_8^{3-}$ $TlSn_9^{3-}$)$_{½}$·en.[28] It is indeed remarkable that the anion cavity defined by the crypt-K^+ cations can on the one hand be so unspecific that it can accommodate three different anions and on the other hand so specific that at least seven of the atoms in each cluster are in essentially identical positions. There is probably no significant interaction between the anion and the en molecules or crypt cations; the shortest contacts are Sn8 to NEN2, 3.71 (8) Å and Sn7 to C316, 3.78 (2) Å. For Sn-N the sum of van der Waals radii is 3.7 Å.[69] Also, the en molecules themselves are not in close enough proximity for any hydrogen bonding, unlike those seen in (2,2,2-crypt-K^+)$_3Sb_7^{3-}$·2en.[23] The 2,2,2-crypt-K^+ cations have normal conformations.

Anion charge assignment

The assignment of the 3- charge to the Sn_9 cluster is derived primarily from the three to one crypt-K^+ to anion ratio. The anion exhibits relatively small and spherical thermal ellipsoids; this is unlikely to be the case if Sn_9^{2-} (D_{3h}) and Sn_9^{4-} (C_{4v}) were equally disordered on the same site (even if both were to occur in D_{3h} configurations the trigonal prismatic atoms should overlap poorly as is discussed later). In any event, the 3- charge necessitates a paramagnetic species and both ESR and magnetic susceptibility studies confirm the paramagnetic character of this compound.

ESR results

ESR measurements were made for a variety of samples, as shown in Table 19. Figure 10 presents several representative spectra (they are not drawn to the same scale in terms of intensity). Even in solution the resonances are fairly broad, and no clear evidence of hyperfine coupling to the two tin nuclei with I = 1/2 (^{117}Sn, 7.7% and ^{119}Sn, 8.7%) was observed, although at low temperatures there are some weak unexplained inflections between the two main signals in the bulk product spectrum, but these may be due to possible impurities or the lack of complete randomness in this sample. However, they might also be the result of hyperfine coupling; at 5 K the ESR spectrum for phase III in the Na-Ge system (see Experimental) which may contain the analogous Ge_9^{3-} anion shows similar weak inflections, but there are many more (>15), which would be appropriate since the only active isotope for germanium has I = 9/2 (^{73}Ge, 7.8%). The fact that the ESR signal is retained in solution and is dependent on orientation for a 'single' crystal is evidence of a distinct paramagnetic species. Above about 150 K, the spectra of the first three samples have essentially two g values ($g_{\parallel} \sim 1.97$ and $g_{\perp} \sim 2.07$) which is appropriate for Sn_9^{3-} as ideally it has axial symmetry. Below 150 K the bulk product and 'single' crystal spectra indicate $g_{\perp}$ may be slightly split; the anion is probably distorted somewhat from the ideal D_{3h} symmetry. As expected, the two g values for static samples coalesce to a single resonance ($g \sim 2.035$) for the solution samples which allow free rotation of the paramagnetic anion.

Table 19. ESR measurements for $(2,2,2\text{-crypt-}K^+)_3Sn_9^{3-} \cdot 1.5en$

Sample	Temperature (K)	Signal	g values
1. Bulk product (reaction 3)[a]	5-292	strong, complex	1.92, 2.07
2. Large 'single' crystal (reaction 3)[b]	4-298	strong	1.982, 2.076
3. Crystals (reaction 3) dissolved in en (frozen solution)	200-250	strong	1.978, 2.075
4. Crystals (reaction 5) dissolved in en, decanted	298	very weak[c]	2.03
5. KSn_2 + crypt + en, solution decanted after 3d	298	weak[c]	2.035
6. Sn metal	298	none	
7. KSn_2 alloy	298	none	
8. en (solvent)	298	none	

[a]Not finely powdered.

[b]Crystal was in no particular orientation, signal appearance changes with a change in orientation. The crystal is probably not truly single.

[c]The weakness of the solution signals may be due in part to the necessity of using capillary tubes because of the solvent's high dielectric constant.

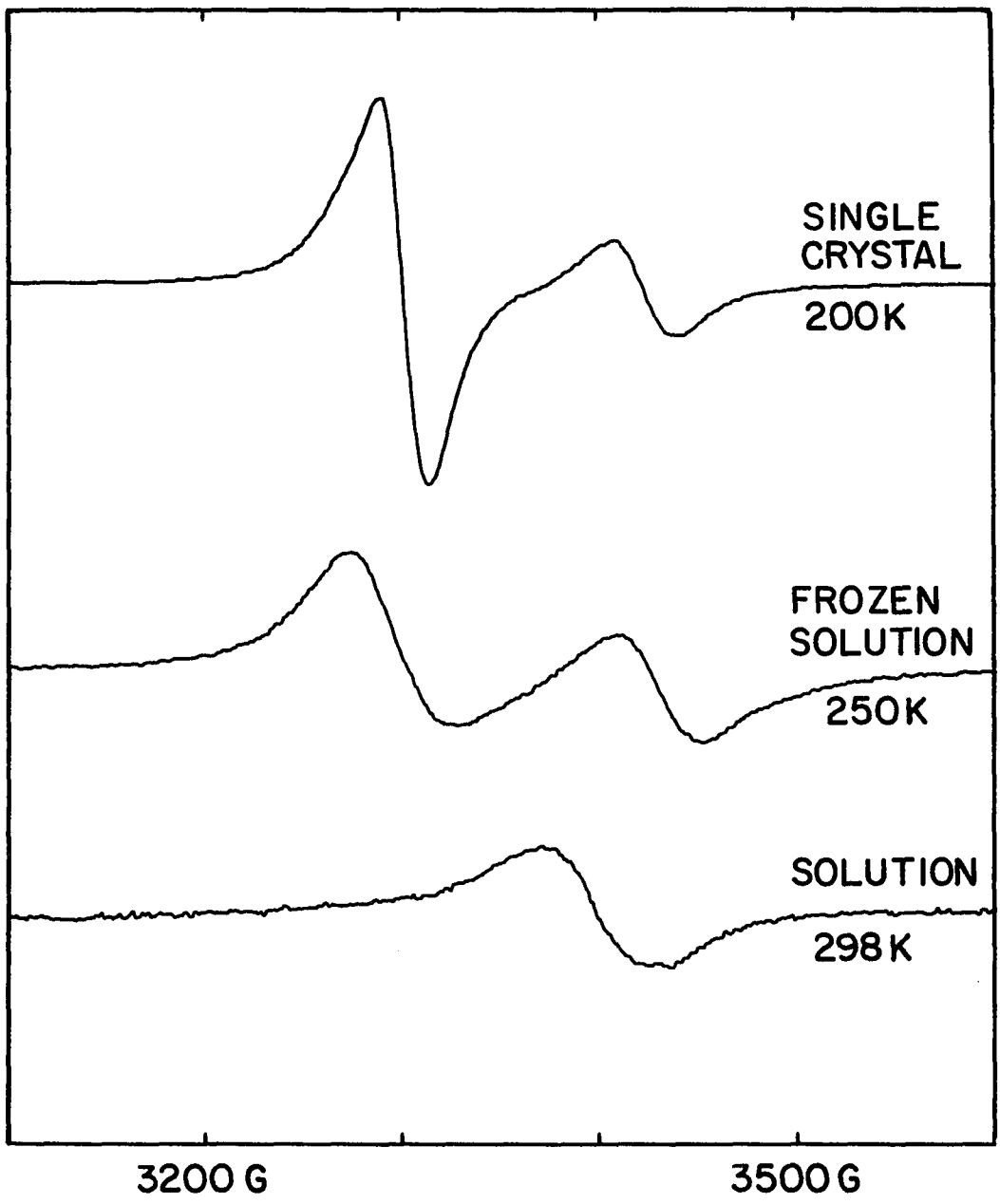

Figure 10. ESR spectra for $(2,2,2\text{-crypt-}K^{+})_3Sn_9^{3-}\cdot 1.5en$: top, 'single' crystal (sample 2, see Table 19) at 9.5935 GHz; middle, frozen en solution (sample 3) at 9.5934 GHz; bottom, solution of KSn_2 + crypt in en (sample 5) at 9.7592 GHz

Magnetic susceptibility

Results of magnetic susceptibility measurements on the bulk products of two of the KSn_2 + crypt reactions that produced $(2,2,2\text{-crypt-}K^+)_3$ - $Sn_9^{3-}\cdot 1.5en$ are listed in Table 20. The data were corrected for the estimated diamagnetic effects of the atomic cores (H,C,N,O,K^+ and Sn^{2+})[70,71] and for the 21 delocalized cluster electrons.[70] The inconsistency of the two samples is probably due to a lack of precision associated with the small sample sizes (possible error of 3-5%) and the likelihood of impurities or decomposition.

The question of the purity of these two samples is rather difficult to address. Visually, the samples appeared reasonably homogeneous although there is certainly small amounts of elemental tin, and perhaps alloy and excess crypt present; however, the Sn_9^{3-} phase (V) and phase IV (the primary product from reaction 4) in this system are not readily distinguishable by eye. It should be noted that recrystallization of the products is generally not a viable option - in this case phase VI (Sn_9^{4-}) would be the likely result. Guinier powder patterns of the products of reaction 3, 4 and 5 were taken, but the multitude of weak, very low angle lines makes it difficult to draw any firm conclusions. Although many lines were similar, all three patterns were different. Probably all three products are inhomogeneous; however, the pattern for the reaction 3 product apparently matches a calculated pattern for Sn_9^{3-} better than that from reaction 5. The reaction 5 magnetic susceptibility sample was the one analyzed by atomic absorption as having exactly a 3Sn:1K mole ratio, but this only suggests that any other phase present

Table 20. Magnetic susceptibility data

	Sample 1	Sample 2
Product from reaction	3	5
Sample weight (mg)	37.9	79.0
Temperature (K)	296 → 100	296 → 93
χ_{296} (emu/mol)[a]	5.45×10^{-3}	2.91×10^{-3}
Curie plot (χ vs $^{1}/_{T}$)		
R[b]	0.9965	0.9983
μ_{eff} (BM)	1.383 (12)	1.054 (8)
χ_{TIP} (emu/mol)	$4.74(1) \times 10^{-3}$	$2.473(8) \times 10^{-3}$
Curie-Weiss plot ($^{1}/_{\chi}$ vs T)		
R	0.9891	0.9795
θ	-579 (12)	-508 (19)

[a]After diamagnetic correction, -1.43×10^{-3} emu/mol.

[b]Linear correlation coefficient.

(probably phase IV) must have a similar ratio. Perhaps phase IV is simply $(crypt\text{-}K^{+})_6Sn_9^{2-}Sn_9^{4-}$ with more solvent molecules than normal to account for the very large volume per crypt, rather than the previously postulated $(crypt\text{-}K^{+})_7Sn_9^{3-}Sn_9^{4-}$. Certainly, the presence of impurities or other phases will greatly influence the magnetic susceptibility results.

Both samples exhibit linear Curie law behavior, as shown in Figure 11 for sample 1. It is not clear why the intercept (χ_{TIP}) should be so far from zero. Curie-Weiss plots are not as satisfactory, as they are much less linear and give very large Weiss constants (θ). It would be surprising if there is actually significant interaction between spins or neighboring clusters as these Weiss constants would suggest, since the anions are separated by the very large crypt cations. The important fact is that the compound is clearly paramagnetic with an effective magnetic moment of approximately 1.38 BM (assuming sample 1 is of higher purity). This value is appropriate for the expected one unpaired electron per mole, although it is admittedly low compared to the spin only value of 1.73 BM.

NMR results

The reaction of the KSn_2 alloy with 2,2,2-crypt has also been investigated by ^{117}Sn and ^{119}Sn solution NMR.[72] Two spectra are shown in Figure 12. Reaction conditions used were similar to those known to produce the Sn_9^{3-} phase, that is, decanting the solution after several days over the alloy residue. With ethylenediamine as the solvent, an extremely broad (fwhm $\sim$ 1100 Hz) resonance was observed, at a chemical shift appropriate for the Sn_9^{4-} anion (δ = -1230 ppm and J = 254 Hz for Na-Sn solutions without crypt[34] but these values vary slightly with different solvents or cations[63]). No fine structure was evident. Since ethylenediamine freezes at only 8°C, reactions in liquid ammonia were also examined as this solvent allows temperatures down to -78°C. In

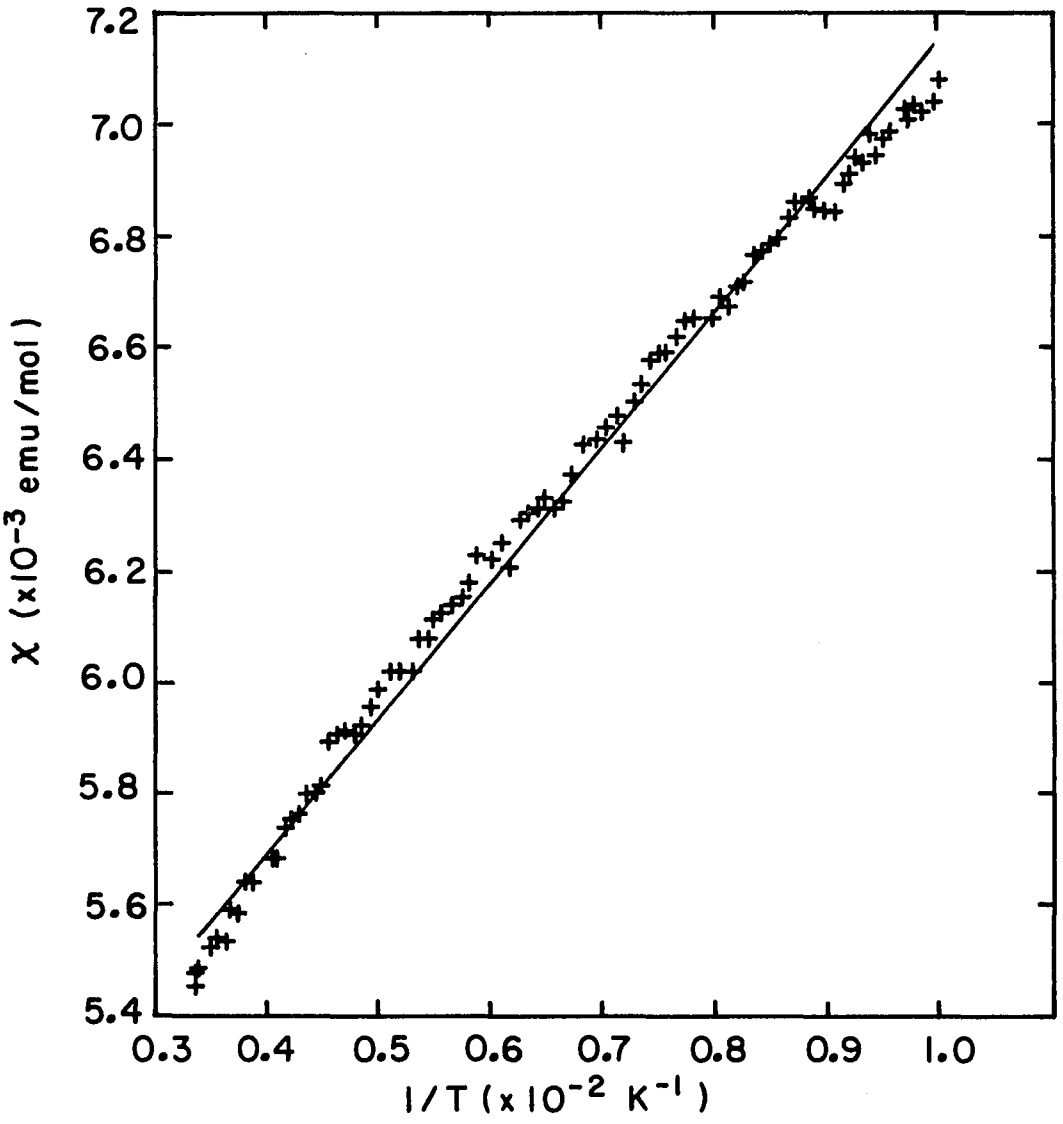

Figure 11. Magnetic susceptibility for $(2,2,2\text{-crypt-}K^{+})_3Sn_9^{3-}\cdot 1.5en$ (sample 1) as χ_{corr} vs. 1/T

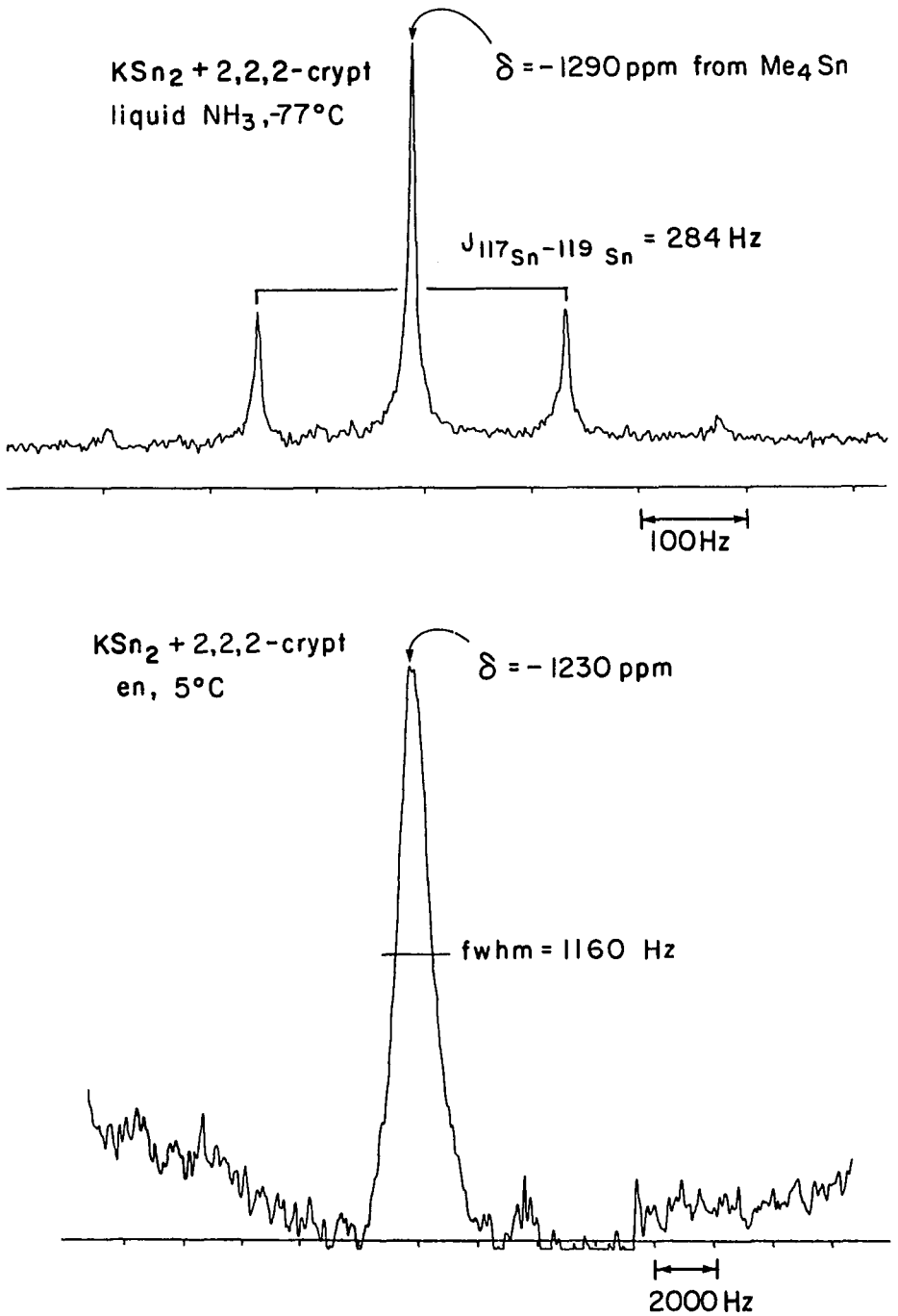

Figure 12. ^{117}Sn NMR spectra (note difference in abscissa scale)

sharp contrast, the signal observed in liquid ammonia is the characteristic Sn_9^{4-} multiplet,[33,34] a singlet (through intramolecular exchange) split by ^{117}Sn - ^{119}Sn coupling. Presumably, the broadening of the signal in ethylenediamine arises from the presence of the paramagnetic Sn_9^{3-} anion, which is not obtained in $NH_3(\ell)$ under similar conditions.

Anion configuration

The nonastannide(3-) anion has a tricapped trigonal prismatic geometry which deviates very little from the ideal D_{3h} symmetry (Figure 9) considering the fact that the site symmetry is only C_1. The bond distances and angles are quite regular; differences between equivalent values are relatively small, though admittedly large compared with the low standard deviations (Table 18). One height of the trigonal prism is about 0.04 Å shorter than the other two but this is probably unimportant. The Sn_9^{3-} cluster has average bond distances of 3.298 Å, 3.058 Å, and 2.944 Å for the height (h) and edge (e) of the trigonal prism and from the prismatic to the capping (c) atoms, respectively.

A comparison of dihedral angles provides the most useful means of distinguishing D_{3h} and C_{4v} configurations for nine-atom clusters, as is shown in Table 21. Sn_9^{3-} is obviously D_{3h} with a dihedral angle of 179.1° for opposed trigonal prism faces, and average values of 17.7° for vicinal cap to cap faces and 41.0° for vicinal prism end to cap faces. These latter two categories of dihedral angles do show significant variation even among the relatively nondistorted D_{3h} species; most noticeable

Table 21. Some dihedral angles (δ,degrees) in nine-atom polyhedra

D_{3h} Type faces		Trigonal prism, (opposed)	Cap to cap, (vicinal)		Prism end to cap, (vicinal)					
D_{3h} Example (Figure 9)		1-4-8,2-3-6	5-6-8,6-7-8		2-3-6,2-5-6					
D_{3h}	Bi_9^{5+}	180	22 (x3)		43 (x6)					
D_{3h}	Sn_9^{3-}	179	17	18 18	40	40	41	41	41	42
C_{2v} (D_{3h}[a])	$TlSn_8^{3-}$	177	16	17[b] 19[b]	35[b]	36[b]	41	41	42	42
~D_{3h}	Sn_9^{4-} [c]	173	21	25 16	42	41	41	52	46	47
C_{2v}	Ge_9^{2-}	171	8	25 23	38	36	44	47	45	45
~C_{4v}	Ge_9^{4-}	162,156	5	32 24	32	33	51	54	53	51
~C_{4v}	Sn_9^{4-} [c]	164,157	2	30 28	34	33	52	50	46	54
C_{4v}	Sn_9^{4-} [d]	158,158	3	30 29	29	32	52	53	54	55
C_{4v}	Type faces	waist, opposed	base	cap to waist, vicinal			waist to waist, vicinal			

[a]Ignoring thallium atom.
[b]Defining planes contain one thallium atom, which effectively reduces δ relative to homoatomic species.
[c]Disordered anion in $(2,1,1\text{-crypt-}Li^+)_4Sn_9^{4-}$.
[d]2,2,2-crypt-Na^+ salt.

is the difference between the average values for Sn_9^{3-}, 17.7° and 41.0°, and those for Bi_9^{5+} (C_{3h} site symmetry), 22° and 43°, respectively. This is not an indication of distortion, but is due strictly to variations in the h:e:c ratios among these D_{3h} species. The vicinal cap to cap angle is sensitive to changes in the h:c ratio, while the vicinal prism end to cap angle correlates linearly with the h:e ratio.

Correlation of the h:e ratio to electron count

The Bi_9^{5+} ion has long been something of an anomaly because it has seemingly two electrons more than required for the closo D_{3h} geometry it adopts, in contrast to the isoelectronic Sn_9^{4-} and Ge_9^{4-} anions which have the expected nido C_{4v} configuration for 22 skeletal electrons. Some explanations of this exception to Wade's rules have noted the elongation of the trigonal prism in Bi_9^{5+} compared to the 20-electron species $B_9H_9^{2-}$, and related it to the high cationic charge of Bi_9^{5+} and consequently poorer orbital overlap.[73,74] It is now clear that the height to edge ratio (h:e) of the trigonal prism has a direct correlation with electron count for D_{3h} nine-atom clusters; this is directly related to the character of the molecular orbital involved (the LUMO for 20-electron and the HOMO for 21- or 22-electron species).[20,75,76]

Table 22 lists the characteristic distances and h:e ratios for known D_{3h} nine-atom species. The 20-electron clusters have a height to edge ratio of about 0.99. The values for Ge_9^{2-} and $B_7H_7C_2(CH_3)_2$ are probably less representative as the former is quite distorted and the latter may be affected by the two C-CH_3 units. The h:e ratio for

Table 22. D_{3h} nine-atom clusters

Cluster	Skeletal e's	h[a]	e	c	h:e	Ref.
Bi_9^{5+}	22	3.74	3.24	3.09	1.15	61
Sn_9^{4-} [b]	22	3.54	3.02	2.93	1.17	this work
Sn_9^{3-}	21	3.30	3.06	2.94	1.08	20, this work
$T\ell Sn_8^{3-}$	20	3.16[c]	3.12	2.96[c]	1.01[c]	28
$B_9H_9^{2-}$	20	1.84	1.90	1.71	0.97	77
$B_7H_7C_2(CH_3)_2$	20	1.77	1.97	1.70[d]	0.90	78
Ge_9^{2-} [e]	20	2.83[e]	2.67	2.56	1.06[e]	22

[a]Height (h), edge (e) and capping (c) distances in Å.

[b]This anion occurs in both D_{3h} and C_{4v} conformations disordered on the same site in $(2,1,1\text{-crypt-}Li^+)_4Sn_9^{4-}$.

[c]The long height and four capping distances involving disordered atoms 6 and 8 were omitted in the calculation; otherwise the values are h=3.21, c=2.93, and h:e=1.03. (Capping distances to Tℓ are of course not used.)

[d]Capping distances to C are not included.

[e]Badly distorted to C_{2v} symmetry. One long height was omitted; otherwise the values are h=2.94 and h:e=1.10.

22-electron species is about 1.16. Again, the Sn_9^{4-} value may be somewhat unreliable because of disorder. Curiously, this value compares well with the h:e ratio of 1.17 for a points on a sphere calculation, with relative values h = 1.42, e = 1.22 and c = 1.14 for a sphere of radius 1.00.[79] Of course, this calculation assumes repulsion between ligands for centered ML_9 type clusters, not bonding atoms as is the case here. The h:e ratio of 1.08 for the 21-electron Sn_9^{3-} is exactly intermediate between that for 20- and 22-electron clusters, which is further confirmation of the correctness of the charge assignment. Note also the trends in h, e and c distances for the three tin species. (The capping distance c is always shorter than h or e because the capping atom has the lower connectivity.) Interestingly, the same elongation trend is observed for actual trigonal prismatic species; h:e for Te_6^{4+} (20 electrons) is 1.17 compared to 1.01 for hexamethyl prismane (18 electrons).[73]

Molecular orbital calculations

Semiempirical energy calculations support these conclusions about the relationship between the electron count and the tricapped trigonal prism dimensions for nine-atom clusters. Extended Hückel molecular orbital (EHMO) calculations were performed for Sn_9^{2-}, Sn_9^{3-}, Sn_9^{4-} and Bi_9^{5+} in various configurations. Previous molecular orbital calculations for nine-atom clusters have included extended Hückel results for Bi_9^{5+},[80] $B_9H_9^{2-}$ [77] and Sn_9^{4-};[73] both normal and relativistically parameterized extended Hückel calculations for Ge_9^{2-}, Ge_9^{4-}, Sn_9^{4-}, Pb_9^{4-} and Bi_9^{5+};[81]

a graph theory topological approach for these same five ions;[74] and SCF-MO-CNDO results for Sn_9^{4-},[21] Ge_9^{2-} and Ge_9^{4-}.[22] All except the first have addressed the relative stability of D_{3h} versus C_{4v} configurations to some extent. However, the effect of trigonal prism elongation for the D_{3h} configuration has never been thoroughly examined. It should be noted that CNDO molecular orbital calculations are not successful for Sn_9^{3-} in any configuration or for Sn_9^{2-} in the C_{4v} configuration because of the open shell character; the extra electron in Sn_9^{3-} is simply ignored, and self-consistency for the C_{4v} Sn_9^{2-} anion cannot be obtained. The extended Hückel approach is therefore preferred here.

The EHMO program[82] as obtained from E. R. Davidson of the University of Washington allows the use of up to three mirror planes in the molecule and involves an iterative procedure to obtain self-consistent charge density, which produces more reasonable HOMO-LUMO energy gaps and charge distributions than some noniterative EHMO procedures.[83] The parameters and idealized cluster geometries used in the calculations are summarized in Table 23 and 24, respectively, while the results are presented in Table 25 and Figure 13.

Comparing the total (one-electron) energies in Table 25, the most stable configurations are indeed the expected ones. Of course, some of the differences in energy are small (<0.5 eV) and may be partially influenced by the actual choice of distances; however, the general trends are certainly real. Of the three D_{3h} geometries, the 1% elongation is favored for Sn_9^{2-}, the 8% elongation is marginally better for Sn_9^{3-}, and the 15% elongation is better for both Sn_9^{4-} and Bi_9^{5+}. For Sn_9^{2-} or

Table 23. EHMO parameters[a]

	zeta[c]	VOIE (eV)[b] Sn^-	Sn^o	Sn^+
Sn 5s	2.13	-7.14	-14.23	-22.78
Sn 5p	1.62	-1.26	- 7.01	-14.98
			Bi^o	Bi^+
Bi 6s	2.56		-16.56	-26.86
Bi 6p	2.01		- 8.14	-15.60

[a]The Wolfsberg-Helmholtz interaction constant, K, was taken to be 1.89 for all orbitals.

[b]Valence orbital ionization energy, calculated as in reference 84 from ionization potentials and atomic spectra energy levels (reference 85) and the electron affinity for Sn (reference 86).

[c]Overlap orbital exponent, reference 87.

Table 24. Distances in idealized polyhedra used in EHMO calculations

Geometry[b]	Distances[a] (Å)	
	Sn_9^{x-}	Bi_9^{5+}
D_{3h} 1%	3.159, 3.121, 2.960[c]	3.434, 3.393, 3.094[d]
D_{3h} 8%	3.298, 3.058, 2.945[e]	3.580, 3.320, 3.094[d]
D_{3h} 15%	3.447, 2.990, 2.930[f]	3.737, 3.241, 3.094[e]
C_{4v}	2.956, 3.242, 2.971, 2.964[e]	3.154, 3.459, 3.170, 3.163[g]

[a] D_{3h} distances: h, e, c (see text); C_{4v} distances: capping atom to capped face, within capped face, capped face to base, within base.

[b] With percent elongation of the trigonal prism.

[c] Based on T&Sn_8^{3-}.

[d] Only h and e changed from observed Bi_9^{5+} proportions to give appropriate percent elongation.

[e] Observed geometry.

[f] Based on the D_{3h} Sn_9^{4-} as found in the 2,1,1-crypt-Li^+ salt but with a 15.3% elongation as in Bi_9^{5+}.

[g] Proportioned as in Sn_9^{4-}.

Table 25. EHMO calculations

Cluster	Geometry	Total energy (eV)	HOMO-LUMO gap (eV)
Sn_9^{2-}	D_{3h} 1%[a]	-365.68	1.58
	D_{3h} 8%	-365.49	1.15
	D_{3h} 15%	-364.97	0.54
Sn_9^{3-}	D_{3h} 1%	-338.25	4.12
	D_{3h} 8%	-338.47	4.30
	D_{3h} 15%	-338.45	4.30
	C_{4v}	-336.86[b]	4.55[b]
	$C_1(\sim D_{3h})$[c]	-338.48	4.20
Sn_9^{4-}	D_{3h} 1%	-309.94	3.60
	D_{3h} 8%	-310.48	3.75
	D_{3h} 15%	-310.82	3.74
	C_{4v}	-311.78	4.02
	$C_1(\sim C_{4v})$[c]	-311.70	3.79
Bi_9^{5+}	D_{3h} 1%	-737.94	5.63
	D_{3h} 8%	-739.16	5.77
	D_{3h} 15%	-740.06	5.61
	C_{4v}	-739.99	6.59

[a]Percent elongation of the trigonal prism.
[b]One cycle only (will not iterate to a consistent charge density).
[c]Actual geometry found from the crystal structure solution.

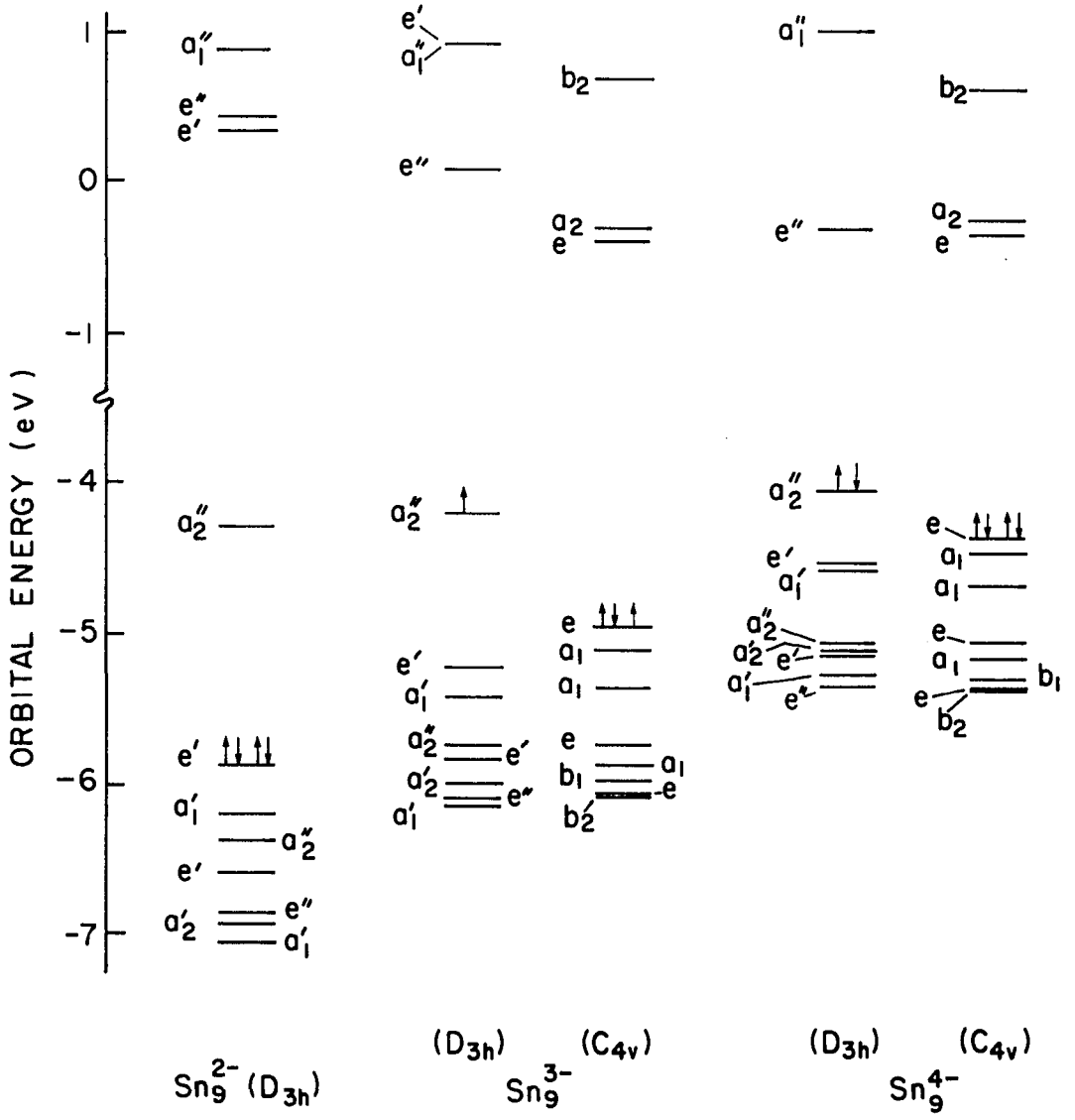

Figure 13. EHMO orbital energies. Arrows denote the HOMO and its occupancy in each case

Sn_9^{3-}, a C_{4v} configuration is not feasible as it would require a partially filled, degenerate HOMO level, e^2 or e^3, respectively. The C_{4v} geometry for Sn_9^{3-} is apparently of much lower stability anyway. For Sn_9^{4-}, the C_{4v} configuration is calculated to be more stable than the 15% elongated D_{3h} geometry by 1.0 eV. However, Bi_9^{5+} is apparently marginally more stable in the 15% D_{3h} configuration (by only 0.1 eV), which does agree with observation.

The HOMO-LUMO gaps in general parallel the total energy trends, although all the C_{4v} configurations have larger gaps than the corresponding D_{3h} ones. (For Sn_9^{3-} the HOMO is of course only partially filled; so properly speaking, the gap energy should be 0.0 eV.) The energy level diagram for Sn_9^{2-} is rather unusual with the surprisingly small HOMO-LUMO gap (1.6 eV) followed by a very large energy separation (4.6 eV) between the LUMO and the second-lowest unoccupied orbital. This may be an indication of low stability for this anion, which has yet to be isolated. (There is a second-hand mention of a ^{119}Sn solution NMR signal extremely far downfield from Me_4Sn ($\delta \approx +2700$ ppm) attributed to Sn_9^{2-}, and a report of a crystalline compound which by analysis was $Li_2Sn_9 \cdot 2.5en$.[63])

The elongation of the trigonal prism for D_{3h} clusters upon successive reduction can be readily understood upon examination of the molecular orbital involved, the LUMO for 20-electron or the HOMO for 21- or 22-electron species. This orbital is of a_2'' symmetry (with mainly p_z atomic orbital contributions) and is strongly σ antibonding along the height, pi bonding for the edges, and weakly bonding to the capping

atoms. (A previous molecular orbital calculation for Bi_9^{5+} [80] is in agreement in this respect; however, Wade and O'Neill[76] believe (for unspecified reasons) that the contribution of the capping atom p_z orbitals is reversed, so that this a_2'' orbital would instead be antibonding to the capping atoms, and overall show net antibonding.) Therefore, the increase in h:e observed upon occupation of this orbital with one or two electrons arises from not only an increase in the height, but partly from a decrease in the edge length of the trigonal prism. These trends are exactly what is found when tin distances for $T\ell Sn_8^{3-}$, Sn_9^{3-}, and Sn_9^{4-} are compared (Table 22). There is little change in the capping distance for these three clusters; the slight decrease observed may be artificial. The addition of electrons to the a_2'' orbital might be expected to shorten the capping distance because of the weakly bonding character; however, this is essentially negated by a corresponding decrease in the amount of capping atom p_z atomic orbital participation upon trigonal prism elongation.

There is no disagreement as to the a_2'' character of the LUMO for 20 skeletal electron D_{3h} clusters (except as to whether the capping distance is bonding or antibonding). However, while the HOMO found here and in other EHMO calculations[73,81] is of e' symmetry, CNDO and some EHMO calculations[77,80] indicate an a_2' symmetry. In this latter case, the a_2' orbital is bonding for the height and antibonding for the trigonal prism edges, so one would expect a similar prism elongation upon <u>removal</u> of two electrons.[75,76] This in fact occurs for $B_9C\ell_9$ which is formally an 18-electron species (h = 2.08 Å, e = 1.80 Å, c = 1.75 Å, and

h:e = 1.16),[75,88] although the back-bonding effect of the chlorine ligands cannot be ignored.

For the 22 electron species Bi_9^{5+} and Sn_9^{4-} these EHMO results do actually agree with the observed configurations, although differences in the total energy are small. It is clearly evident that the elongation of the trigonal prism not only allows the accommodation of the extra two electrons, but also produces a D_{3h} configuration which is of at least similar stability to that for the C_{4v} geometry. Also the change from Sn_9^{4-} to Bi_9^{5+} increases the relative stability of the D_{3h} configuration. Other molecular orbital calculations[21,73,81] also predict a minimal difference in energy between C_{4v} and D_{3h} geometries, suggesting there is a very low barrier to interconversion. Sn_9^{4-} is certainly fluxional in solution as demonstrated by ^{119}Sn NMR.[33] Also, while Sn_9^{4-} is of approximate C_{4v} geometry in $(crypt\text{-}Na^+)_4Sn_9^{4-}$ and also in the unusual salt $(crypt\text{-}K^+)_3(KSn_9)^{3-}$ which has infinite chains - K^+ - Sn_9^{4-} - K^+ - Sn_9^{4-} - running through the cell,[18] the anion seems to occur in both D_{3h} and C_{4v} geometries (disordered) in $(2,1,1\text{-}crypt\text{-}Li^+)_4Sn_9^{4-}$. Similarly, Bi_9^{5+} is essentially D_{3h} in the salt $Bi_9^{5+}Bi^+(HfCl_6^{2-})_3$[61] (the site symmetry is C_{3h}), but is about 25% distorted toward C_{4v} (via C_{2v}) in $Bi_{12}Cl_{14}$.[89] Dipole effects[22] and solid state packing forces probably are of importance in the relative stability of the two configurations.

The calculated charge distributions for the four clusters are given in Table 26. There are no real surprises, with the atoms of higher connectivity having the more positive charge. The charge separations are however, much smaller (and more reasonable) than those obtained

Table 26. Calculated charge distributions

Cluster	Geometry	Charges
Sn_9^{2-}	D_{3h} 1%	prism = -0.21 cap = -0.24
Sn_9^{3-}	D_{3h} 8%	prism = -0.32 cap = -0.36
Sn_9^{4-}	C_{4v}	apex = -0.44 waist = -0.41 base = -0.48
Bi_9^{5+}	D_{3h} 15%	prism = +0.57 cap = +0.52

through CNDO calculations. Also, for the C_{4v} Sn_9^{4-} anion the base atoms here have the most negative character in contrast to CNDO calculations which put the highest negative charge on the apex atom.[21]

Conclusions

The synthesis of Sn_9^{3-} was certainly unexpected, both because it was a new tin anion and because of its open shell, paramagnetic character. The previous investigations[19,21] of Na-Sn alloy reactions produced only two compounds, $(crypt\text{-}Na^+)_4Sn_9^{4-}$ and $(crypt\text{-}Na^+)_2Sn_5^{2-}$. As was observed in the antimony system, the subtle switch from sodium to potassium alloys has served here to allow isolation of new anions. The compositions of the other two products of the reaction of KSn_2 are as yet unknown (phase IV and VI, see Experimental), so it is difficult to speculate on the course of the reaction. If phase VI does contain Sn_9^{4-} as expected, it would seem that the presence of alloy residue causes eventual reduction of Sn_9^{3-} to Sn_9^{4-} (presumably the more stable anion)

with corresponding formation of tin metal. If this is the case, one might expect phase IV to contain a more oxidized anion such as Sn_9^{2-} since this compound formed when reaction times were short; however, the unit cell dimensions seem to point to a mixture of Sn_9^{4-} and Sn_9^{3-} in phase IV.

Sn_9^{3-} is unique as a paramagnetic Zintl anion with an odd total number of electrons, but it is unlikely to be the only such exception; as previously mentioned, the isoelectronic Ge_9^{3-} anion may indeed exist. However, molecular orbital considerations indicate that it is the nondegenerate nature of the LUMO for the 20 skeletal electron nine-atom closo configuration which allows the accommodation of this extra electron. Therefore, the choice of possible configurations for odd-electron species is restricted to those with nondegenerate frontier orbitals; otherwise the degenerate open shell level would cause Jahn-Teller instability. For closo configurations, the only possibilities (besides a nine-vertex cluster isoelectronic to Sn_9^{3-}) would be an eight-vertex dodecahedron or an eleven-vertex octadecahedron,[76] which have not as yet been observed for Zintl anions.

Incomplete Studies

The $(2,2,2\text{-crypt-Na}^+)_2Ge_4^{2-}$ structure

The final positional and thermal parameters for $(2,2,2\text{-crypt-Na}^+)_2$ - Ge_4^{2-} are listed in Table 27, while distances and angles for this structure appear in Appendix A. Figure 14 shows the Ge_4^{2-} anion as it occurs in the cell in two disordered images, each at 0.50 occupancy, related by the center of symmetry at the origin.

Table 27. Positional and thermal parameters for (2,2,2-crypt-Na)$_2$Ge$_4$

Atom	x	y	z	B11	B22	B33	B12	B13	B23
Ge1[a]	0.1539(5)	0.0346(6)	0.0534(4)	9.3(3)	11.6(3)	9.8(3)	5.1(2)	0.7(2)	0.8(2)
Ge2	0.0000	0.0000	0.1537(8)	12.4(4)	12.4	10.2(5)	6.2	0.0	0.0
Na	0.3333	0.6667	0.4034(6)	4.9(2)	4.9	3.9(3)	2.5	0.0	0.0
O1	0.1154(8)	0.6240(8)	0.2781(6)	6.0(4)	6.2(4)	3.1(3)	3.6(3)	0.1(3)	0.1(3)
O2	0.1963(7)	0.7566(8)	0.4996(6)	4.1(3)	6.1(4)	2.8(3)	2.5(3)	0.1(2)	0.2(3)
N1	0.3333	0.6667	0.1135(13)	5.4(5)	5.4	3.1(6)	2.7	0.0	0.0
N2	0.3333	0.6667	0.6552(12)	4.0(4)	4.0	3.2(6)	2.0	0.0	0.0
C1	0.2125(11)	0.6700(12)	0.0725(9)	4.5(5)	6.2(6)	3.0(4)	2.5(4)	-0.4(4)	0.0(4)
C2	0.0923(13)	0.5826(14)	0.1513(9)	5.6(6)	7.6(7)	2.9(4)	2.8(5)	-1.1(4)	-1.8(4)
C3	0.1227(13)	0.7521(12)	0.2977(10)	6.4(6)	5.5(6)	4.6(5)	3.4(5)	-0.5(5)	-0.8(4)
C4	0.0917(11)	0.7570(13)	0.4315(10)	4.8(5)	6.9(6)	4.0(5)	3.5(5)	-1.4(4)	-0.6(4)
C5	0.1546(10)	0.7274(12)	0.6234(8)	4.2(5)	6.3(6)	2.8(4)	2.5(4)	0.3(3)	0.0(4)
C6	0.2789(12)	0.7533(12)	0.6978(9)	5.6(6)	5.5(5)	3.2(4)	3.2(5)	0.0(4)	-0.2(4)

[a] Ge atoms are at 0.50 occupancy.

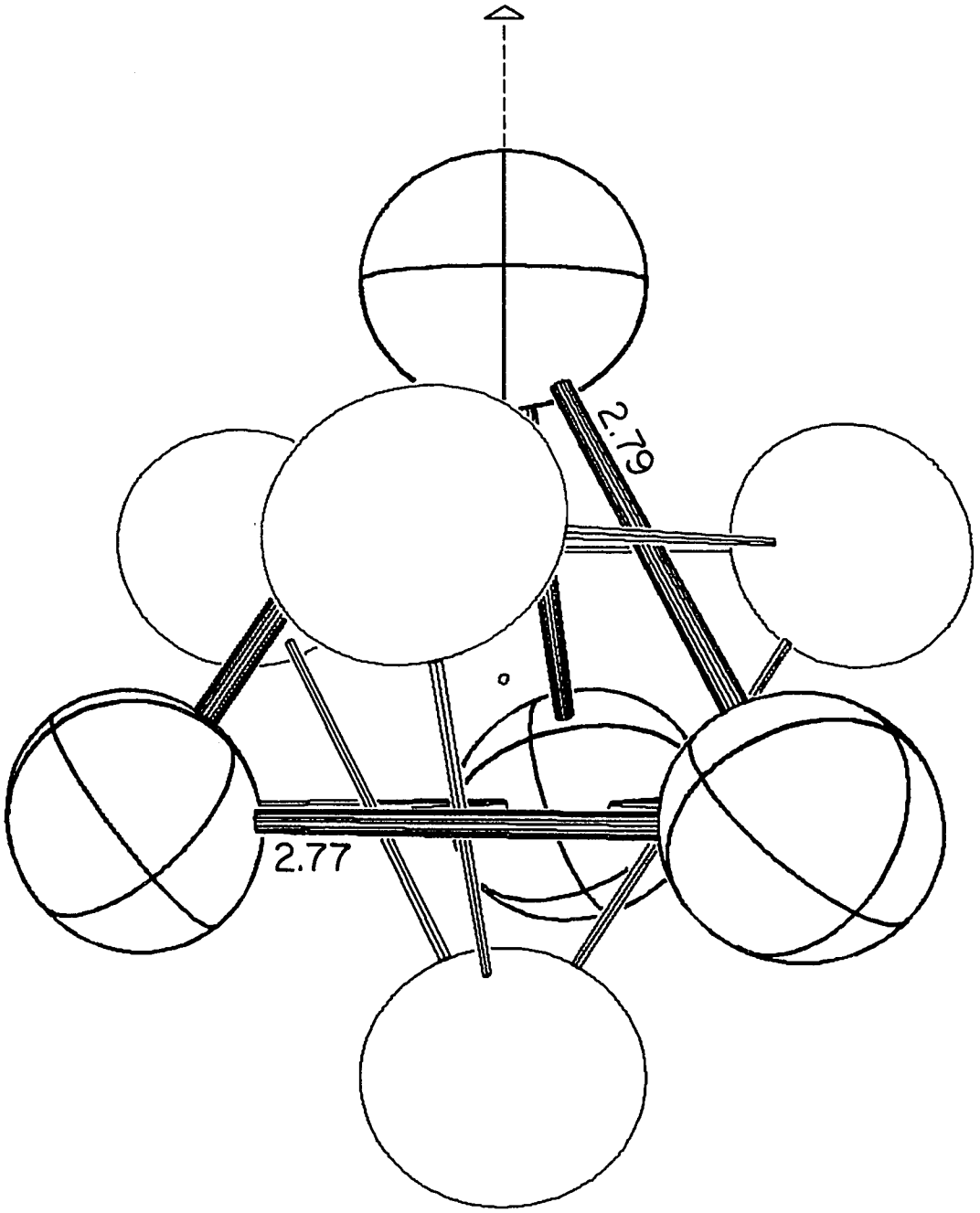

Figure 14. The Ge_4^{2-} anion showing both 0.50 occupancy tetrahedra with C_3 axis vertical

The two inversion-related crypt-Na^+ cations have three-fold symmetry with axes at 1/3,2/3,z and 2/3,1/3,-z; their configuration and packing is nearly identical to that in the middle half of the $(2,2,2\text{-crypt-}Na^+)_2$ - Pb_5^{2-} structure[19] ($P\bar{3}c1$ with a doubled c axis). The sodium atom is similarly off the midpoint of the N-N axis by 0.21 Å; this is an indication of the extent the Na^+ ion is undersized for the 2,2,2-crypt cavity.

The Ge_4^{2-} anion is essentially tetrahedral, only slightly elongated to C_{3v} symmetry, with bond distances of 2.769 (8) Å between basal atoms and 2.793 (9) Å for basal to apex atoms. The two Ge_4^{2-} images actually combine to give a fairly regular cube with distances between the two of 1.987 (7) and 1.946 (7) Å. In spite of the high agreement factors (R = 0.170), the standard deviations for bond distances in this structure are very comparable to those in similar structures (the Ge-Ge distances are somewhat less precise but that is to be expected with the relatively small electron density at each position).

The Ge_4^{2-} anion as an 18-electron tetrahedral cluster is unusual but not unprecedented. Rudolph and coworkers have identified the analogous Sn_4^{2-} anion based on an NMR resonance in solutions of Na-Sn alloys in en.[35] It is interesting to note that Ge_4^{2-} is isoelectronic with the hypothetical $B_4H_4^{2-}$ anion. The Ge_4^{2-} anion with either exact T_d or C_{3v} symmetry would require two unpaired electrons in the highest e-orbital and should be first-order Jahn-Teller unstable; ESR measurements on this compound indicate no unpaired spin density. A study of Sn_4^{2-} by Rothman, Bartell and Lohr[59] using effective potential calculations predicts a minimum in total valence energy for a compressed tetrahedron (D_{2d}), and

also predicts fluxional behavior, related to a second-order Jahn-Teller effect, through three compressed and three elongated tetrahedra (D_{2d}). Since the crystal symmetry forces Ge_4^{2-} in this compound to have at least C_{3v} symmetry, the relatively large thermal ellipsoids observed and the left-over electron density near the cluster on a difference map may be the result of the occurrence of such D_{2d} structures in all their possible orientations, giving average tetrahedral symmetry.

The Ge-Ge bond distances (2.781 Å average) are also surprisingly long. Comparable distances in Ge_9^{4-} and Ge_9^{2-} average 2.623 and 2.649 Å, respectively;[22] the tetrahedral cluster in the alloy NaGe which formally is Ge_4^{4-} has distances which average 2.56 Å.[41] The 20-electron tetrahedral clusters $Sn_2Bi_2^{2-}$ and $Pb_2Sb_2^{2-}$ appear to have normal bond lengths; it is hard to understand why the 18-electron count for Ge_4^{2-} should result in bond lengths about 0.2 Å too long. However, the study by Rothman et al. does predict a similar lengthening of bond distances for Sn_4^{2-} (3.26 Å) compared to Sn_9^{4-} (3.02 Å) or Sn_5^{2-} (2.95 Å).

It is interesting that the alloy used in the reaction to produce this compound does contain tetrahedral Ge_4 units, formally with a 4- charge, so the cluster unit seemingly remains intact. A 4- charge is according to experience too high for the cluster to retain in solution. It is unfortunate that the high agreement factors and disorder problems in this structure prevent a precise description of the Ge_4^{2-} anion; in actual fact one cannot be completely certain the anion is truly 'naked'. The isolation of this anion in a lower symmetry salt would be useful,

though the known tendency of tetrahedral species toward disorder might still cause difficulty.

The $(2,1,1\text{-crypt-}Li^+)_4Sn_9^{4-}$ structure

Table 28 lists the positional and thermal parameters for $(2,1,1\text{-crypt-}Li^+)_4Sn_9^{4-}$. The two (disordered 50:50) Sn_9^{4-} configurations A (C_{4v}) and B (D_{3h}) are shown in Figure 15 and 16, and distances are given in Table 29. Remaining distances for the crypt cations and angles for the structure appear in Appendix A.

There were several indications that the Sn_9^{4-} anion could be resolved into these two components. First, the distances and dihedral angles for the unresolved cluster imply a configuration about halfway between C_{4v} and D_{3h} symmetry. The most telling distances are the diagonals across what would be the basal square face of the C_{4v} configuration. The values are Sn1-Sn3 = 3.856 (7) Å and Sn2-Sn4 = 4.352 (7) Å. These should be equal for C_{4v} symmetry, while Sn1-Sn3 would be one height of the trigonal prism for D_{3h} symmetry. The most important dihedral angles are 169° between planes (1,5,6) and (3,7,8) which would be the opposed faces of the trigonal prism and 9° between planes (1,2,3) and (1,3,4) which are the vicinal triangles in what would be the square base of the C_{4v} configuration (see Table 21 for comparison). All these values are midway between those expected for D_{3h} and C_{4v} configurations. Secondly, some of the tin atoms in the unresolved cluster had wildly elongated 'thermal' ellipsoids suggesting positional disorder, and the elongation directions were correct for a C_{4v}-D_{3h} disorder.

Table 28. Positional and thermal parameters for (2,1,1-crypt-Li)$_4$Sn$_9$

Atom	x	y	z	B11	B22	B33	B12	B13	B23
Sn1	0.3395(2)	0.1912(1)	0.7555(2)	3.8(2)	3.9(2)	5.1(2)	0.4(1)	-1.8(1)	-0.8(2)
Sn2	0.1557(2)	0.1879(1)	0.7002(3)	3.3(2)	3.1(2)	9.7(3)	0.0(1)	-2.4(2)	0.6(2)
Sn8	0.2329(2)	0.0643(1)	0.8274(2)	7.9(2)	3.0(2)	2.9(2)	-0.1(2)	-1.1(1)	0.1(1)
Sn3A[a]	0.1300(5)	0.1349(3)	0.8454(5)	4.5(4)	8.4(5)	6.3(4)	2.5(4)	0.0(3)	2.3(4)
Sn3B	0.1568(7)	0.1424(2)	0.8686(6)	14.9(8)	4.6(5)	6.2(5)	2.2(5)	5.9(5)	-1.4(4)
Sn4A	0.3062(5)	0.1392(2)	0.9019(4)	9.6(5)	5.3(4)	1.5(3)	-1.4(4)	-2.4(3)	-0.3(3)
Sn4B	0.3436(7)	0.1259(3)	0.8888(6)	10.9(7)	14.3(8)	9.9(6)	-9.2(6)	-8.0(5)	6.6(6)
Sn5A	0.4111(4)	0.1111(2)	0.7508(5)	2.1(3)	2.8(3)	9.8(5)	0.9(3)	-1.9(3)	1.3(3)
Sn5B	0.4095(5)	0.1118(3)	0.7150(7)	2.8(4)	5.8(5)	17.9(9)	0.0(4)	-0.5(4)	-1.0(5)
Sn6A	0.3036(4)	0.1460(2)	0.5921(5)	4.4(3)	3.0(3)	6.0(4)	-0.7(3)	-0.2(3)	-1.0(3)
Sn6B	0.2724(5)	0.1464(2)	0.5948(3)	10.3(5)	3.5(3)	0.7(2)	0.7(3)	-0.4(3)	1.1(2)
Sn7A	0.1301(4)	0.1029(2)	0.6649(5)	5.7(4)	1.6(3)	6.5(4)	-1.4(3)	-5.5(3)	0.2(3)
Sn7B	0 1066(5)	0.1038(2)	0.6979(6)	5.4(4)	3.2(4)	12.0(6)	0.8(3)	-2.8(4)	-0.3(4)
Sn9A	0.2970(4)	0.0622(2)	0.6419(4)	6.3(4)	1.7(3)	5.0(3)	0.0(3)	-1.4(3)	-0.6(3)
Sn9B	0.2658(5)	0.0620(2)	0.6457(4)	7.3(4)	3.7(3)	1.7(3)	0.3(3)	0.4(3)	-0.3(3)

Atom	x	y	z	B	Atom	x	y	z	B
L11[b]	0.252(4)	0.323(2)	0.431(4)	3.0(13)	L13	0.760(4)	0.186(2)	0.536(4)	3.1(14)
N100	0.123(2)	0.338(1)	0.509(2)	4.1(7)	N300	0.670(2)	0.239(1)	0.513(2)	4.7(8)
C101	0.095(3)	0.372(2)	0.491(3)	6.3(13)	C301	0.579(3)	0.225(2)	0.548(3)	6.8(13)
C102	0.180(3)	0.403(2)	0.478(3)	6.5(13)	C302	0.595(3)	0.197(1)	0.629(3)	5.5(12)
O103	0.225(2)	0.3893(9)	0.411(2)	5.0(7)	O303	0.648(2)	0.168(1)	0.600(2)	6.5(9)
C104	0.303(3)	0.407(1)	0.400(3)	4.1(11)	C304	0.662(3)	0.132(1)	0.663(3)	5.0(11)
C105	0.352(3)	0.387(1)	0.337(3)	3.5(9)	C305	0.728(3)	0.108(1)	0.618(3)	5.6(11)

[a] A and B denote the disordered pairs of Sn atoms at 0.50 occupancy.

[b] The first digit refers to the crypt, the latter two to the position within the crypt.

Table 28. Continued

Atom	x	y	z	B	Atom	x	y	z	B
O106	0.359(2)	0.3470(8)	0.367(2)	4.3(6)	O306	0.802(2)	0.1317(9)	0.593(2)	4.7(7)
C107	0.395(3)	0.323(2)	0.313(3)	5.4(13)	C307	0.866(3)	0.114(1)	0.541(3)	5.3(11)
C108	0.411(3)	0.280(1)	0.346(3)	4.6(10)	C308	0.939(3)	0.143(2)	0.526(3)	5.8(14)
N109	0.333(2)	0.268(1)	0.394(2)	4.1(8)	N309	0.892(2)	0.176(1)	0.482(2)	4.6(8)
C110	0.276(3)	0.244(2)	0.333(3)	5.7(14)	C310	0.952(3)	0.212(2)	0.490(3)	6.8(13)
C111	0.180(3)	0.251(1)	0.357(3)	4.9(11)	C311	0.926(3)	0.224(1)	0.587(3)	3.7(10)
O112	0.161(2)	0.2921(9)	0.352(2)	4.0(7)	O312	0.834(2)	0.2309(8)	0.596(2)	3.8(6)
C113	0.076(3)	0.300(1)	0.374(3)	5.0(11)	C313	0.806(3)	0.271(1)	0.553(3)	4.8(11)
C114	0.061(3)	0.303(1)	0.467(3)	4.8(11)	C314	0.711(3)	0.270(1)	0.568(3)	5.1(11)
C115	0.149(3)	0.328(2)	0.592(3)	5.9(13)	C315	0.662(4)	0.245(2)	0.420(4)	7.2(15)
C116	0.208(3)	0.294(1)	0.602(3)	4.2(10)	C316	0.663(3)	0.207(1)	0.369(3)	4.1(10)
O117	0.291(2)	0.3067(8)	0.554(2)	3.9(6)	O317	0.734(2)	0.184(1)	0.394(2)	6.2(8)
C118	0.362(3)	0.277(1)	0.548(3)	4.7(10)	C318	0.811(3)	0.194(1)	0.347(3)	3.4(10)
C119	0.342(3)	0.249(1)	0.478(3)	4.8(11)	C319	0.875(4)	0.168(2)	0.385(4)	10.1(20)
L12	0.555(5)	0.427(2)	0.756(5)	3.2(17)	L14	0.448(5)	0.062(2)	0.248(5)	3.8(17)
N200	0.518(2)	0.492(1)	0.803(2)	5.6(10)	N400	0.522(2)	0.079(1)	0.374(2)	3.7(8)
C201	0.565(4)	0.495(2)	0.894(4)	8.3(15)	C401	0.490(3)	0.114(1)	0.416(3)	5.1(11)
C202	0.644(3)	0.469(1)	0.900(3)	5.8(12)	C402	0.482(3)	0.144(1)	0.335(3)	4.7(10)
O203	0.627(2)	0.429(1)	0.867(2)	6.7(9)	O403	0.408(2)	0.1236(9)	0.284(2)	4.6(7)
C204	0.689(3)	0.403(1)	0.877(3)	6.5(12)	C404	0.388(2)	0.147(1)	0.204(2)	4.3(9)
C205	0.658(3)	0.365(2)	0.841(3)	5.9(12)	C405	0.327(3)	0.125(1)	0.149(3)	5.3(11)
O206	0.629(2)	0.376(1)	0.750(2)	5.9(8)	O406	0.379(2)	0.0823(8)	0.143(2)	4.1(6)
C207	0.584(3)	0.345(1)	0.704(3)	4.1(11)	C407	0.326(3)	0.052(1)	0.101(3)	5.0(11)
C208	0.562(3)	0.359(1)	0.622(3)	5.2(11)	C408	0.382(3)	0.018(1)	0.085(3)	5.4(10)
N209	0.502(2)	0.392(1)	0.630(2)	6.0(10)	N409	0.432(2)	0.008(1)	0.167(2)	4.7(9)
C210	0.500(4)	0.424(2)	0.557(4)	6.7(14)	C410	0.520(3)	-0.005(2)	0.153(3)	6.3(13)
C211	0.588(3)	0.449(2)	0.562(3)	5.2(13)	C411	0.580(3)	0.022(2)	0.144(3)	6.5(14)

Table 28. Continued

Atom	x	y	z	B	Atom	x	y	z	B
O212	0.601(2)	0.4665(9)	0.646(2)	5.3(8)	O412	0.577(2)	0.059(1)	0.210(2)	6.2(8)
C213	0.549(3)	0.505(2)	0.645(3)	5.6(14)	C413	0.630(3)	0.044(1)	0.285(3)	6.3(12)
C214	0.548(3)	0.519(2)	0.746(3)	6.7(14)	C414	0.617(3)	0.076(2)	0.342(3)	6.3(12)
C215	0.431(4)	0.493(2)	0.819(4)	10.3(17)	C415	0.500(3)	0.045(1)	0.435(3)	5.1(10)
C216	0.401(4)	0.453(2)	0.835(4)	9.8(17)	C416	0.400(3)	0.034(1)	0.430(3)	4.5(12)
O217	0.422(2)	0.4219(9)	0.783(2)	5.6(8)	O417	0.385(2)	0.0251(8)	0.337(2)	4.0(6)
C218	0.372(3)	0.418(2)	0.695(3)	6.7(14)	C418	0.402(3)	-0.017(1)	0.318(3)	5.8(11)
C219	0.412(3)	0.383(2)	0.652(3)	6.5(13)	C419	0.379(3)	-0.019(2)	0.221(3)	6.0(12)

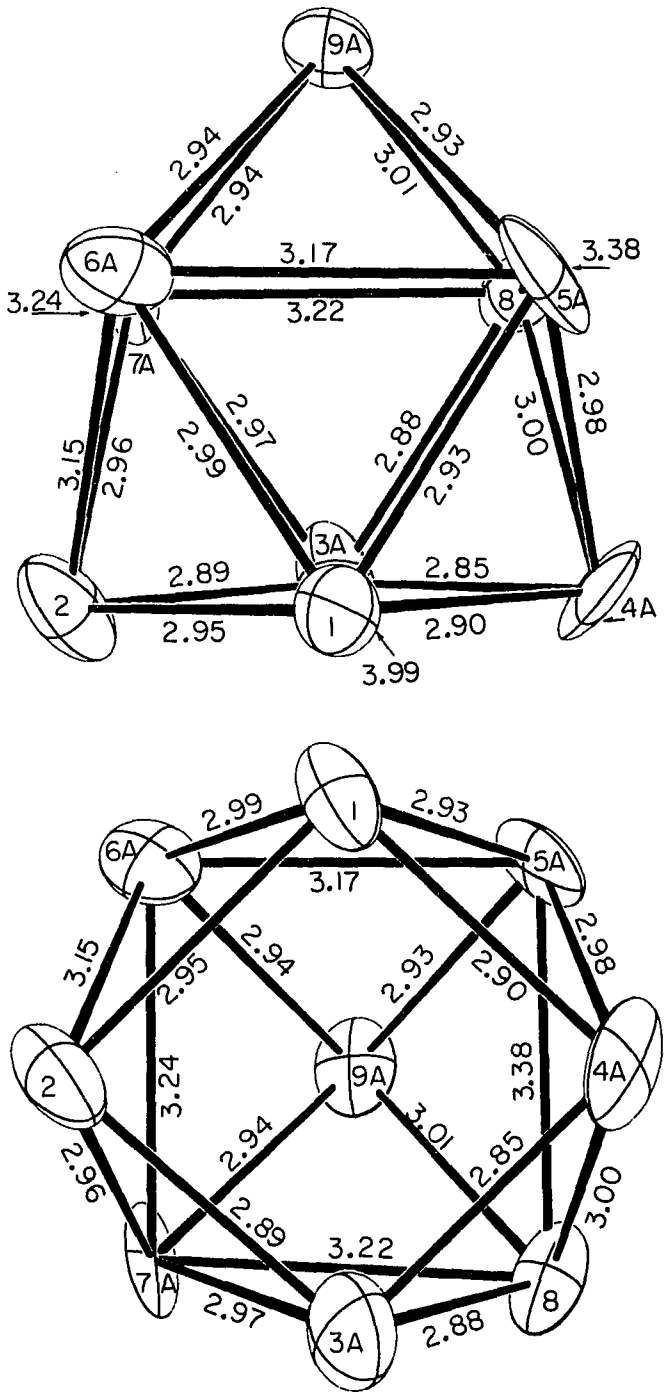

Figure 15. Two views of Sn_9^{4-} cluster A ($\sim C_{4v}$) in $(2,1,1\text{-crypt-}Li^+)_4Sn_9^{4-}$

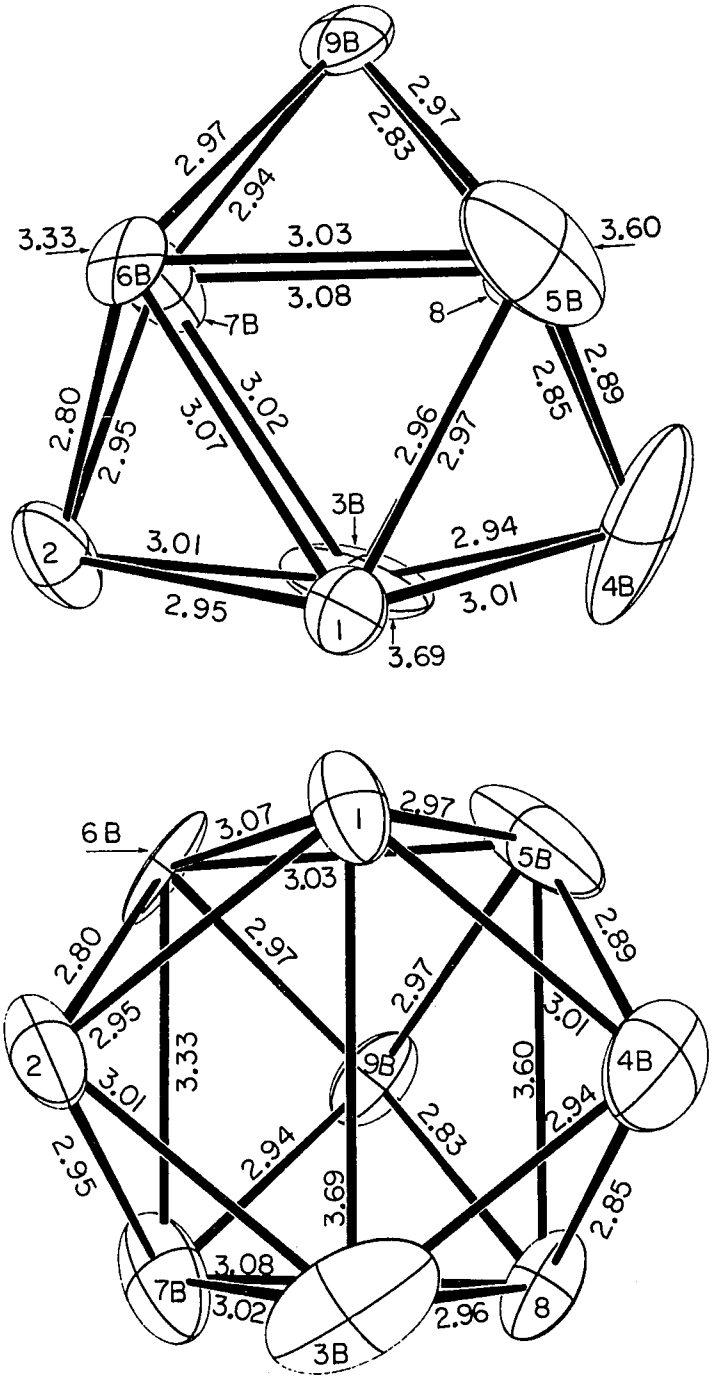

Figure 16. Two views of Sn_9^{4-} cluster B ($\sim D_{3h}$) in $(2,1,1\text{-crypt-}Li^+)_4Sn_9^{4-}$

Table 29. Distances in Sn_9^{4-} A and B in $(2,1,1\text{-crypt-}Li^+)_4Sn_9^{4-}$

A (C_{4v})		B ($\sim D_{3h}$)	
Sn-Sn	Distance (Å)	Sn-Sn	Distance (Å)
1 - 2	2.949 (5)	1 - 3B	3.693 (10)
2 - 3A	2.889 (9)	5B - 8	3.599 (9)
3A - 4A	2.845 (11)	6B - 7B	3.330 (11)
1 - 4A	2.901 (7)	1 - 5B	2.965 (9)
5A - 6A	3.168 (10)	1 - 6B	3.072 (7)
6A - 7A	3.242 (9)	5B - 6B	3.031 (12)
7A - 8	3.224 (8)	3B - 7B	3.025 (12)
5A - 8	3.378 (7)	3B - 8	2.964 (9)
5A - 9A	2.932 (9)	7B - 8	3.078 (9)
6A - 9A	2.945 (9)	1 - 2	2.949 (5)
7A - 9A	2.935 (9)	3B - 2	3.007 (9)
8 - 9A	3.012 (7)	6B - 2	2.798 (8)
1 - 5A	2.930 (7)	7B - 2	2.951 (8)
1 - 6A	2.988 (8)	1 - 4B	3.013 (11)
2 - 6A	3.154 (8)	3B - 4B	2.940 (15)
2 - 7A	2.959 (7)	5B - 4B	2.894 (15)
3A - 7A	2.973 (11)	8 - 4B	2.854 (12)
3A - 8	2.882 (9)	5B - 9B	2.975 (11)
4A - 8	3.002 (8)	6B - 9B	2.966 (9)
4A - 5A	2.981 (10)	7B - 9B	2.939 (10)
1 - 3A	3.991 (9)	8 - 9B	2.833 (6)
2 - 4A	4.196 (8)	2 - 4B	4.592 (11)

After resolving six of the nine tin atoms into two positions, one does indeed obtain two configurations of approximately C_{4v} and D_{3h} symmetry. The resolved atoms are separated by 0.48 (1) Å to 0.76 (1) Å. Cluster A is fairly regular with reasonable bond distances and dihedral angles (see Table 21) for C_{4v} geometry. Distances average 2.956 Å for the capping atom to the capped face, 3.253 Å within the capped face, 2.984 Å for the capped face to the base and 2.896 Å within the base;

comparable values for the Sn_9^{4-} anion in $(2,2,2\text{-crypt-}Na^+)_4Sn_9^{4-}$ [21] are 2.956, 3.242, 2.971 and 2.964 Å, respectively. The base and capped face of the unicapped square antiprism are within ±0.015 and ±0.013 Å of planarity, respectively; the dihedral angle between these planes is 2.0°.

Cluster B is not as regular, retaining some badly elongated ellipsoids, but the D_{3h} geometry is still clearly evident in the bond distances and dihedral angles (see Table 21). The height (h), edge (e) and capping (c) distances for the tricapped trigonal prism average 3.541 Å, 3.023 Å and 2.927 Å, respectively, and the h:e ratio is 1.17; these values are indeed appropriate for a 22 skeletal electron D_{3h} cluster as seen in Table 22 and 24.

The EHMO calculations previously described indicate the C_{4v} configuration for Sn_9^{4-} is preferred over the 15% elongated D_{3h} geometry by a difference of 1.0 eV in total energy. However, the elongation observed here is 17%, for which this calculated difference decreases to only 0.4 eV (for an idealized D_{3h} cluster proportioned according to the distances in cluster B the calculated total energy is -311.34 eV). The Sn_9^{4-} anion is known to be fluxional in solution.[33] The C_{4v} configuration certainly occurs in the 2,2,2-crypt-Na^+ salt; perhaps solid state effects in this 2,1,1-crypt-Li^+ salt help to stabilize the D_{3h} configuration.

The cations in this compound have essentially C_2 symmetry, similar to those found in $(2,1,1\text{-crypt-}Li^+)I^-$.[90] Bond distances range from 2.02 (8) to 2.30 (7) Å for Li-O and from 2.21 (7) to 2.40 (8) Å for Li-N. This is the first structure of a polyatomic anion with 2,1,1-crypt-Li^+ cations. Unfortunately, while the switch from 2,2,2-crypt to the smaller,

less symmetrical 2,1,1-crypt ligand does avoid the three-fold symmetry which often causes disorder, it seems it does not eliminate anion disorder problems.

FUTURE WORK

Clearly, many homo- and heteropolyatomic anions remain to be discovered. Although investigations of the homoatomic systems have been reasonably thorough, some have involved only one alkali metal and the 2,2,2-crypt ligand. Simply switching from sodium to potassium alloys served here to produce the new Sb_4^{2-} and Sn_9^{3-} anions. There are several homopolyatomic anions whose presence is indicated, but which have yet to be structurally characterized. For example, both the original Zintl investigations[8,9] and ^{207}Pb NMR results prove the Pb_9^{4-} anion exists in solution.[34] Sn_4^{2-} has been identified by solution NMR,[35] and there is a second-hand mention of the NMR identification of Sn_9^{2-} as well as analysis of a compound of stoichiometry $Li_2Sn_9 \cdot 2.5en$;[63] however, the small HOMO-LUMO gap found in the EHMO calculations for Sn_9^{2-} may indicate a lack of stability. One can also speculate as to whether isoelectronic anions to known species might exist, such as Ge_5^{2-}, Sn_{10}^{2-}, Sb_{11}^{3-} or Bi_7^{3-}. Also, the paramagnetic Sn_9^{3-} anion is evidence that these clusters are not restricted to even numbers of electrons. The analogous Ge_9^{3-} anion may indeed occur in the 2,2,1-crypt-Na^+ salt.

Investigations of heteroatomic systems have really just begun. So far, most reactions have involved 1:1:1 ternary alloy compositions; other stoichiometries will certainly produce new anions. There are many possibilities just in terms of isoelectronic analogs of known anions. An example is Sn_8Bi^{3-} for which some solution ^{119}Sn NMR evidence exists,[63] and which may be one product of the $KSn_2 + K_3Bi_2$ reactions. However,

the discoveries of $Sn_2Bi_2^{2-}$, $Pb_2Sb_2^{2-}$, and $TlSn_9^{3-}$ demonstrate that the combination of elements from different groups can lead to quite new configurations. Because of their electronic requirements, group IV elements favor closo (or nido) clusters while group V elements favor relatively open and valence-precise anions - the proper combination should produce clusters of intermediate-type configurations. Some hindrances to the successful synthesis and structural characterization of these heteropolyatomic anions include the relative stability of the homopolyatomic species (decanting solutions from the alloy residue before crystal growth is recommended in this respect), the higher probability of multiphase products (for example, members of the $Sn_{9-x}Pb_x^{4-}$ family coexist in solution),[34] and the possibility of anion disorder and corresponding inability to distinguish heteroatoms due to the lack of specificity sometimes provided by the crypt cations (as with $Sn_2Bi_2^{2-}$ and $Pb_2Sb_2^{2-}$).

For both homo- and heteroatomic systems, the choice of alloy and reaction conditions is clearly important. The use of different crypt ligands should be beneficial, although the reactions of 2,2,1-crypt and 2,1,1-crypt here have not been encouraging because of the difficulty of producing crystalline compounds. Because the crypt cations in these structures do dominate the crystal packing, the choice of crypt ligand and corresponding metal cation should be an important factor in anion stability. This dominance (and the disorder problems which often follow) might be minimized if the larger crypt cations are used for the bulkier anions with relatively small charges, while the more reduced or smaller

anions are isolated with the relatively small crypt cations. Another choice in the latter case would be the use of alkaline earth-crypt cations as this would cut the number of crypts per anion in half; $(2,2,2\text{-crypt-}Ba^{2+})_2Se_4^{2-}$ is an example of such a salt.[91] The elusive Pb_9^{4-} anion might be a good candidate for such a change.

The possible effects of the use of ternary alloys in production of new homopolyatomic anions cannot be ignored. While the ease of formation of the new Sb_4^{2-} anion with the ternary alloys KAuSb, KGeSb and KPbSb may be attributed to the change from sodium to potassium cations, it is a fact that large crystals of the Bi_4^{2-} salt are more rapidly formed in the ternary $KSn_2 + K_3Bi_2$ reaction than in previous binary K_3Bi_2 reactions. Of more interest is the unusual compound $(\text{crypt-}K^+)_3(KSn_9)^{3-}$ formed from a reaction of the ternary alloy KHgSn.[18]

There have been several interesting reports recently involving reactions of Zintl anions. Sn_9^{4-} or Pb_9^{4-} will reportedly react with $Pt(PPh_3)_4$ in en to form $(PPh_3)_2PtSn_9^{4-}$ or $(PPh_3)_2PtPb_9^{4-}$ as identified by ^{119}Sn, ^{207}Pb and ^{31}P NMR.[92] Also, Haushalter and Krause have made use of the strong reducing power of these anions in their intriguing electroless metallization reactions to surface modify polyimides,[93] certain inorganic solids, or even the transition metals Pt and Pd.[94] Such investigations of polyatomic anion reactions should prove to be worthwhile endeavors but the basis of that research must first be the thorough knowledge of the synthesis and structure of the anions themselves.

LITERATURE CITED

1. Joannis, A. Compt. Rend. 1891, 113, 795-798; 1892, 114, 585-587.
2. Kraus, C. A. J. Am. Chem. Soc. 1907, 29, 1557-1571.
3. Smyth, F. H. J. Am. Chem. Soc. 1917, 39, 1299-1312.
4. Peck, E. B. J. Am. Chem. Soc. 1918, 40, 335-347.
5. Kraus, C. A.; Kurtz, H. F. J. Am. Chem. Soc. 1925, 47, 43-60.
6. Kraus, C. A. J. Am. Chem. Soc. 1922, 44, 1216-1239.
7. Kraus, C. A. J. Electrochem. Soc. 1924, 45, 175-186.
8. Zintl, E.; Goubeau, J.; Dullenkopf, W. Z. Phys. Chem., Abt. A 1931, 154, 1-46.
9. Zintl, E.; Harder, A. Z. Phys. Chem., Abt. A 1931, 154, 47-91.
10. Zintl, E.; Dullenkopf, W. Z. Phys. Chem., Abt. B 1932, 16, 183-194.
11. Zintl, E.; Kaiser, H. Z. Anorg. Allg. Chem. 1933, 211, 113-131.
12. Cisar, A.; Corbett, J. D. Inorg. Chem. 1977, 16, 2482-2487.
13. Johnson, W. C.; Wheatly, A. C. Z. Anorg. Allg. Chem. 1934, 216, 273-287.
14. Schäfer, H.; Eisenmann, B.; Müller, W. Angew. Chem., Int. Ed. Engl. 1973, 9, 694-712.
15. von Schnering, H.-G. Angew. Chem., Int. Ed. Engl. 1981, 20, 33-51.
16. Dietrich, B.; Lehn, J. M.; Sauvage, J. P. Tetrahedron Lett. 1969, 34, 2885-2888.
17. Lehn, J. M. Struct. and Bond. 1973, 16, 1-69.
18. Corbett, J. D.; Critchlow, S. C.; Burns, R. C. In "Rings, Clusters, and Polymers of the Main Group Elements"; Cowley, A., Ed.; American Chemical Society: Washington, D.C., 1983; ACS Symp. Ser. No. 232; Chapter 6.
19. Edwards, P.; Corbett, J. D. Inorg. Chem. 1977, 16, 903-907.

20. Critchlow, S. C.; Corbett, J. D. J. Am. Chem. Soc. 1983, 105, 5715-5716.

21. Corbett, J. D.; Edwards, P. J. Am. Chem. Soc. 1977, 99, 3313-3317.

22. Belin, C. H. E.; Corbett, J. D.; Cisar, A. J. Am. Chem. Soc. 1977, 99, 7163-7169.

23. Critchlow, S. C.; Corbett, J. D. Inorg. Chem. 1984, 23, accepted.

24. Adolphson, D. G.; Corbett, J. D.; Merryman, D. J. J. Am. Chem. Soc. 1976, 98, 7234-7239.

25. Belin, C. H. E. J. Am. Chem. Soc. 1980, 102, 6036-6040.

26. Critchlow, S. C.; Corbett, J. D. Inorg. Chem. 1982, 21, 3286-3290.

27. Burns, R. C.; Corbett, J. D. J. Am. Chem. Soc. 1981, 103, 2627-2632.

28. Burns, R. C.; Corbett, J. D. J. Am. Chem. Soc. 1982, 104, 2804-2810.

29. Wade, K. Adv. Inorg. Chem. Radiochem. 1976, 18, 1-66.

30. Kummer, D.; Diehl, L. Angew. Chem., Int. Ed. Engl. 1970, 9, 895.

31. Diehl, L.; Khodadadeh, K.; Kummer, D.; Strähle, J. Chem. Ber. 1976, 109, 3404-3418.

32. Teller, R. G.; Krause, L. J.; Haushalter, R. C. Inorg. Chem. 1983, 22, 1809-1812.

33. Rudolph, R. W.; Wilson, W. L.; Parker, F.; Taylor, R. C.; Young, D. C. J. Am. Chem. Soc. 1978, 100, 4629.

34. Rudolph, R. W.; Taylor, R. C.; Young, D. C. In "Fundamental Research in Homogeneous Catalysis"; Tsutsui, M., Ed.; Plenum: New York, 1979; pp. 997-1005.

35. Rudolph, R. W.; Wilson, W. L.; Taylor, R. C. J. Am. Chem. Soc. 1981, 103, 2480-2481.

36. Critchlow, S. C.; Corbett, J. D. J. Chem. Soc., Chem. Commun. 1981, 236-237.

37. Clark, C. M.; Smith, D. K.; Johnson, G. J. "A Fortran IV Program for Calculating X-Ray Powder Diffraction Patterns--Version 5", Department of Geosciences, Pennsylvania State University, 1973.

38. Hansen, M.; Anderko, K. "Constitution of Binary Alloys", 2nd ed.; McGraw-Hill: New York, 1958; pp. 881-882.

39. Hewaidy, I. F.; Busmann, E.; Klemm, W. Z. Anorg. Allg. Chem. 1964, 328, 283-293.

40. Hansen, M.; Anderko, K. "Constitution of Binary Alloys", 2nd ed.; McGraw-Hill: New York, 1958; p. 768.

41. Witte, J.; von Schnering, H.-G. Z. Anorg. Allg. Chem. 1964, 327, 260-273.

42. Bailey, D. M.; Skelton, W. H.; Smith, J. F. J. Less Common Met. 1976, 64, 233-240.

43. Müller, W., Dissertation, Eduard-Zintl-Institut der Technischen Hochschule Darmstadt, West Germany, 1975.

44. Cisar, A.; Corbett, J. D. Inorg. Syn. 1983, 22, in press.

45. Stierman, R. J.; Gschneidner, K. A., Department of Materials Science and Engineering, Iowa State University, to be published.

46. Cisar, A.; Corbett, J. D. Inorg. Chem. 1977, 16, 632-635.

47. Burns, R. C.; Corbett, J. D. Inorg. Chem. 1981, 20, 4433-4434.

48. Belin, C. H. E.; Charbonnel, M. M. Inorg. Chem. 1982, 21, 2504-2506.

49. Burns, R. C.; Corbett, J. D., Ames Laboratory, Iowa State University, unpublished research.

50. Corbett, J. D., Ames Laboratory, Iowa State University, unpublished research.

51. Schroeder, D. R.; Jacobson, R. A. Inorg. Chem. 1973, 12, 210-213.

52. Jacobson, R. A. J. Appl. Crystallogr. 1976, 9, 115-118.

53. Karcher, B., Ph. D. Dissertation, Iowa State University, 1981.

54. Takusagawa, F., Ames Laboratory, Iowa State University, unpublished program, 1976.

55. Lapp, R. L.; Jacobson, R. A., Ames Laboratory, Iowa State University, unpublished program, 1979.

56. Powell, D. R.; Jacobson, R. A., Ames Laboratory, Iowa State University, unpublished program, 1979.

57. "International Tables for X-Ray Crystallography", Vol. III; Kynoch Press: Birmingham, England, 1968.

58. Johnson, C. K. "ORTEP: A Fortran Thermal-Ellipsoid Plot Program for Crystal Structure Illustrations", ORNL Report 3794, Oak Ridge National Laboratory, Oak Ridge, TN, 1970.

59. Rothman, M. J.; Bartell, L. S.; Lohr, L. L., Jr. J. Am. Chem. Soc. 1981, 103, 2482-2483.

60. Main, P. "MULTAN 80, A System of Computer Programs for the Automatic Solution of Crystal Structures for X-Ray Diffraction Data", University of York Printing Unit: York, United Kingdom, 1980.

61. Friedman, R. M.; Corbett, J. D. Inorg. Chem. 1973, 12, 1134-1139.

62. Hart, R. R.; Robin, M. B.; Kuebler, N. A. J. Chem. Phys. 1965, 42, 3631-3638.

63. Wilson, W. L., Ph. D. Dissertation, University of Michigan, 1982.

64. Dahlmann, W.; v. Schnering, H.-G. Naturwissenschaften 1972, 59, 420; 1973, 60, 429.

65. Schmettow, W.; von Schnering, H.-G. Angew. Chem., Int. Ed. Engl. 1977, 16, 857.

66. Leung, Y. C.; Waser, J.; van Houten, S.; Vos, A.; Wiegers, G. A.; Wiebenga, F. H. Acta Crystallogr., Sect. B 1957, 10, 574-576.

67. Hönle, W.; von Schnering, H.-G. Z. Anorg. Allg. Chem. 1978, 440, 171-182.

68. Hamilton, W. C.; Ibers, J. C. "Hydrogen Bonding in Solids"; Benjamin: New York, 1968; p. 16.

69. Bondi, A. J. Phys. Chem. 1964, 68, 441-452.

70. Drago, R. S. "Physical Methods in Chemistry"; W. B. Saunders Co.: Philadelphia, 1977; p. 413.

71. Selwood, P. W. "Magnetochemistry", 2nd ed.; Interscience: New York, 1956; p. 78.

72. Burns, R. C., Department of Chemistry, McMaster University, Hamilton, Ontario, Canada, private communication, 1982.

73. Burns, R. C.; Gillespie, R. J.; Garnes, J. A.; McGlinchey, M. J. Inorg. Chem. 1982, 21, 799-807.

74. King, R. B. Inorg. Chim. Acta 1982, 57, 79-86.

75. Wade, K.; O'Neill, M. E. J. Molec. Str. 1983, 103, 259-268.

76. Wade, K.; O'Neill, M. E. Polyhedron, 1983, 2, 963-966.

77. Guggenberger, L. J. Inorg. Chem. 1968, 11, 2260-2264.

78. Koetzle, T. F.; Scarbrough, F. E.; Lipscomb, W. N. Inorg. Chem. 1968, 7, 1076-1084.

79. Guggenberger, L. J.; Muetterties, E. L. J. Am. Chem. Soc. 1976, 98, 7221-7225.

80. Corbett, J. D.; Rundle, R. E. Inorg. Chem. 1964, 3, 1408-1412.

81. Lohr, L. L. Inorg. Chem. 1981, 20, 4229-4235.

82. Schaffer, A. M.; Gouterman, M.; Davidson, E. R. Theoret. Chim. Acta (Berl.) 1973, 30, 9-30.

83. Baetzold, R. C. Adv. in Catalysis 1976, 25, 1-55.

84. McGlynn, S. P.; Vanquickenborne, L. G.; Kinoshita, M.; Carroll, D. G. "Introduction to Applied Quantum Chemistry"; Holt, Rinehart and Winston, Inc.: New York, 1972; Chapter 4.

85. Moore, C. E. "Atomic Energy Levels", Natl. Stand. Ref. Data Ser., Natl. Bur. Stand. (U.S.) 1971, NSRDS-NBS 35, Vol. III.

86. Politzer, P. Trans. Faraday Soc. 1968, 64, 2241-2246.

87. Cusachs, L. C.; Corrington, J. H. In "Sigma Molecular Orbital Theory"; Sinanoglu, O.; Wiberg, K. B., Eds.; Yale University Press: New Haven, Conn., 1970; Chapter IV-4.

88. Hursthouse, M. B.; Kane, J.; Massey, A. G. Nature 1970, 228, 659-660.

89. Hershaft, A.; Corbett, J. D. Inorg. Chem. 1963, 2, 979-985.

90. Moras, D.; Weiss, R. Acta Crystallogr., Sect. B 1973, 29, 400-403.

91. Koenig, T.; Eisenmann, B.; Schäfer, H. Z. Anorg. Allg. Chem. 1983, 498, 99-104.

92. Teixidor, F.; Luetkens, M. L., Jr.; Rudolph, R. W. J. Am. Chem. Soc. 1983, 105, 149-150.

93. Haushalter, R. C. Angew. Chem., Int. Ed. Engl. 1983, 22, 558-559; Angew. Chem. Suppl. 1983, 766-777.

94. Krause, L.; Haushalter, R. Thin Solid Films 1983, 102, 161-171.

ACKNOWLEDGEMENTS

I would especially like to thank Professor John D. Corbett for his advice and patience throughout these investigations.

I also thank Dr. R. A. Jacobson and members of his research group for the use of the diffractometers and access to the crystallographic programs; in particular I am grateful to J. Richardson for his assistance with the low temperature data collection set-up.

F. Laabs is thanked for the microprobe analyses, R. Stierman kindly assisted with the magnetic susceptibility work, and G. Lukat was a great help in obtaining the ESR spectra.

Especial thanks are due to Dr. R. C. Burns for the NMR data as well as for many valuable discussions. The past and present members of Physical and Inorganic Chemistry Group IX of the Ames Laboratory will always be fondly remembered for their help and friendship.

Last, but by no means least, I wish to thank my parents and family whose encouragement, love and understanding have sustained me throughout my educational years.

APPENDIX A: ADDITIONAL DISTANCES AND ANGLES

Table A. 1. Additional distances (Å) in (2,2,2-crypt-K)$_2$Sn$_2$Bi$_2$.en

Atom	Atom	Distance	Atom	Atom	Distance	Atom	Atom	Distance	Atom	Atom	Distance
K1	N10	2.99(4)	K1	O33	2.77(3)	K2	N40	2.96(4)	K2	O63	2.84(3)
K1	N19	3.00(4)	K1	O16	2.88(2)	K2	N49	2.91(4)	K2	O46	2.88(3)
K1	O13	2.75(3)	K1	O26	2.86(3)	K2	O43	2.79(2)	K2	O56	2.83(3)
K1	O23	2.78(3)	K1	O36	2.85(3)	K2	O53	2.88(2)	K2	O66	2.84(3)
N10	C11	1.50(6)	N19	C18	1.45(5)	N40	C41	1.53(6)	N49	C48	1.46(7)
N10	C21	1.45(6)	N19	C28	1.46(5)	N40	C51	1.48(6)	N49	C58	1.52(6)
N10	C31	1.42(6)	N19	C38	1.50(6)	N40	C61	1.49(7)	N49	C68	1.52(7)
O13	C12	1.37(6)	O16	C15	1.46(5)	O43	C42	1.31(6)	O46	C45	1.45(5)
O13	C14	1.38(5)	O16	C17	1.40(6)	O43	C44	1.54(6)	O46	C47	1.40(8)
O23	C22	1.35(7)	O26	C25	1.47(4)	O53	C52	1.41(6)	O56	C55	1.50(5)
O23	C24	1.43(5)	O26	C27	1.37(5)	O53	C54	1.44(4)	O56	C57	1.43(6)
O33	C32	1.31(7)	O36	C35	1.48(5)	O63	C62	1.46(6)	O66	C65	1.36(5)
O33	C34	1.44(6)	O36	C37	1.37(6)	O63	C64	1.55(4)	O66	C67	1.35(7)
C11	C12	1.60(7)	C27	C28	1.54(6)	C41	C42	1.45(7)	C57	C58	1.38(7)
C14	C15	1.57(6)	C31	C32	1.52(8)	C44	C45	1.43(7)	C61	C62	1.64(7)
C17	C18	1.51(7)	C34	C35	1.36(7)	C47	C48	1.57(9)	C64	C65	1.34(6)
C21	C22	1.63(8)	C37	C38	1.58(7)	C51	C52	1.60(6)	C67	C68	1.51(8)
C24	C25	1.39(7)				C54	C55	1.41(7)			
NEN1	CEN1	1.2(3)	CEN2	NEN2	1.4(2)	SnBi1	C12	3.99(4)	SnBi3	C22	4.05(5)
CEN1	CEN2	1.9(2)				SnBi1	C32	4.01(5)	SnBi4	CEN1	4.09(18)

Table A.2. Additional angles (deg) in (2,2,2-crypt-K)$_2$Sn$_2$Bi$_2$.en

Atom	Atom	Atom	Angle	Atom	Atom	Atom	Angle	Atom	Atom	Atom	Angle	Atom	Atom	Atom	Angle
N10	K1	N19	178.9(8)	N19	K1	O26	59.6(8)	N40	K2	N49	178.0(10)	N49	K2	O56	62.5(9)
N10	K1	O13	61.2(9)	N19	K1	O36	61.2(8)	N40	K2	O43	61.9(9)	N49	K2	O66	59.8(10)
N10	K1	O23	60.3(9)	O13	K1	O16	59.3(8)	N40	K2	O53	61.6(9)	O43	K2	O46	59.6(9)
N10	K1	O33	59.6(10)	O23	K1	O26	59.8(9)	N40	K2	O63	59.8(9)	O53	K2	O56	58.6(8)
N19	K1	O16	61.1(8)	O33	K1	O36	59.4(10)	N49	K2	O46	61.6(10)	O63	K2	O66	59.8(8)
K1	N10	C11	109(3)	K1	N19	C18	109(3)	K2	N40	C41	107(3)	K2	N49	C48	113(3)
K1	N10	C21	112(3)	K1	N19	C28	107(3)	K2	N40	C51	111(3)	K2	N49	C58	106(3)
K1	N10	C31	112(3)	K1	N19	C38	109(3)	K2	N40	C61	114(3)	K2	N49	C68	111(3)
C11	N10	C21	108(4)	C18	N19	C28	109(3)	C41	N40	C51	105(3)	C48	N49	C58	109(4)
C11	N10	C31	110(4)	C18	N19	C38	110(3)	C41	N40	C61	111(4)	C48	N49	C68	107(4)
C21	N10	C31	106(4)	C28	N19	C38	113(3)	C51	N40	C61	109(4)	C58	N49	C68	111(4)
K1	O13	C12	123(2)	K1	O26	C25	112(2)	K2	O43	C42	113(2)	K2	O56	C55	115(2)
K1	O13	C14	125(3)	K1	O26	C27	118(2)	K2	O43	C44	116(2)	K2	O56	C57	116(2)
C12	O13	C14	104(3)	C25	O26	C27	112(3)	C42	O43	C44	116(3)	C55	O56	C57	115(3)
K1	O16	C15	113(2)	K1	O33	C32	119(3)	K2	O46	C45	118(3)	K2	O63	C62	120(2)
K1	O16	C17	115(2)	K1	O33	C34	116(3)	K2	O46	C47	117(3)	K2	O63	C64	112(2)
C15	O16	C17	113(3)	C32	O33	C34	114(4)	C45	O46	C47	107(3)	C62	O63	C64	111(3)
K1	O23	C22	118(3)	K1	O36	C35	111(2)	K2	O53	C52	112(2)	K2	O66	C65	115(3)
K1	O23	C24	119(2)	K1	O36	C37	115(2)	K2	O53	C54	116(2)	K2	O66	C67	121(3)
C22	O23	C24	111(3)	C35	O36	C37	111(3)	C52	O53	C54	112(3)	C65	O66	C67	110(4)
N10	C11	C12	113(4)	O26	C25	C24	113(3)	N40	C41	C42	109(4)	O56	C55	C54	109(4)
O13	C12	C11	108(4)	O26	C27	C28	105(3)	O43	C42	C41	118(4)	O56	C57	C58	113(4)
O13	C14	C15	108(3)	N19	C28	C27	112(4)	O43	C44	C45	114(4)	N49	C58	C57	118(4)
O16	C15	C14	109(3)	N10	C31	C32	112(5)	O46	C45	C44	107(3)	N40	C61	C62	106(4)
O16	C17	C18	112(4)	O33	C32	C31	115(4)	O46	C47	C48	112(5)	O63	C62	C61	106(4)
N19	C18	C17	116(4)	O33	C34	C35	113(4)	N49	C48	C47	114(5)	O63	C64	C65	109(3)
N10	C21	C22	109(4)	O36	C35	C34	107(3)	N40	C51	C52	105(3)	O66	C65	C64	118(4)
O23	C22	C21	109(4)	O36	C37	C38	110(3)	O53	C52	C51	111(3)	O66	C67	C68	108(4)
O23	C24	C25	113(3)	N19	C38	C37	110(4)	O53	C54	C55	109(3)	N49	C68	C67	113(5)
NEN1	CEN1	CEN2	67(12)	CEN1	CEN2	NEN2	124(12)								

Table A.3. Additional distances (Å) in (2,2,2-crypt-K)$_2$Pb$_2$Sb$_2$.en

Atom	Atom	Distance	Atom	Atom	Distance	Atom	Atom	Distance	Atom	Atom	Distance
K1	N10	3.02(3)	K1	O33	2.80(2)	K2	N40	2.95(3)	K2	O63	2.86(2)
K1	N19	2.99(3)	K1	O16	2.87(2)	K2	N49	2.94(3)	K2	O46	2.87(2)
K1	O13	2.78(2)	K1	O26	2.89(2)	K2	O43	2.81(2)	K2	O56	2.80(2)
K1	O23	2.77(2)	K1	O36	2.90(2)	K2	O53	2.85(2)	K2	O66	2.86(2)
N10	C11	1.42(5)	N19	C18	1.51(4)	N40	C41	1.48(4)	N49	C48	1.35(5)
N10	C21	1.45(5)	N19	C28	1.48(4)	N40	C51	1.47(4)	N49	C58	1.49(5)
N10	C31	1.46(5)	N19	C38	1.47(4)	N40	C61	1.41(5)	N49	C68	1.58(5)
O13	C12	1.41(5)	O16	C15	1.48(4)	O43	C42	1.44(4)	O46	C45	1.50(4)
O13	C14	1.49(4)	O16	C17	1.42(5)	O43	C44	1.46(4)	O46	C47	1.35(5)
O23	C22	1.33(5)	O26	C25	1.44(4)	O53	C52	1.40(5)	O56	C55	1.45(4)
O23	C24	1.44(4)	O26	C27	1.37(4)	O53	C54	1.42(4)	O56	C57	1.48(4)
O33	C32	1.33(5)	O36	C35	1.43(4)	O63	C62	1.45(5)	O66	C65	1.38(4)
O33	C34	1.40(4)	O36	C37	1.39(5)	O63	C64	1.51(4)	O66	C67	1.47(5)
C11	C12	1.57(5)	C27	C28	1.55(4)	C41	C42	1.48(5)	C57	C58	1.58(5)
C14	C15	1.45(5)	C31	C32	1.58(6)	C44	C45	1.46(6)	C61	C62	1.57(5)
C17	C18	1.52(5)	C34	C35	1.46(5)	C47	C48	1.56(6)	C64	C65	1.46(6)
C21	C22	1.61(6)	C37	C38	1.58(5)	C51	C52	1.58(5)	C67	C68	1.43(6)
C24	C25	1.44(5)				C54	C55	1.46(5)			
NEN1	CEN2	1.46(14)	CEN3	NEN4	1.39(12)	PbSb1	NEN1	3.87(8)	PbSb2	C12	3.96(4)
CEN2	CEN3	1.47(15)				PbSb1	C32	3.99(4)	PbSb4	C64	3.99(3)

Table A.4. Additional angles (deg) in (2,2,2-crypt-K)$_2$Pb$_2$Sb$_2$.en

Atom	Atom	Atom	Angle	Atom	Atom	Atom	Angle	Atom	Atom	Atom	Angle	Atom	Atom	Atom	Angle
N10	K1	N19	179.3(7)	N19	K1	O26	60.3(6)	N40	K2	N49	179.3(8)	N49	K2	O56	62.2(8)
N10	K1	O13	60.5(7)	N19	K1	O36	59.7(7)	N40	K2	O43	62.8(7)	N49	K2	O66	62.4(8)
N10	K1	O23	60.9(7)	O13	K1	O16	60.2(7)	N40	K2	O53	61.5(7)	O43	K2	O46	59.2(6)
N10	K1	O33	60.8(8)	O23	K1	O26	58.8(6)	N40	K2	O63	60.5(7)	O53	K2	O56	58.7(7)
N19	K1	O16	60.3(7)	O33	K1	O36	60.1(7)	N49	K2	O46	59.2(8)	O63	K2	O66	58.0(7)
K1	N10	C11	110(2)	K1	N19	C18	110(2)	K2	N40	C41	108(2)	K2	N49	C48	115(3)
K1	N10	C21	111(2)	K1	N19	C28	110(2)	K2	N40	C51	112(2)	K2	N49	C58	108(2)
K1	N10	C31	112(2)	K1	N19	C38	113(2)	K2	N40	C61	111(2)	K2	N49	C68	110(2)
C11	N10	C21	109(3)	C18	N19	C28	109(2)	C41	N40	C51	108(3)	C48	N49	C58	112(3)
C11	N10	C31	109(3)	C18	N19	C38	106(2)	C41	N40	C61	110(3)	C48	N49	C68	109(3)
C21	N10	C31	106(3)	C28	N19	C38	110(2)	C51	N40	C61	108(3)	C58	N49	C68	102(3)
K1	O13	C12	120(2)	K1	O26	C25	114(2)	K2	O43	C42	114(2)	K2	O56	C55	117(2)
K1	O13	C14	118(2)	K1	O26	C27	118(2)	K2	O43	C44	117(2)	K2	O56	C57	117(2)
C12	O13	C14	110(2)	C25	O26	C27	111(2)	C42	O43	C44	116(2)	C55	O56	C57	110(2)
K1	O16	C15	110(2)	K1	O33	C32	116(2)	K2	O46	C45	117(2)	K2	O63	C62	120(2)
K1	O16	C17	118(2)	K1	O33	C34	117(2)	K2	O46	C47	119(2)	K2	O63	C64	117(2)
C15	O16	C17	115(2)	C32	O33	C34	115(3)	C45	O46	C47	108(3)	C62	O63	C64	111(2)
K1	O23	C22	118(2)	K1	O36	C35	110(2)	K2	O53	C52	115(2)	K2	O66	C65	119(2)
K1	O23	C24	119(2)	K1	O36	C37	118(2)	K2	O53	C54	116(2)	K2	O66	C67	115(2)
C22	O23	C24	111(3)	C35	O36	C37	111(2)	C52	O53	C54	110(2)	C65	O66	C67	112(3)
N10	C11	C12	114(3)	O26	C25	C24	108(3)	N40	C41	C42	112(3)	O56	C55	C54	107(3)
O13	C12	C11	108(3)	O26	C27	C28	111(2)	O43	C42	C41	114(3)	O56	C57	C58	107(3)
O13	C14	C15	106(3)	N19	C28	C27	113(2)	O43	C44	C45	114(3)	N49	C58	C57	109(3)
O16	C15	C14	110(3)	N10	C31	C32	109(3)	O46	C45	C44	105(3)	N40	C61	C62	116(3)
O16	C17	C18	110(3)	O33	C32	C31	116(3)	O46	C47	C48	114(3)	O63	C62	C61	107(3)
N19	C18	C17	112(3)	O33	C34	C35	112(3)	N49	C48	C47	114(4)	O63	C64	C65	107(3)
N10	C21	C22	111(3)	O36	C35	C34	110(3)	N40	C51	C52	110(3)	O66	C65	C64	112(3)
O23	C22	C21	113(3)	O36	C37	C38	109(3)	O53	C52	C51	111(3)	O66	C67	C68	113(3)
O23	C24	C25	113(3)	N19	C38	C37	112(3)	O53	C54	C55	110(3)	N49	C68	C67	115(3)
NEN1	CEN2	CEN3	100(9)	CEN2	CEN3	NEN4	124(9)								

Table A.5. Additional distances (Å) in (2,2,2-crypt-K)$_2$Sb$_4$

Atom	Atom	Distance	Atom	Atom	Distance
K	O6	2.749(6)	K	O13	2.847(7)
K	O16	2.773(5)	K	O23	2.816(7)
K	O26	2.780(5)	K	NO	2.963(7)
K	O3	2.831(8)	K	N9	2.990(6)
O3	C2a	1.504(2)	O23	C24	1.395(1)
O3	C2b	1.440(3)	O6	C5	1.458(1)
O3	C4	1.441(2)	O6	C7	1.442(1)
O13	C12a	1.501(2)	O16	C15	1.408(1)
O13	C12b	1.515(2)	O16	C17	1.419(1)
O13	C14	1.420(1)	O26	C25	1.435(1)
O23	C22a	1.547(2)	O26	C27	1.401(1)
O23	C22b	1.428(2)			
NO	C1a	1.397(2)	NO	C21	1.447(2)
NO	C1b	1.544(3)	N9	C8	1.477(1)
NO	C11a	1.466(2)	N9	C18	1.483(1)
NO	C11b	1.489(3)	N9	C28	1.479(1)
C1a	C2a	1.467(3)	C4	C5	1.417(2)
C1b	C2b	1.556(4)	C14	C15	1.502(1)
C11a	C12a	1.465(3)	C24	C25	1.476(2)
C11b	C12b	1.638(3)	C7	C8	1.526(1)
C21	C22a	1.159(3)	C17	C18	1.512(1)
C21	C22b	1.503(3)	C27	C28	1.537(1)
C1a	C1b	0.693(3)	C12a	C12b	0.973(3)
C11a	C11b	0.757(3)	C22a	C22b	0.902(3)
C2a	C2b	0.980(4)			
C1a	C2b	1.464(3)	C11a	C12b	1.309(3)
C1b	C2a	1.098(3)	C11b	C12a	1.292(3)

Table A.6. Additional angles (deg) in (2,2,2-crypt-K)$_2$Sb$_4$

Atom	Atom	Atom	Angle	Atom	Atom	Atom	Angle
O3	K	O6	61.8(2)	O23	K	NO	61.7(2)
O3	K	NO	60.5(2)	O6	K	N9	60.9(2)
O13	K	O16	60.8(2)	O26	K	N9	60.4(2)
O13	K	NO	61.2(2)	O16	K	N9	60.5(1)
O23	K	O26	61.0(2)	NO	K	N9	179.6(2)
K	O3	C2a	115.4(10)	K	O23	C24	109.2(6)
K	O3	C2b	116.7(11)	C22a	O23	C24	126.3(11)
K	O3	C4	104.9(6)	C22b	O23	C24	95.6(11)
C2a	O3	C4	128.6(12)	K	O6	C5	115.6(6)
C2b	O3	C4	95.3(13)	K	O6	C7	119.3(5)
K	O13	C12a	118.1(9)	C5	O6	C7	111.7(7)
K	O13	C12b	113.4(9)	K	O26	C25	114.7(5)
C12a	O13	C14	124.7(10)	K	O26	C27	120.8(4)
K	O13	C14	107.7(5)	C25	O26	C27	112.5(6)
C12b	O13	C14	97.3(10)	K	O16	C15	116.7(4)
K	O23	C22a	112.0(9)	K	O16	C17	120.8(4)
K	O23	C22b	116.0(9)	C15	O16	C17	110.8(6)
K	NO	C1a	112.5(9)	C11a	NO	C21	118.7(11)
K	NO	C1b	105.8(10)	C11b	NO	C21	94.4(12)
K	NO	C11a	109.9(8)	K	N9	C8	108.3(4)
K	NO	C11b	106.4(10)	K	N9	C18	108.6(4)
K	NO	C21	109.3(6)	K	N9	C28	109.6(4)
C1a	NO	C11a	109.4(13)	C8	N9	C18	111.1(6)
C1b	NO	C11b	117.6(15)	C8	N9	C28	109.9(6)
C1a	NO	C21	96.5(12)	C18	N9	C28	109.2(6)
C1b	NO	C21	122.3(13)				
NO	C1a	C2a	115.6(17)	O3	C4	C5	111.4(11)
NO	C1b	C2b	110.0(19)	O13	C14	C15	108.0(7)
NO	C11b	C12b	105.6(17)	O23	C24	C25	108.2(9)
NO	C11a	C12a	119.8(15)	O6	C5	C4	110.2(9)
NO	C21	C22a	128.4(15)	O16	C15	C14	109.9(7)
NO	C21	C22b	120.8(13)	O26	C25	C24	111.0(8)
O3	C2a	C1a	110.4(17)	O6	C7	C8	106.7(7)
O3	C2b	C1b	98.8(19)	O16	C17	C18	108.7(7)
O13	C12b	C11b	97.2(15)	O26	C27	C28	109.3(6)
O13	C12a	C11a	107.8(15)	N9	C8	C7	112.7(7)
O23	C22a	C21	122.8(19)	N9	C18	C17	113.6(7)
O23	C22b	C21	108.7(15)	N9	C28	C27	112.6(6)

Table A.7. Additional distances (Å) in (2,2,2-crypt-K)$_3$Sb$_7$.2en

Atom	Atom	Distance	Atom	Atom	Distance	Atom	Atom	Distance
K1	O103	2.89(1)	K2	O203	2.84(1)	K3	O303	2.85(1)
K1	O106	2.82(1)	K2	O206	2.76(1)	K3	O306	2.86(1)
K1	O112	2.75(1)	K2	O212	2.83(1)	K3	O312	2.85(1)
K1	O115	2.91(1)	K2	O215	2.81(2)	K3	O315	2.83(1)
K1	O120	2.87(1)	K2	O220	2.87(1)	K3	O320	2.83(1)
K1	O123	2.81(1)	K2	O223	2.88(2)	K3	O323	2.86(1)
K1	N100	2.99(1)	K2	N200	2.96(1)	K3	N300	2.92(1)
K1	N109	3.04(2)	K2	N209	2.99(2)	K3	N309	2.87(1)
N100	C101	1.50(3)	N200	C201	1.47(2)	N300	C301	1.46(2)
N100	C110	1.51(3)	N200	C210	1.50(2)	N300	C310	1.50(2)
N100	C118	1.47(2)	N200	C218	1.44(2)	N300	C318	1.50(2)
N109	C108	1.49(3)	N209	C208	1.49(3)	N309	C308	1.50(2)
N109	C117	1.44(3)	N209	C217	1.45(3)	N309	C317	1.48(2)
N109	C125	1.50(3)	N209	C225	1.49(4)	N309	C325	1.47(2)
O103	C102	1.42(2)	O203	C202	1.43(2)	O303	C302	1.42(2)
O103	C104	1.45(2)	O203	C204	1.46(2)	O303	C304	1.45(2)
O106	C105	1.42(2)	O206	C205	1.42(3)	O306	C305	1.42(2)
O106	C107	1.43(2)	O206	C207	1.43(3)	O306	C307	1.44(2)
O112	C111	1.44(3)	O212	C211	1.46(2)	O312	C311	1.45(2)
O112	C113	1.44(3)	O212	C213	1.46(2)	O312	C313	1.42(2)
O115	C114	1.44(3)	O215	C214	1.38(3)	O315	C314	1.41(2)
O115	C116	1.48(3)	O215	C216	1.45(3)	O315	C316	1.43(2)
O120	C119	1.44(2)	O220	C219	1.44(3)	O320	C319	1.42(2)
O120	C121	1.40(2)	O220	C221	1.44(3)	O320	C321	1.45(2)
O123	C122	1.42(2)	O223	C222	1.40(3)	O323	C322	1.43(2)
O123	C124	1.46(2)	O223	C224	1.45(3)	O323	C324	1.42(2)
C101	C102	1.53(3)	C201	C202	1.55(3)	C301	C302	1.58(3)
C104	C105	1.52(3)	C204	C205	1.52(3)	C304	C305	1.51(3)
C107	C108	1.50(3)	C207	C208	1.57(4)	C307	C308	1.54(3)
C110	C111	1.54(3)	C210	C211	1.49(3)	C310	C311	1.55(3)
C113	C114	1.40(4)	C213	C214	1.53(3)	C313	C314	1.53(3)
C116	C117	1.50(3)	C216	C217	1.58(4)	C316	C317	1.52(3)
C118	C119	1.49(3)	C218	C219	1.55(3)	C318	C319	1.52(2)
C121	C122	1.51(3)	C221	C222	1.49(3)	C321	C322	1.51(2)
C124	C125	1.52(3)	C224	C225	1.52(4)	C324	C325	1.48(3)
NEN1	CEN1	1.50(4)	NEN3	CEN3	1.79(4)	Sb4	C107	3.89(2)
CEN1	CEN2	1.64(4)	CEN3	CEN4	1.24(6)	Sb5	C221	3.71(2)
CEN2	NEN2	1.48(3)	CEN4	NEN4	1.74(5)	Sb7	C321	3.95(2)
						Sb3	NEN1	3.90(3)

Table A.8. Additional angles (deg) in (2,2,2-crypt-K)$_3$Sb$_7$.2en

Atom	Atom	Atom	Angle,	Atom	Atom	Atom	Angle	Atom	Atom	Atom	Angle
N100	K1	N109	179.5(4)	N200	K2	N209	178.3(5)	N300	K3	N309	179.0(4)
N100	K1	O103	61.1(4)	N200	K2	O203	61.3(4)	N300	K3	O303	61.2(4)
N100	K1	O112	62.4(4)	N200	K2	O212	61.2(4)	N300	K3	O312	61.0(4)
N100	K1	O120	59.6(4)	N200	K2	O220	60.8(4)	N300	K3	O320	61.2(4)
N109	K1	O106	59.5(4)	N209	K2	O206	59.8(4)	N309	K3	O306	62.5(4)
N109	K1	O115	58.6(4)	N209	K2	O215	61.9(5)	N309	K3	O315	62.0(4)
N109	K1	O123	61.7(4)	N209	K2	O223	60.9(5)	N309	K3	O323	60.8(4)
O103	K1	O106	59.7(4)	O203	K2	O206	59.9(4)	O303	K3	O306	59.3(3)
O112	K1	O115	59.9(4)	O212	K2	O215	60.0(4)	O312	K3	O315	59.6(4)
O120	K1	O123	60.0(3)	O220	K2	O223	58.4(4)	O320	K3	O323	59.1(3)
K1	N100	C101	108.1(11)	K2	N200	C201	109.4(10)	K3	N300	C301	108.6(10)
K1	N100	C110	108.1(11)	K2	N200	C210	109.0(10)	K3	N300	C310	111.4(10)
K1	N100	C118	111.5(11)	K2	N200	C218	108.8(11)	K3	N300	C318	108.4(10)
C101	N100	C110	108.4(15)	C201	N200	C210	108.7(14)	C301	N300	C310	111.3(14)
C101	N100	C118	110.2(15)	C201	N200	C218	109.3(15)	C301	N300	C318	109.4(13)
C110	N100	C118	110.4(15)	C210	N200	C218	111.6(14)	C310	N300	C318	107.6(14)
K1	N109	C108	108.5(12)	K2	N209	C208	105.7(13)	K3	N309	C308	110.2(10)
K1	N109	C117	112.4(12)	K2	N209	C217	108.0(14)	K3	N309	C317	110.0(10)
K1	N109	C125	106.2(11)	K2	N209	C225	107.3(15)	K3	N309	C325	110.2(10)
C108	N109	C117	109.7(16)	C208	N209	C217	114.9(19)	C308	N309	C317	107.9(13)
C108	N109	C125	110.8(16)	C208	N209	C225	108.7(19)	C308	N309	C325	109.6(14)
C117	N109	C125	109.2(16)	C217	N209	C225	111.8(10)	C317	N309	C325	108.9(14)
K1	O103	C102	114.8(11)	K2	O203	C202	114.5(10)	K3	O303	C302	119.4(10)
K1	O103	C104	112.1(10)	K2	O203	C204	113.9(11)	K3	O303	C304	115.1(10)
C102	O103	C104	111.4(14)	C202	O203	C204	106.9(14)	C302	O303	C304	108.2(14)
K1	O106	C105	117.7(10)	K2	O206	C205	119.1(11)	K3	O306	C305	116.0(10)
K1	O106	C107	118.7(11)	K2	O206	C207	123.5(12)	K3	O306	C307	115.9(10)
C105	O106	C107	109.9(14)	C205	O206	C207	109.1(16)	C305	O306	C307	110.6(14)
K1	O112	C111	117.8(12)	K2	O212	C211	116.0(10)	K3	O312	C311	118.0(10)
K1	O112	C113	119.5(13)	K2	O212	C213	115.1(10)	K3	O312	C313	116.1(10)

Table A.8. Continued

Atom	Atom	Atom	Angle,	Atom	Atom	Atom	Angle	Atom	Atom	Atom	Angle
C111	O112	C113	111.0(17)	C211	O212	C213	110.0(14)	C311	O312	C313	109.9(14)
K1	O115	C114	109.8(12)	K2	O215	C214	116.8(12)	K3	O315	C314	116.4(11)
K1	O115	C116	118.5(12)	K2	O215	C216	117.3(13)	K3	O315	C316	117.8(10)
C114	O115	C116	116.7(16)	C214	O215	C216	109.8(18)	C314	O315	C316	111.1(14)
K1	O120	C119	116.7(10)	K2	O220	C219	116.9(12)	K3	O320	C319	118.9(9)
K1	O120	C121	115.7(10)	K2	O220	C221	114.5(11)	K3	O320	C321	118.2(9)
C119	O120	C121	111.1(14)	C219	O220	C221	108.4(15)	C319	O320	C321	109.6(12)
K1	O123	C122	115.0(10)	K2	O223	C222	117.9(12)	K3	O323	C322	116.8(9)
K1	O123	C124	115.2(10)	K2	O223	C224	117.4(15)	K3	O323	C324	117.3(9)
C122	O123	C124	109.6(14)	C222	O223	C224	111.5(19)	C322	O323	C324	110.7(12)
N100	C101	C102	112.1(17)	N200	C201	C202	113.1(16)	N300	C301	C302	112.7(14)
O103	C102	C101	108.6(16)	O203	C202	C201	106.5(15)	O303	C302	C301	107.2(15)
O103	C104	C105	107.7(14)	O203	C204	C205	108.0(17)	O303	C304	C305	107.2(15)
O106	C105	C104	109.4(15)	O206	C205	C204	107.3(18)	O306	C305	C304	109.8(16)
O106	C107	C108	107.4(17)	O206	C207	C208	105.5(18)	O306	C307	C308	108.7(15)
N109	C108	C107	111.3(18)	N209	C208	C207	108.4(19)	N309	C308	C307	113.4(15)
N100	C110	C111	113.2(17)	N200	C210	C211	112.6(15)	N300	C310	C311	111.6(16)
O112	C111	C110	109.0(18)	O212	C211	C210	108.0(16)	O312	C311	C310	107.7(16)
O112	C113	C114	110.6(21)	O212	C213	C214	107.8(16)	O312	C313	C314	110.6(16)
O115	C114	C113	114.7(22)	O215	C214	C213	110.2(18)	O315	C314	C313	108.9(16)
O115	C116	C117	109.0(18)	O215	C216	C217	108.3(21)	O315	C316	C317	110.5(15)
N109	C117	C116	113.6(18)	N209	C217	C216	112.7(21)	N309	C317	C316	113.6(15)
N100	C118	C119	112.2(16)	N200	C218	C219	113.1(17)	N300	C318	C319	112.6(14)
O120	C119	C118	109.2(16)	O220	C219	C218	106.8(17)	O320	C319	C318	107.8(14)
O120	C121	C122	108.8(15)	O220	C221	C222	109.3(17)	O320	C321	C322	109.7(14)
O123	C122	C121	111.6(16)	O223	C222	C221	110.3(18)	O323	C322	C321	109.5(14)
O123	C124	C125	107.8(16)	O223	C224	C225	105.6(23)	O323	C324	C325	109.2(15)
N109	C125	C124	112.7(17)	N209	C225	C224	115.4(24)	N309	C325	C324	113.9(15)
NEN1	CEN1	CEN2	104.1(21)	NEN3	CEN3	CEN4	86.9(29)				
CEN1	CEN2	NEN2	104.4(21)	NEN4	CEN4	CEN3	90.7(30)				

Table A.9. Additional distances (Å) in (2,2,2-crypt-K)$_3$Sn$_9$·1.5en

Atom	Atom	Distance	Atom	Atom	Distance	Atom	Atom	Distance
K1	O11	2.909(16)	K2	O21	2.831(15)	K3	O31	2.805(13)
K1	O12	2.833(18)	K2	O22	2.840(13)	K3	O32	2.830(13)
K1	O13	2.815(14)	K2	O23	2.844(13)	K3	O33	2.878(13)
K1	O14	2.824(18)	K2	O24	2.809(12)	K3	O34	2.798(14)
K1	O15	2.831(15)	K2	O25	2.787(14)	K3	O35	2.812(13)
K1	O16	2.777(17)	K2	O26	2.802(13)	K3	O36	2.831(13)
K1	N11	2.997(17)	K2	N21	2.979(18)	K3	N31	3.004(16)
K1	N12	3.011(25)	K2	N22	3.008(15)	K3	N32	3.030(14)
N11	C11	1.49(3)	N21	C21	1.50(3)	N31	C31	1.46(3)
N11	C17	1.46(3)	N21	C27	1.52(3)	N31	C37	1.48(2)
N11	C113	1.44(3)	N21	C213	1.47(3)	N31	C313	1.51(3)
N12	C16	1.49(4)	N22	C26	1.52(2)	N32	C36	1.47(2)
N12	C112	1.51(4)	N22	C212	1.49(3)	N32	C312	1.48(3)
N12	C118	1.52(4)	N22	C218	1.50(3)	N32	C318	1.51(2)
O11	C12	1.45(3)	O21	C22	1.44(3)	O31	C32	1.44(2)
O11	C13	1.41(3)	O21	C23	1.44(3)	O31	C33	1.43(3)
O12	C14	1.39(3)	O22	C24	1.45(3)	O32	C34	1.42(2)
O12	C15	1.42(3)	O22	C25	1.43(2)	O32	C35	1.45(2)
O13	C18	1.46(3)	O23	C28	1.46(3)	O33	C38	1.44(2)
O13	C19	1.42(3)	O23	C29	1.45(2)	O33	C39	1.41(2)
O14	C110	1.42(3)	O24	C210	1.45(2)	O34	C310	1.44(2)
O14	C111	1.41(3)	O24	C211	1.40(3)	O34	C311	1.48(3)
O15	C114	1.42(3)	O25	C214	1.41(3)	O35	C314	1.41(3)
O15	C115	1.41(3)	O25	C215	1.41(2)	O35	C315	1.45(2)
O16	C116	1.42(3)	O26	C216	1.42(2)	O36	C316	1.45(2)
O16	C117	1.45(3)	O26	C217	1.41(2)	O36	C317	1.45(2)
C11	C12	1.53(3)	C21	C22	1.44(4)	C31	C32	1.53(3)
C13	C14	1.43(4)	C23	C24	1.41(4)	C33	C34	1.50(3)
C15	C16	1.57(4)	C25	C26	1.52(3)	C35	C36	1.48(3)
C17	C18	1.55(3)	C27	C28	1.52(4)	C37	C38	1.46(3)
C19	C110	1.53(4)	C29	C210	1.47(3)	C39	C310	1.47(3)
C111	C112	1.56(4)	C211	C212	1.55(3)	C311	C312	1.46(3)
C113	C114	1.55(3)	C213	C214	1.49(3)	C313	C314	1.56(3)
C115	C116	1.43(4)	C215	C216	1.48(3)	C315	C316	1.52(3)
C117	C118	1.52(5)	C217	C218	1.49(3)	C317	C318	1.49(3)
Sn8	NEN2	3.71(8)	NEN1	CEN1	1.13(12)	NEN3	CEN3	1.36(14)
Sn7	C316	3.78(2)	CEN1	CEN2	1.45(9)	CEN3	CEN3	1.92(21)
Sn6	C111	3.91(3)	CEN2	NEN2	1.82(8)	CEN3	NEN3	1.56(14)

Table A.10. Additional angles (deg) in (2,2,2-crypt-K)$_3$Sn$_9$·1.5en

Atom	Atom	Atom	Angle	Atom	Atom	Atom	Angle	Atom	Atom	Atom	Angle
N11	K1	N12	178.2(6)	N21	K2	N22	178.2(4)	N31	K3	N32	179.2(4)
N11	K1	O11	59.9(4)	N21	K2	O21	62.1(4)	N31	K3	O31	59.7(4)
N11	K1	O13	61.0(4)	N21	K2	O23	60.6(4)	N31	K3	O33	60.2(4)
N11	K1	O15	61.7(4)	N21	K2	O25	60.6(4)	N31	K3	O35	61.3(4)
N12	K1	O12	60.7(6)	N22	K2	O22	60.5(4)	N32	K3	O32	61.0(4)
N12	K1	O14	61.5(6)	N22	K2	O24	59.2(4)	N32	K3	O34	60.3(4)
N12	K1	O16	60.3(6)	N22	K2	O26	60.7(4)	N32	K3	O36	59.9(4)
O11	K1	O12	57.9(5)	O21	K2	O22	59.8(4)	O31	K3	O32	59.6(4)
O13	K1	O14	59.5(4)	O23	K2	O24	59.9(4)	O33	K3	O34	59.5(4)
O15	K1	O16	59.2(5)	O25	K2	O26	59.3(4)	O35	K3	O36	60.2(4)
K1	N11	C11	110.1(12)	K2	N21	C21	106.5(14)	K3	N31	C31	111.5(11)
K1	N11	C17	108.2(12)	K2	N21	C27	110.0(13)	K3	N31	C37	108.2(10)
K1	N11	C113	107.1(12)	K2	N21	C213	108.9(12)	K3	N31	C313	107.3(11)
C11	N11	C17	109.9(16)	C21	N21	C27	113.0(18)	C31	N31	C37	109.0(15)
C11	N11	C113	109.1(16)	C21	N21	C213	111.5(18)	C31	N31	C313	111.6(15)
C17	N11	C113	112.3(17)	C27	N21	C213	106.9(17)	C37	N31	C313	109.2(15)
K1	N12	C16	108.0(17)	K2	N22	C26	109.6(10)	K3	N32	C36	107.5(10)
K1	N12	C112	105.6(16)	K2	N22	C212	109.9(11)	K3	N32	C312	108.3(11)
K1	N12	C118	107.0(18)	K2	N22	C218	107.6(11)	K3	N32	C318	111.1(10)
C16	N12	C112	108.9(23)	C26	N22	C212	108.2(15)	C36	N32	C312	111.4(15)
C16	N12	C118	114.3(24)	C26	N22	C218	107.7(14)	C36	N32	C318	109.8(14)
C112	N12	C118	112.6(24)	C212	N22	C218	113.8(15)	C312	N32	C318	108.7(14)
K1	O11	C12	116.3(13)	K2	O21	C22	114.6(12)	K3	O31	C32	119.4(11)
K1	O11	C13	113.2(13)	K2	O21	C23	111.3(13)	K3	O31	C33	115.5(12)
C12	O11	C13	111.7(18)	C22	O21	C23	114.3(17)	C32	O31	C33	110.7(15)
K1	O12	C14	117.0(15)	K2	O22	C24	113.3(12)	K3	O32	C34	111.8(10)
K1	O12	C15	118.7(15)	K2	O22	C25	114.0(11)	K3	O32	C35	113.6(10)
C14	O12	C15	112.5(21)	C24	O22	C25	112.0(16)	C34	O32	C35	109.3(14)
K1	O13	C18	114.7(12)	K2	O23	C28	115.6(14)	K3	O33	C38	114.5(11)
K1	O13	C19	115.8(13)	K2	O23	C29	110.7(11)	K3	O33	C39	112.4(11)

Table A. 10. Continued

Atom	Atom	Atom	Angle	Atom	Atom	Atom	Angle	Atom	Atom	Atom	Angle
C18	O13	C19	110.3(17)	C28	O23	C29	103.8(18)	C38	O33	C39	112.7(15)
K1	O14	C110	115.3(14)	K2	O24	C210	116.0(10)	K3	O34	C310	114.9(11)
K1	O14	C111	115.8(14)	K2	O24	C211	121.5(12)	K3	O34	C311	119.6(11)
C110	O14	C111	105.8(19)	C210	O24	C211	107.4(15)	C310	O34	C311	109.6(15)
K1	O15	C114	114.7(13)	K2	O25	C214	117.8(12)	K3	O35	C314	119.6(12)
K1	O15	C115	112.6(13)	K2	O25	C215	121.4(11)	K3	O35	C315	112.4(10)
C114	O15	C115	109.8(18)	C214	O25	C215	112.0(15)	C314	O35	C315	109.9(15)
K1	O16	C116	117.8(14)	K2	O26	C216	111.7(10)	K3	O36	C316	116.5(10)
K1	O16	C117	115.5(15)	K2	O26	C217	119.3(10)	K3	O36	C317	115.0(10)
C116	O16	C117	111.6(20)	C216	O26	C217	110.5(13)	C316	O36	C317	109.1(14)
N11	C11	C12	113.3(18)	N21	C21	C22	114.8(22)	N31	C31	C32	114.4(17)
O11	C12	C11	105.5(18)	O21	C22	C21	111.6(21)	O31	C32	C31	107.4(16)
O11	C13	C14	108.9(21)	O21	C23	C24	108.5(21)	O31	C33	C34	107.6(17)
O12	C14	C13	111.8(23)	O22	C24	C23	109.4(21)	O32	C34	C33	105.5(16)
O12	C15	C16	105.3(23)	O22	C25	C26	107.4(17)	O32	C35	C36	109.2(16)
N12	C16	C15	113.8(25)	N22	C26	C25	110.4(16)	N32	C36	C35	113.1(16)
N11	C17	C18	112.1(19)	N21	C27	C28	112.0(21)	N31	C37	C38	116.1(16)
O13	C18	C17	104.6(18)	O23	C28	C27	106.1(23)	O33	C38	C37	107.0(16)
O13	C19	C110	109.5(21)	O23	C29	C210	107.3(17)	O33	C39	C310	109.2(17)
O14	C110	C19	105.8(21)	O24	C210	C29	107.2(16)	O34	C310	C39	107.7(16)
O14	C111	C112	104.5(21)	O24	C211	C212	105.9(18)	O34	C311	C312	107.5(17)
N12	C112	C111	111.6(24)	N22	C212	C211	111.4(18)	N32	C312	C311	117.6(18)
N11	C113	C114	114.0(19)	N21	C213	C214	114.5(19)	N31	C313	C314	113.1(17)
O15	C114	C113	107.9(19)	O25	C214	C213	109.0(18)	O35	C314	C313	107.5(18)
O15	C115	C116	110.0(22)	O25	C215	C216	106.6(16)	O35	C315	C316	108.9(16)
O16	C116	C115	110.4(22)	O26	C216	C215	113.2(16)	O36	C316	C315	105.5(15)
O16	C117	C118	103.6(24)	O26	C217	C218	109.5(16)	O36	C317	C318	109.0(16)
N12	C118	C117	107.7(26)	N22	C218	C217	114.6(17)	N32	C318	C317	111.7(16)
NEN1	CEN1	CEN2	108(8)	CEN3	CEN3	NEN3	54(6)				
CEN1	CEN2	NEN2	86(4)								

Table A. 11. Distances (Å) in (2,2,2-crypt-Na)$_2$Ge$_4$

Atom	Atom	Distance	Atom	Atom	Distance
Ge1	Ge1	2.769(8)	Ge1	Ge2'	1.946(7)
Ge1	Ge2	2.793(9)	Ge1	Ge1'	3.408(10)
Ge1	Ge1'	1.987(7)	Ge2	Ge2'	3.400(19)
Na	O1	2.674(9)	Na	N1	3.205(16)
Na	O2	2.500(8)	Na	N2	2.784(15)
N1	C1	1.473(12)	C4	O2	1.415(13)
C1	C2	1.507(16)	O2	C5	1.433(11)
C2	O1	1.461(12)	C5	C6	1.537(15)
O1	C3	1.441(14)	C6	N2	1.485(12)
C3	C4	1.529(16)			

Table A. 12. Angles (deg) in (2,2,2-crypt-Na)$_2$Ge$_4$

Atom	Atom	Atom	Angle	Atom	Atom	Atom	Angle
Ge1	Ge1	Ge2	60.3(1)	Ge1	Ge2	Ge1	59.4(2)
Ge1	Ge1	Ge1	60.0				
N1	Na	N2	180.0	N2	Na	O2	64.8(2)
N1	Na	O1	58.8(2)	O1	Na	O2	65.0(2)
Na	N1	C1	107.9(6)	Na	O2	C4	118.6(6)
Na	O1	C2	123.9(7)	Na	O2	C5	121.0(6)
Na	O1	C3	99.3(6)	Na	N2	C6	108.5(6)
C1	N1	C1	111.0(6)	C3	C4	O2	107.7(9)
N1	C1	C2	111.2(9)	C4	O2	C5	109.0(7)
C1	C2	O1	112.5(10)	O2	C5	C6	107.3(8)
C2	O1	C3	112.5(8)	C5	C6	N2	110.9(8)
O1	C3	C4	106.6(9)	C6	N2	C6	110.4(6)

Table A.12. Additional distances (Å) in (2,1,1-crypt-Li)$_4$Sn$_9$

Atom	Atom	Distance	Atom	Atom	Distance	Atom	Atom	Distance	Atom	Atom	Distance
Li1	O103	2.30(7)	Li2	O203	2.02(8)	Li3	O303	2.07(7)	Li4	O403	2.23(9)
Li1	O106	2.08(7)	Li2	O206	2.05(8)	Li3	O306	2.13(7)	Li4	O406	2.04(8)
Li1	O112	2.13(7)	Li2	O212	2.28(8)	Li3	O312	2.11(7)	Li4	O412	2.08(8)
Li1	O117	2.05(6)	Li2	O217	2.09(8)	Li3	O317	2.21(7)	Li4	O417	2.10(8)
Li1	N100	2.36(7)	Li2	N200	2.39(9)	Li3	N300	2.30(8)	Li4	N400	2.31(8)
Li1	N109	2.32(7)	Li2	N209	2.40(8)	Li3	N309	2.21(7)	Li4	N409	2.24(9)
N100	C101	1.28(6)	N200	C201	1.57(7)	N300	C301	1.57(6)	N400	C401	1.44(6)
C101	C102	1.70(7)	C201	C202	1.52(7)	C301	C302	1.58(7)	C401	C402	1.61(6)
C102	O103	1.33(6)	C202	O203	1.45(6)	C302	O303	1.35(6)	C402	O403	1.54(5)
O103	C104	1.34(5)	O203	C204	1.31(6)	O303	C304	1.59(6)	O403	C404	1.50(5)
C104	C105	1.41(6)	C204	C205	1.50(7)	C304	C305	1.47(6)	C404	C405	1.47(6)
C105	O106	1.43(5)	C205	O206	1.51(6)	C305	O306	1.46(6)	C405	O406	1.65(6)
O106	C107	1.30(6)	O206	C207	1.43(6)	O306	C307	1.40(5)	O406	C407	1.46(5)
C107	C108	1.56(7)	C207	C208	1.39(6)	C307	C308	1.49(7)	C407	C408	1.47(6)
C108	N109	1.47(6)	C208	N209	1.47(6)	C308	N309	1.50(6)	C408	N409	1.52(6)
N109	C110	1.51(6)	N209	C210	1.55(7)	N309	C310	1.53(6)	N409	C410	1.43(6)
C110	C111	1.53(7)	C210	C211	1.61(8)	C310	C311	1.60(7)	C410	C411	1.32(8)
C111	O112	1.44(6)	C211	O212	1.43(6)	C311	O312	1.45(5)	C411	O412	1.60(6)
O112	C113	1.38(5)	O212	C213	1.54(6)	O312	C313	1.56(6)	O412	C413	1.51(6)
C113	C114	1.45(6)	C213	C214	1.62(7)	C313	C314	1.47(6)	C413	C414	1.40(7)
C114	N100	1.65(6)	C214	N200	1.36(7)	C314	N300	1.49(6)	C414	N400	1.54(6)
N100	C115	1.38(6)	N200	C215	1.36(7)	N300	C315	1.46(6)	N400	C415	1.52(6)
C115	C116	1.46(7)	C215	C216	1.46(9)	C315	C316	1.50(7)	C415	C416	1.57(6)
C116	O117	1.53(5)	C216	O217	1.35(7)	C316	O317	1.40(5)	C416	O417	1.48(5)
O117	C118	1.49(5)	O217	C218	1.56(6)	O317	C318	1.43(5)	O417	C418	1.47(6)
C118	C119	1.46(6)	C218	C219	1.51(8)	C318	C319	1.44(8)	C418	C419	1.53(6)
C119	N109	1.44(6)	C219	N209	1.45(6)	C319	N309	1.54(8)	C419	N409	1.47(6)
Sn4A	C313	3.84(5)	Sn7A	C215	3.87(7)	Sn7B	C214	3.83(6)	Sn9A	C416	3.74(5)
Sn4A	C405	3.83(4)	Sn7A	C308	3.87(5)	Sn7B	C215	3.83(7)	Sn9B	C215	3.87(6)

Table A. 14. Angles (deg) in (2,1,1-crypt-Li)$_4$Sn$_9$

Atom	Atom	Atom	Angle	Atom	Atom	Atom	Angle	Atom	Atom	Atom	Angle	Atom	Atom	Atom	Angle
Sn2	Sn1	Sn6A	64.2(2)	Sn2	Sn6A	Sn7A	55.1(2)	Sn5A	Sn8	Sn9A	54.3(2)	Sn1	Sn6A	Sn2	57.3(2)
Sn4A	Sn1	Sn5A	61.5(2)	Sn2	Sn7A	Sn6A	60.9(2)	Sn7A	Sn8	Sn9A	56.0(2)	Sn2	Sn7A	Sn3A	58.3(2)
Sn1	Sn2	Sn6A	58.5(2)	Sn8	Sn7A	Sn3A	55.2(2)	Sn5A	Sn9A	Sn6A	65.2(2)	Sn3A	Sn8	Sn4A	57.8(2)
Sn3A	Sn2	Sn7A	61.1(2)	Sn3A	Sn8	Sn7A	57.9(2)	Sn8	Sn9A	Sn5A	69.2(2)	Sn2	Sn1	Sn4A	91.7(2)
Sn2	Sn3A	Sn7A	60.6(2)	Sn4A	Sn8	Sn5A	55.3(2)	Sn6A	Sn9A	Sn7A	66.9(2)	Sn1	Sn2	Sn3A	86.2(2)
Sn8	Sn3A	Sn4A	63.2(2)	Sn6A	Sn5A	Sn9A	57.6(2)	Sn8	Sn9A	Sn7A	65.6(2)	Sn2	Sn3A	Sn4A	94.1(3)
Sn1	Sn4A	Sn5A	59.7(2)	Sn8	Sn5A	Sn9A	56.5(2)	Sn5A	Sn1	Sn6A	64.7(2)	Sn1	Sn4A	Sn3A	88.0(3)
Sn8	Sn4A	Sn3A	59.0(2)	Sn5A	Sn6A	Sn9A	57.2(2)	Sn6A	Sn2	Sn7A	64.0(2)	Sn8	Sn5A	Sn6A	91.2(2)
Sn1	Sn5A	Sn6A	58.5(2)	Sn7A	Sn6A	Sn9A	56.4(2)	Sn8	Sn3A	Sn7A	66.8(2)	Sn5A	Sn6A	Sn7A	89.7(2)
Sn8	Sn5A	Sn4A	55.9(2)	Sn6A	Sn7A	Sn9A	56.7(2)	Sn8	Sn4A	Sn5A	68.8(2)	Sn8	Sn7A	Sn6A	92.7(2)
Sn1	Sn6A	Sn5A	56.8(2)	Sn8	Sn7A	Sn9A	58.3(2)	Sn1	Sn5A	Sn4A	58.8(2)	Sn5A	Sn8	Sn7A	86.4(2)
Sn2	Sn1	Sn3B	52.4(2)	Sn2	Sn3B	Sn7B	58.6(2)	Sn8	Sn7B	Sn3B	58.1(2)	Sn3B	Sn1	Sn5B	88.2(2)
Sn3B	Sn1	Sn4B	50.8(2)	Sn8	Sn3B	Sn4B	57.8(3)	Sn3B	Sn8	Sn7B	60.0(2)	Sn3B	Sn1	Sn6B	84.3(2)
Sn1	Sn3B	Sn2	51.0(2)	Sn1	Sn5B	Sn4B	61.9(3)	Sn1	Sn2	Sn6B	64.6(2)	Sn1	Sn3B	Sn7B	88.9(3)
Sn1	Sn3B	Sn4B	52.5(3)	Sn6B	Sn5B	Sn9B	59.2(2)	Sn3B	Sn2	Sn7B	61.0(3)	Sn1	Sn3B	Sn8	90.0(3)
Sn8	Sn5B	Sn4B	50.7(3)	Sn1	Sn6B	Sn2	60.1(2)	Sn1	Sn4B	Sn5B	60.2(3)	Sn1	Sn5B	Sn8	91.8(2)
Sn8	Sn5B	Sn9B	50.0(2)	Sn5B	Sn6B	Sn9B	59.5(2)	Sn8	Sn4B	Sn3B	61.5(3)	Sn8	Sn5B	Sn6B	86.6(2)
Sn2	Sn6B	Sn7B	56.8(2)	Sn2	Sn7B	Sn3B	60.4(2)	Sn8	Sn9B	Sn7B	64.4(2)	Sn1	Sn6B	Sn7B	95.1(2)
Sn7B	Sn6B	Sn9B	55.3(2)	Sn8	Sn7B	Sn9B	56.1(2)	Sn5B	Sn9B	Sn6B	61.4(3)	Sn5B	Sn6B	Sn7B	94.3(3)
Sn2	Sn7B	Sn6B	52.5(2)	Sn3B	Sn8	Sn4B	60.7(3)	Sn1	Sn2	Sn3B	76.6(2)	Sn3B	Sn7B	Sn6B	91.7(3)
Sn6B	Sn7B	Sn9B	56.1(2)	Sn7B	Sn8	Sn9B	59.4(2)	Sn6B	Sn2	Sn7B	70.8(2)	Sn8	Sn7B	Sn6B	90.8(2)
Sn4B	Sn8	Sn5B	51.7(3)	Sn5B	Sn1	Sn6B	60.2(2)	Sn1	Sn4B	Sn3B	76.7(3)	Sn3B	Sn8	Sn5B	90.0(2)
Sn5B	Sn8	Sn9B	53.5(2)	Sn8	Sn3B	Sn7B	61.8(2)	Sn8	Sn4B	Sn5B	77.5(3)	Sn5B	Sn8	Sn7B	88.4(2)
Sn2	Sn1	Sn6B	55.3(2)	Sn1	Sn5B	Sn6B	61.6(2)	Sn8	Sn9B	Sn5B	76.5(3)	Sn2	Sn1	Sn4B	100.7(2)
Sn4B	Sn1	Sn5B	57.9(3)	Sn1	Sn6B	Sn5B	58.1(2)	Sn6B	Sn9B	Sn7B	68.7(3)	Sn2	Sn3B	Sn4B	101.0(4)
N100	Li1	O103	74(2)	N200	Li2	O203	80(3)	N300	Li3	O303	78(2)	N400	Li4	O403	73(3)
N100	Li1	N109	138(3)	N200	Li2	N209	128(4)	N300	Li3	N309	128(3)	N400	Li4	N409	136(4)
N100	Li1	O112	81(2)	N200	Li2	O212	76(3)	N300	Li3	O312	80(3)	N400	Li4	O412	77(3)

Table A. 14. Continued

Atom	Atom	Atom	Angle	Atom	Atom	Atom	Angle	Atom	Atom	Atom	Angle	Atom	Atom	Atom	Angle
N100	Li1	O117	81(2)	N200	Li2	O217	77(3)	N300	Li3	O317	76(2)	N400	Li4	O417	80(3)
O103	Li1	O106	72(2)	O203	Li2	O206	77(3)	O303	Li3	O306	79(3)	O403	Li4	O406	75(3)
O106	Li1	N109	77(2)	O206	Li2	N209	75(3)	O306	Li3	N309	75(2)	O406	Li4	N409	77(3)
N109	Li1	O112	79(2)	N209	Li2	O212	78(3)	N309	Li3	O312	77(2)	N409	Li4	O412	84(3)
N109	Li1	O117	81(2)	N209	Li2	O217	78(3)	N309	Li3	O317	78(2)	N409	Li4	O417	79(3)
C101	N100	C114	112(3)	C201	N200	C214	111(4)	C301	N300	C314	114(3)	C401	N400	C414	122(4)
C101	N100	C115	121(4)	C201	N200	C215	106(4)	C301	N300	C315	107(4)	C401	N400	C415	105(3)
C114	N100	C115	111(3)	C214	N200	C215	116(4)	C314	N300	C315	119(4)	C414	N400	C415	111(3)
C108	N109	C110	108(3)	C208	N209	C210	119(4)	C308	N309	C310	106(4)	C408	N409	C410	115(3)
C108	N109	C119	120(3)	C208	N209	C219	117(4)	C308	N309	C319	112(4)	C408	N409	C419	109(3)
C110	N109	C119	111(4)	C210	N209	C219	107(4)	C310	N309	C319	108(4)	C410	N409	C419	114(4)
N100	C101	C102	109(4)	N200	C201	C202	112(4)	N300	C301	C302	108(4)	N400	C401	C402	102(3)
C101	C102	O103	106(4)	C201	C202	O203	113(4)	C301	C302	O303	105(4)	C401	C402	O403	99(3)
C102	O103	C104	113(4)	C202	O203	C204	117(4)	C302	O303	C304	117(3)	C402	O403	C404	109(3)
O103	C104	C105	111(4)	O203	C204	C205	109(4)	O303	C304	C305	104(3)	O403	C404	C405	109(3)
C104	C105	O106	105(3)	C204	C205	O206	102(4)	C304	C305	O306	111(4)	C404	C405	O406	100(3)
C105	O106	C107	115(3)	C205	O206	C207	114(3)	C305	O306	C307	118(3)	C405	O406	C407	112(3)
O106	C107	C108	117(4)	O206	C207	C208	108(4)	O306	C307	C308	110(4)	O406	C407	C408	107(3)
C107	C108	N109	107(4)	C207	C208	N209	109(4)	C307	C308	N309	101(4)	C407	C408	N409	110(3)
N109	C110	C111	109(4)	N209	C210	C211	109(4)	N309	C310	C311	97(3)	N409	C410	C411	117(5)
C110	C111	O112	109(4)	C210	C211	O212	112(4)	C310	C311	O312	112(3)	C410	C411	O412	117(4)
C111	O112	C113	113(3)	C211	O212	C213	106(3)	C311	O312	C313	112(3)	C411	O412	C413	102(3)
O112	C113	C114	113(4)	O212	C213	C214	104(4)	O312	C313	C314	102(4)	O412	C413	C414	98(4)
N100	C114	C113	110(3)	N200	C214	C213	115(4)	N300	C314	C313	110(4)	C413	C414	C415	98(3)
N100	C115	C116	118(4)	N200	C215	C216	109(5)	N300	C315	C316	113(4)	N400	C415	C416	112(3)
C115	C116	O117	105(3)	C215	C216	O217	123(5)	C315	C316	O317	110(4)	C415	C416	O417	105(3)
C116	O117	C118	117(3)	C216	O217	C218	117(4)	C316	O317	C318	112(3)	C416	O417	C418	112(3)
O117	C118	C119	110(3)	O217	C218	C219	104(4)	O317	C318	C319	103(4)	O417	C418	C419	101(3)
N109	C119	C118	112(4)	N209	C219	C218	109(4)	N309	C319	C318	113(5)	N409	C419	C418	112(4)

APPENDIX B: CALCULATED AND OBSERVED STRUCTURE FACTORS (x10) FOR $(2,2,2\text{-crypt-}K^{+})_2Pb_2Sb_2^{2-}\cdot en$

L =-14

H	K	FO	FC
9	0	284	291
9	2	426	369
10	0	366	389
10	1	404	365

L =-13

H	K	FO	FC
9	0	357	327
9	2	481	406
10	1	496	432
10	3	385	328
10	5	308	177
11	0	414	336
11	1	364	302
11	2	287	237

L =-12

H	K	FO	FC
8	0	258	178
8	1	290	264
8	3	304	245
9	0	484	453
10	1	435	369
10	3	329	331
11	0	377	402
11	2	324	347
11	3	336	224
12	5	403	406

L =-11

H	K	FO	FC
7	0	255	305
7	1	464	387
7	2	368	304
8	0	401	409
8	4	563	547
9	0	324	198
9	2	351	356
9	4	395	340
10	0	292	302
10	1	472	417
10	2	348	325
10	4	373	392
11	0	411	314
11	1	382	377
11	2	366	362
11	3	440	434
11	5	342	352
12	1	386	358
12	3	462	472
12	4	447	375
12	5	439	432
13	2	297	222

L =-10

H	K	FO	FC
7	0	724	709
7	2	785	708
7	3	561	554
8	1	616	518
8	2	758	710
8	3	294	304
8	4	721	715
9	4	381	469
9	5	391	350
10	0	284	249
10	2	400	383
10	3	391	373
10	4	406	351
10	5	509	434
11	0	462	402
11	1	399	324
11	3	742	680
12	1	279	243

L = -9

H	K	FO	FC
6	0	910	861
6	1	864	776
6	2	739	622
7	0	996	917
7	1	459	460
7	2	1072	1010
7	3	566	565
7	4	1057	1007
8	1	561	602
8	3	426	499
8	4	688	638
9	0	460	379
9	2	518	501
9	3	373	313
10	2	356	301
10	3	257	235

L = -8

H	K	FO	FC
6	0	870	850
6	1	414	305
6	2	564	512
6	3	967	919
7	0	375	404
7	1	815	797
7	2	748	837
7	3	366	356
7	4	901	903
8	0	710	622
8	1	664	594
8	2	454	441
8	3	437	467
9	0	839	754
9	1	526	454
9	2	675	650

L = -7

H	K	FO	FC
5	0	342	290
5	1	376	288
5	2	1117	959
6	0	506	500
6	1	379	305
6	2	290	336
6	3	548	601
7	0	497	390
7	1	1198	1118
7	2	286	240
7	3	464	608
8	0	1698	1506
8	1	274	183
8	2	1144	1069

L = -6

H	K	FO	FC
4	0	264	232
4	1	1369	1185
5	0	486	440
5	1	968	905
5	2	747	711
5	3	332	369
6	0	237	156
6	1	1584	1461
6	2	227	252
6	3	633	538
7	0	1292	1159
7	1	1100	1068

L = -5

H	K	FO	FC
4	0	1179	1161
4	1	1663	1526
4	2	2036	1910
5	0	792	737
5	1	1237	1141
5	2	893	890

L = -4

H	K	FO	FC
3	0	1687	1455
3	1	1945	1678
4	0	626	543
4	1	1626	1562
4	2	856	838

L = -3

H	K	FO	FC
2	0	1711	1518
3	0	2151	1829
3	1	942	858

L = -2

H	K	FO	FC
2	0	324	278
2	1	1695	1613

L = -1

H	K	FO	FC
1	0	2447	1949

L = 0

H	K	FO	FC
-12	-8	432	461
-12	-6	276	245
-12	-5	314	319
-12	-4	313	391
-12	-2	461	504
-11	0	308	279
-11	-11	429	429
-11	-9	351	380
-11	-7	387	390
-11	-5	557	588
-11	-3	624	614
-11	-1	505	537
-10	-12	274	339
-10	-10	291	267
-10	-6	352	400
-10	-4	302	351
-10	-2	431	432
-10	-1	486	494
-9	-16	316	184
-9	-15	326	328
-9	-13	269	264
-9	-9	327	240
-9	-7	374	399
-9	-6	286	275
-9	-4	249	277
-9	-3	302	345
-9	-1	522	518
-8	-17	398	320
-8	-15	376	365
-8	-9	568	599
-8	-8	279	252
-8	-7	802	831
-8	-6	393	436
-8	-5	366	343
-8	-4	452	436
-8	-3	551	594
-8	-2	284	288
-8	-1	785	809
-7	-18	365	295
-7	-16	461	464
-7	-14	359	399
-7	-10	790	794
-7	-9	277	266
-7	-8	1147	1205
-7	-6	704	724
-7	-3	552	555
-7	-2	943	1012
-6	-17	319	416
-6	-15	346	323
-6	-14	431	480
-6	-12	552	614
-6	-11	520	577
-6	-9	751	809
-6	-7	604	672
-6	-6	329	279
-6	-5	503	474
-6	-4	592	603
-6	-3	904	883
-6	-2	683	739
-6	-1	1166	1135
-5	-20	337	232
-5	-19	397	272
-5	-18	443	457
-5	-16	483	504
-5	-15	417	424
-5	-13	431	362
-5	-12	723	779
-5	-11	569	629
-5	-10	846	902
-5	-9	315	293
-5	-8	725	779
-5	-7	605	684
-5	-6	933	928
-5	-5	1190	1264
-5	-4	946	925
-5	-3	1283	1304
-5	-2	1015	948
-5	-1	271	364
-4	-21	369	253
-4	-19	331	394
-4	-18	310	230
-4	-15	665	697
-4	-14	405	390
-4	-13	880	866
-4	-12	542	617
-4	-11	1053	1123
-4	-10	639	717
-4	-9	687	706
-4	-8	723	734
-4	-7	1162	1247
-4	-6	884	921
-4	-5	2063	2117
-4	-4	1118	1102
-4	-3	1653	1587
-4	-2	740	675
-4	-1	2064	1927
-3	-15	326	313
-3	-14	577	555
-3	-12	938	970
-3	-11	335	401
-3	-10	373	356
-3	-9	867	860
-3	-8	390	466
-3	-7	707	711
-3	-6	394	333
-3	-4	2032	2006
-3	-3	590	553
-3	-2	2268	2033
-3	-1	1575	1491
-2	-17	569	579
-2	-15	597	578
-2	-14	307	322
-2	-12	367	406
-2	-11	432	477
-2	-9	1223	1282
-2	-8	253	204
-2	-7	1732	1775
-2	-6	588	619
-2	-5	853	849
-2	-4	764	756
-2	-3	975	986
-2	-2	424	445
-2	-1	1803	1666
-1	-20	338	225
-1	-19	452	444
-1	-18	354	315
-1	-17	781	798
-1	-16	508	508
-1	-15	792	786
-1	-14	730	665
-1	-13	506	526
-1	-11	870	873
-1	-10	982	998
-1	-9	1792	1938
-1	-8	1882	1995
-1	-7	2278	2370
-1	-6	1048	1107
-1	-5	1083	1131
-1	-4	626	642
-1	-3	1475	1510
-1	-2	1867	1833
-1	-1	2466	2197
0	2	2356	2837
0	4	1920	1926
0	6	3154	3130
0	8	3286	3320
0	10	2037	1967
0	12	1077	913
0	14	1139	947
0	16	1452	1184
0	18	957	712
0	20	405	283
0	24	366	231
0-24		374	243
0-18		772	722
0-16		1179	1239
0-14		889	924
0-12		933	952
0-10		1919	2041
0	-8	3061	3358
0	-6	3326	3392
0	-4	2153	2125
1	0	2125	1892
1	1	2480	2410
1	2	1868	1959
1	3	1478	1596
1	4	638	717
1	5	992	1106
1	6	1033	1151
1	7	2072	2352
1	8	1648	2016
1	9	1845	1949
1	10	1014	1007
1	11	862	933
1	13	526	489
1	14	748	619
1	15	897	785
1	16	700	477
1	17	944	774
1	18	484	366
1	19	574	444
1	20	331	229
1	24	351	196
2	0	276	288
2	1	1864	1760
2	2	463	443
2	3	1023	1016
2	4	821	767
2	5	891	893
2	6	661	624
2	7	1694	1757
2	8	251	242
2	9	1351	1322
2	10	288	296
2	11	533	516
2	12	382	330
2	15	520	607
2	17	708	602
2	19	418	311
3	0	1370	1202
3	1	1591	1439
3	2	2169	1958
3	3	587	562
3	4	1886	1825
3	5	210	179
3	6	580	588
3	7	791	793
3	8	495	533
3	9	902	866
3	10	504	466
3	11	362	324
3	12	1016	993
3	14	694	612
3	15	397	340
3	16	310	248
3	17	323	197
4	0	412	331
4	1	2028	1843
4	2	775	662
4	3	1700	1627
4	4	1187	1129
4	5	2166	2119
4	6	906	879
4	7	1269	1230
4	8	715	684
4	9	727	748
4	10	659	668
4	11	1108	1089
4	12	600	603
4	13	922	895

H	K	FO	FC
-13	-4	312	260
-13	-1	297	302
-12	0	535	552
-12	-11	360	359
-12	-10	386	398
-12	-8	291	266
-12	-5	266	286
-12	-2	314	337
-11	-13	296	276
-11	-12	364	359
-11	-9	274	308
-11	-8	291	184
-11	-4	395	439
-11	-3	634	667
-11	-2	293	319
-11	-1	301	289
-10	-14	348	292
-10	-13	300	355
-10	-7	266	283
-10	-6	329	349
-10	-5	414	455
-10	-4	407	474
-10	-3	384	414
-9	0	574	565
-9	-13	440	430
-9	-11	378	445
-9	-8	509	558
-9	-7	523	569

L = 1

10	4	601	618	-8	-8	422	477	-4	-13	731	738	-1	-3	1444	1277	2	4	407	349	5	17	582	568	-14	-2	452	401
10	6	398	440	-8	-7	375	436	-4	-12	967	1005	-1	-2	1448	1338	2	5	2082	2050	6	0	1790	1816	-13	-9	285	371
10	7	385	379	-8	-6	868	870	-4	-11	875	872	-1	-1	2121	1925	2	6	908	899	6	1	1135	1119	-13	-7	281	241
10	9	359	345	-8	-4	1047	1079	-4	-10	373	416	0	0	1124	970	2	7	1307	1327	6	2	1543	1507	-13	-1	486	454
10	12	305	360	-8	-2	885	905	-4	-9	731	759	0	1	418	425	2	8	644	610	6	3	576	613	-12	-4	298	297
11	0	275	347	-7	0	546	533	-4	-8	308	277	0	2	1537	1402	2	9	474	463	6	4	739	703	-12	-3	274	279
11	1	551	551	-7	-14	382	379	-4	-7	1332	1376	0	3	562	535	2	10	953	929	6	5	482	439	-12	-1	282	259
11	3	585	549	-7	-12	762	738	-4	-6	598	565	0	4	814	779	2	11	1003	1011	6	6	1090	1068	-11	-14	402	433
11	5	603	598	-7	-10	529	535	-4	-5	1180	1160	0	5	400	392	2	13	1245	1211	6	7	649	615	-11	-13	299	205
11	7	383	346	-7	-9	301	203	-4	-4	1514	1520	0	6	1240	1284	2	14	506	526	6	8	1534	1494	-11	-11	290	195
11	10	282	300	-7	-7	555	554	-4	-3	2004	1914	0	7	1039	1153	2	15	812	753	6	9	1008	987	-11	-10	318	350
11	11	446	433	-7	-6	383	398	-4	-2	1146	980	0	8	1382	1449	2	16	475	402	6	10	911	901	-11	-9	277	253
12	0	436	442	-7	-4	1310	1343	-4	-1	1619	1543	0	9	396	450	2	18	368	325	6	11	460	450	-11	-7	335	352
				-7	-3	326	308	-3	0	3134	2690	0	10	1188	1187	2	19	310	245	6	12	282	288	-11	-6	575	564
	L =	2		-7	-2	1007	1017	-3	-22	336	215	0	11	848	865	2	21	447	353	6	14	444	375	-11	-5	313	331
H	K	FO	FC	-7	-1	413	369	-3	-19	298	215	0	12	451	434	3	1	1144	1122	6	16	473	422	-11	-4	528	559
-13	-9	359	314	-6	0	1780	1655	-3	-17	368	370	0	13	526	491	3	2	816	775	6	18	375	322	-11	-3	532	535
-13	-7	367	328	-6	-19	417	319	-3	-15	677	740	0	15	419	348	3	3	1619	1628	7	0	1789	1781	-11	-2	529	574
-13	-1	305	325	-6	-17	333	280	-3	-14	436	501	0	16	529	414	3	4	1746	1861	7	1	500	491	-11	-1	349	356
-12	0	376	337	-6	-16	341	301	-3	-13	370	400	0	17	481	459	3	5	1174	1146	7	2	985	978	-10	-15	320	327
-12	-12	307	144	-6	-14	473	424	-3	-12	613	714	0	18	496	407	3	6	1310	1264	7	3	262	298	-10	-13	631	671
-12	-6	267	130	-6	-13	467	494	-3	-10	871	916	0	24	320	139	3	7	1142	1169	7	4	798	772	-10	-11	604	587
-12	-2	260	222	-6	-12	1033	1067	-3	-9	412	527	0	-18	463	372	3	8	382	324	7	5	283	300	-10	-9	321	324
-11	-12	359	360	-6	-11	511	492	-3	-8	641	634	0	-17	477	430	3	9	500	478	7	6	934	920	-10	-8	352	371
-11	-6	382	457	-6	-10	805	846	-3	-7	1047	1082	0	-16	433	375	3	10	663	666	7	7	471	473	-10	-7	763	828
-11	-4	488	518	-6	-9	565	605	-3	-6	1394	1502	0	-15	344	394	3	11	789	777	7	8	1039	1033	-10	-6	409	433
-11	-2	374	427	-6	-8	758	767	-3	-5	962	944	0	-13	469	506	3	12	853	866	7	9	387	376	-10	-5	1084	1111
-10	0	279	324	-6	-7	653	652	-3	-4	1436	1406	0	-12	405	475	3	13	488	467	7	10	727	724	-10	-3	1211	1229
-10	-15	409	341	-6	-6	1516	1498	-3	-3	832	826	0	-11	689	782	3	14	416	393	7	12	484	466	-10	-1	843	864
-10	-13	629	610	-6	-5	609	628	-3	-2	1860	1771	0	-10	971	1140	3	15	466	514	7	16	551	528	-9	0	946	1012
-10	-12	270	329	-6	-4	1893	1936	-3	-1	2175	1902	0	-9	415	416	3	17	342	328	7	18	423	354	-9	-16	417	373
-10	-11	549	562	-6	-3	505	531	-2	-21	306	292	0	-8	1289	1427	4	0	225	248	8	1	892	843	-9	-15	328	258
-10	-9	508	456	-6	-2	1739	1671	-2	-17	422	430	0	-7	1125	1182	4	1	1039	1067	8	2	557	520	-9	-14	418	457
-10	-7	522	565	-6	-1	886	916	-2	-15	483	591	0	-6	1197	1246	4	2	1008	1024	8	5	239	228	-9	-13	450	466
-10	-5	982	1021	-5	0	1772	1707	-2	-13	448	528	0	-5	395	422	4	3	546	542	8	6	368	443	-9	-12	526	529
-10	-4	283	342	-5	-21	417	347	-2	-12	303	245	0	-4	794	742	4	4	1270	1231	8	7	483	453	-9	-11	356	371
-10	-3	798	793	-5	-19	405	373	-2	-11	511	602	1	0	755	749	4	5	529	561	8	8	315	293	-9	-10	657	634
-10	-2	364	367	-5	-18	392	267	-2	-9	1146	1216	1	1	625	595	4	6	641	602	8	9	540	526	-9	-8	448	484
-10	-1	606	631	-5	-16	411	454	-2	-8	633	620	1	2	1539	1504	4	7	966	943	8	15	350	342	-9	-7	350	319
-9	0	1091	1073	-5	-15	622	613	-2	-7	1651	1887	1	3	881	898	4	8	324	296	9	0	326	331	-9	-6	1018	1125
-9	-16	374	341	-5	-13	1006	1028	-2	-6	639	661	1	4	2194	2106	4	9	731	687	9	1	321	278	-9	-5	575	584
-9	-14	466	442	-5	-12	467	449	-2	-5	891	927	1	5	974	912	4	10	463	440	9	4	427	418	-9	-4	967	986
-9	-13	525	522	-5	-11	1215	1269	-2	-4	430	432	1	6	1211	1171	4	12	440	490	9	5	336	322	-9	-3	784	800
-9	-12	333	390	-5	-10	1185	1221	-2	-3	915	989	1	7	851	953	4	14	508	481	9	6	303	309	-9	-2	821	856
-9	-11	491	490	-5	-9	755	787	-2	-2	730	758	1	8	807	853	4	15	330	348	9	7	305	354	-9	-1	285	347
-9	-10	402	426	-5	-8	1232	1308	-1	0	3191	2752	1	9	1015	1062	4	16	495	480	9	9	277	322	-8	-14	390	468
-9	-8	722	778	-5	-7	1106	1183	-1	-24	338	135	1	10	1047	986	4	18	330	353	9	12	352	228	-8	-12	438	421
-9	-7	315	389	-5	-6	853	845	-1	-16	585	654	1	11	693	709	5	0	739	785	9	13	295	235	-8	-10	493	499
-9	-6	671	678	-5	-5	2247	2387	-1	-15	450	391	1	12	692	706	5	1	1820	1757	10	1	272	307	-8	-9	433	499
-9	-5	1080	1099	-5	-4	835	843	-1	-14	481	522	1	14	631	632	5	2	214	179	10	2	415	464	-8	-7	452	491
-9	-4	983	1008	-5	-3	2490	2537	-1	-12	369	350	1	15	369	312	5	3	765	758	10	4	633	610	-8	-6	589	627
-9	-3	1089	1139	-5	-2	1533	1465	-1	-11	494	541	1	16	482	511	5	4	619	659	10	6	337	352	-8	-4	827	845
-9	-2	782	834	-5	-1	1532	1559	-1	-10	716	862	1	17	546	595	5	5	864	819	10	10	268	200	-8	-2	701	705
-9	-1	320	313	-4	0	215	237	-1	-9	879	1029	1	19	336	246	5	6	510	488	11	3	436	473	-8	-1	346	397
-8	0	350	308	-4	-22	330	306	-1	-8	811	953	1	20	469	344	5	7	952	954	11	7	303	268	-7	0	255	198
-8	-14	336	372	-4	-20	358	366	-1	-7	649	688	2	0	1222	1255	5	9	1212	1182					-7	-18	363	273
-8	-12	625	644	-4	-17	346	342	-1	-6	854	932	2	1	1188	1158	5	11	727	711		L =	3		-7	-14	317	267
-8	-10	320	319	-4	-15	362	354	-1	-5	967	955	2	2	999	974	5	14	311	284	H	K	FO	FC	-7	-12	648	680
-8	-9	330	363	-4	-14	737	789	-1	-4	456	414	2	3	2583	2461	5	15	616	547	-14	0	429	412	-7	-11	404	418

-7-10	607	628	-3-15	656	672	0 20	453	310	3 9	939	913	8 7	262	280	-9 -4	607	661	-5 -2	1085	1071
-7 -9	683	683	-3-14	380	404	0 22	336	188	3 10	368	365	8 11	269	127	-9 -2	907	959	-5 -1	995	1035
-7 -8	531	529	-3-13	1107	1166	0-20	429	302	3 11	492	427	8 14	300	282	-9 -1	509	510	-4-22	421	289
-7 -7	279	221	-3-12	310	314	0-17	330	519	3 12	720	736	8 15	310	296	-8 0	830	800	-4-20	445	386
-7 -6	979	1071	-3-11	979	1017	0-15	403	521	3 13	391	345	9 1	303	248	-8-17	334	280	-4-16	314	287
-7 -5	384	407	-3-10	404	399	0-14	760	937	3 14	559	516	9 2	292	366	-8-16	339	375	-4-15	689	589
-7 -4	1253	1243	-3 -9	641	594	0-12	937	1060	3 15	479	452	9 3	364	400	-8-15	412	301	-4-14	977	976
-7 -3	617	578	-3 -8	390	332	0-11	470	483	3 17	364	329	9 5	576	600	-8-12	369	332	-4-13	664	675
-7 -2	706	752	-3 -7	848	936	0-10	758	845	4 0	603	573	9 7	257	242	-8-11	372	387	-4-12	870	894
-7 -1	788	827	-3 -6	443	596	0 -9	621	670	4 1	1046	1035	10 0	261	175	-8-10	596	608	-4-11	728	828
-6 0	660	628	-3 -5	1404	1442	0 -8	498	551	4 2	506	513	10 2	275	360	-8 -9	370	360	-4-10	737	745
-6-21	348	223	-3 -4	671	660	0 -7	398	391	4 3	750	740	10 4	439	486	-8 -8	480	462	-4 -9	1085	1117
-6-20	417	214	-3 -3	2536	2567	0 -6	744	734	4 4	486	506	10 6	380	389	-8 -7	505	498	-4 -7	911	1012
-6-14	572	545	-3 -2	1246	1130	0 -5	564	597	4 5	332	320	11 0	268	187	-8 -6	232	229	-4 -6	1340	1484
-6-13	576	552	-2-20	329	263	0 -4	2198	2129	4 6	454	448				-8 -5	606	629	-4 -5	1416	1501
-6-12	559	483	-2-19	347	323	1 0	2320	2228	4 7	1063	1048	L = 4			-8 -4	233	205	-4 -4	1605	1661
-6-11	665	681	-2-15	329	410	1 1	466	496	4 8	478	462	H K	FO	FC	-8 -2	810	830	-4 -3	1560	1641
-6-10	609	604	-2-14	635	613	1 2	2539	2368	4 9	770	718	-14 0	504	463	-8 -1	635	648	-3-23	340	268
-6 -9	341	407	-2-13	454	462	1 3	1477	1515	4 10	610	621	-14 -7	347	306	-7 0	302	269	-3-21	510	398
-6 -8	855	896	-2-12	415	400	1 4	2201	2162	4 11	267	232	-13 -7	345	362	-7-18	377	389	-3-20	311	310
-6 -7	259	235	-2-11	622	684	1 5	1936	1934	4 12	377	429	-13 -1	371	400	-7-16	419	334	-3-19	421	374
-6 -6	658	648	-2-10	769	820	1 6	2384	2341	5 1	1649	1672	-12-12	327	283	-7-13	293	250	-3-17	450	427
-6 -5	446	509	-2 -9	624	640	1 7	930	876	5 2	249	202	-12 -7	288	310	-7-12	314	287	-3-16	577	546
-6 -4	1235	1277	-2 -8	853	927	1 8	1480	1489	5 3	924	946	-12 -4	344	355	-7-11	345	285	-3-15	581	489
-6 -3	1032	974	-2 -7	830	1004	1 9	810	763	5 5	579	574	-12 -2	270	270	-7-10	634	641	-3-13	1401	1489
-6 -2	1590	1533	-2 -6	999	1084	1 10	1092	1069	5 6	461	482	-11-15	300	261	-7 -9	397	427	-3-11	1127	1203
-6 -1	984	913	-2 -5	1155	1226	1 11	820	798	5 7	1352	1324	-11-14	320	322	-7 -8	621	671	-3-10	565	710
-5 0	994	960	-2 -4	1760	1749	1 12	1229	1205	5 8	277	255	-11-13	291	226	-7 -7	761	725	-3 -9	690	744
-5-19	446	369	-2 -3	953	1002	1 13	556	471	5 9	886	895	-11-12	474	432	-7 -6	440	474	-3 -8	1173	1311
-5-15	437	440	-2 -2	1901	1825	1 14	901	808	5 11	637	650	-11-11	296	278	-7 -5	316	300	-3 -7	1349	1531
-5-14	345	296	-2 -1	631	515	1 16	831	723	5 15	301	240	-11 -8	292	196	-7 -4	393	320	-3 -6	774	857
-5-13	927	928	-1 0	2810	2286	1 18	480	369	5 17	435	418	-11 -7	314	347	-7 -3	378	379	-3 -5	2590	2932
-5-12	333	230	-1-14	324	322	1 22	586	406	6 0	1688	1713	-11 -6	405	431	-7 -2	761	743	-3 -4	502	591
-5-11	1008	1058	-1-12	524	614	2 0	751	751	6 1	859	863	-11 -5	616	629	-7 -1	834	816	-3 -3	1955	2176
-5 -9	471	470	-1-10	987	1029	2 1	1996	1930	6 2	1194	1195	-11 -4	649	647	-6-11	510	530	-3 -2	1813	1654
-5 -8	547	605	-1 -9	302	331	2 2	1136	1115	6 3	319	331	-11 -3	308	286	-6-10	452	467	-2 0	2184	1935
-5 -7	759	805	-1 -8	863	901	2 3	2713	2640	6 4	425	443	-11 -2	513	506	-6 -9	997	1062	-2-14	760	835
-5 -6	916	954	-1 -7	909	963	2 4	337	306	6 5	243	241	-11 -1	420	448	-6 -8	391	356	-2-13	628	707
-5 -5	1706	1821	-1 -6	1675	1770	2 5	2704	2698	6 6	939	945	-10 0	545	521	-6 -7	984	995	-2-12	905	1030
-5 -4	316	307	-1 -5	760	749	2 6	946	937	6 7	840	806	-10-13	529	529	-6 -5	557	550	-2-11	475	572
-5 -3	1433	1378	-1 -4	1775	1663	2 7	1606	1621	6 8	805	797	-10-11	501	452	-6 -4	457	467	-2-10	762	850
-5 -2	883	927	-1 -2	2313	2062	2 8	1086	1032	6 9	453	499	-10 -9	437	410	-6 -3	581	581	-2 -9	264	323
-5 -1	798	760	-1 -1	1477	1295	2 9	1076	1069	6 10	855	826	-10 -8	398	424	-6 -2	264	263	-2 -8	1223	1321
-4 0	482	462	0 0	764	652	2 10	668	645	6 11	255	182	-10 -7	276	325	-6 -1	1074	1110	-2 -7	318	323
-4-22	437	338	0 1	1619	1493	2 11	1262	1270	6 14	354	349	-10 -6	325	416	-5 0	349	339	-2 -6	1670	1672
-4-20	417	331	0 2	2450	2288	2 13	1267	1204	6 16	609	527	-10 -5	966	992	-5-22	342	188	-2 -5	1075	1088
-4-16	525	489	0 3	263	114	2 15	1092	1003	6 18	320	335	-10 -3	1047	1077	-5-16	320	291	-2 -4	1731	1673
-4-14	618	609	0 4	2017	1994	2 18	363	212	7 0	729	767	-10 -2	422	501	-5-15	446	475	-2 -3	1646	1561
-4-12	1042	1058	0 5	586	582	2 19	333	285	7 2	583	592	-10 -1	422	458	-5-14	574	625	-2 -2	2176	1865
-4-10	673	780	0 6	739	729	2 21	339	311	7 3	403	395	-9 0	346	341	-5-13	586	751	-2 -1	638	586
-4 -9	529	525	0 7	364	317	3 0	571	585	7 6	450	513	-9-14	391	376	-5-12	697	765	-1 0	1044	1050
-4 -8	520	571	0 8	603	600	3 1	1388	1338	7 7	344	367	-9-12	355	366	-5-11	434	457	-1-13	364	310
-4 -7	288	327	0 9	697	701	3 2	1365	1267	7 8	710	714	-9-11	269	281	-5 -9	336	246	-1-12	749	812
-4 -6	1404	1466	0 10	927	866	3 3	1229	1211	7 9	481	443	-9-10	271	318	-5 -8	457	458	-1-10	587	587
-4 -4	1630	1639	0 11	554	569	3 4	971	1003	7 10	488	494	-9 -9	690	720	-5 -7	538	494	-1 -7	667	666
-4 -3	477	490	0 12	1223	1060	3 5	1491	1479	7 14	333	276	-9 -8	471	533	-5 -6	1135	1114	-1 -6	1185	1258
-4 -2	1108	1081	0 14	1026	875	3 6	574	541	8 1	348	333	-9 -7	588	658	-5 -5	838	855	-1 -5	354	385
-4 -1	399	411	0 15	617	546	3 7	649	653	8 3	371	427	-9 -6	598	652	-5 -4	1200	1269	-1 -4	1917	1815
-3-21	411	336	0 17	545	497	3 8	321	266	8 5	467	435	-9 -5	293	326	-5 -3	964	916	-1 -3	372	396

-1	-2	1418	1274	2	9	322	333	7	2	339	333	-9	-17	528	452	-5	-9	633	680	-1	-6	403	440	2	13	383	411
-1	-1	209	110	2	10	383	333	7	4	360	390	-9	-15	487	469	-5	-8	471	427	-1	-5	236	315	2	14	595	566
0	0	1502	1381	2	11	1185	1164	7	6	495	542	-9	-11	395	393	-5	-7	616	699	-1	-4	1229	1186	3	0	502	499
0	1	1104	982	2	13	1084	1071	8	1	291	268	-9	-9	753	783	-5	-6	941	1034	-1	-3	312	333	3	1	633	675
0	2	1478	1384	2	14	301	319	8	2	478	502	-9	-7	842	867	-5	-5	482	447	-1	-2	1514	1410	3	2	475	503
0	3	563	547	2	15	402	350	8	3	629	677	-9	-6	256	189	-5	-4	1282	1375	-1	-1	225	117	3	3	544	544
0	4	2507	2408	2	16	405	389	8	5	569	536	-9	-5	388	381	-5	-3	885	902	0	0	709	637	3	4	635	638
0	6	1670	1639	2	19	329	253	8	6	402	388	-9	-4	450	483	-4	-15	658	713	0	1	995	936	3	5	937	921
0	7	734	734	2	20	383	236	8	7	377	363	-9	-3	480	481	-4	-14	737	698	0	2	1085	1001	3	6	740	733
0	8	518	479	2	21	457	371	8	8	386	347	-9	-1	1097	1081	-4	-13	844	891	0	3	643	617	3	7	412	382
0	9	933	885	3	0	555	555	8	11	460	433	-8	0	1661	1662	-4	-12	597	624	0	4	1508	1487	3	8	512	528
0	10	829	777	3	1	505	499	8	13	407	295	-8	-18	428	363	-4	-11	1130	1223	0	5	577	458	3	9	451	441
0	11	522	516	3	2	724	684	9	1	350	376	-8	-16	454	419	-4	-10	336	414	0	6	1063	1054	3	10	481	491
0	12	1063	958	3	3	283	296	9	3	666	675	-8	-14	499	529	-4	-9	1111	1204	0	7	807	789	3	11	448	441
0	14	891	822	3	4	1208	1186	9	4	294	361	-8	-13	286	265	-4	-8	383	410	0	9	821	778	3	12	549	559
0	15	431	348	3	5	238	277	9	5	394	502	-8	-11	276	272	-4	-7	1465	1667	0	10	404	386	3	13	343	382
0	16	500	407	3	6	1134	1091	9	7	277	339	-8	-10	873	877	-4	-6	1167	1333	0	11	545	442	3	15	307	263
0	17	321	232	3	7	648	609	9	9	274	217	-8	-9	539	582	-4	-5	1606	1845	0	12	708	652	4	0	1215	1226
0	20	468	326	3	8	433	460	10	1	263	233	-8	-8	1234	1311	-4	-4	1154	1254	0	13	320	324	4	2	884	892
0	-16	309	382	3	10	442	415	10	4	340	358	-8	-7	396	444	-4	-3	2189	2330	0	15	394	353	4	3	850	872
0	-15	335	386	3	11	291	285	10	6	274	266	-8	-6	970	1001	-3	0	1649	1453	0	17	509	383	4	4	267	261
0	-14	647	753	3	12	535	569					-8	-5	427	402	-3	-21	313	329	0	20	318	223	4	5	787	800
0	-12	838	963	3	13	403	388		L =	5		-8	-4	300	323	-3	-19	375	432	0	-17	310	401	4	6	896	893
0	-11	436	498	3	14	628	614	H	K	FO	FC	-8	-3	602	681	-3	-18	363	365	0	-15	285	276	4	7	349	364
0	-10	732	827	3	15	278	259	-14	-8	322	314	-8	-2	1308	1334	-3	-16	426	474	0	-14	286	260	4	8	631	670
0	-9	794	827	3	16	392	352	-14	-5	268	251	-8	-1	543	561	-3	-15	661	700	0	-13	281	316	4	10	613	623
0	-8	423	451	3	20	346	276	-14	-1	348	387	-7	0	1802	1750	-3	-14	695	796	0	-12	529	706	4	11	458	441
0	-7	639	749	4	0	867	874	-13	-9	292	231	-7	-18	371	302	-3	-13	890	1009	0	-11	428	444	4	12	424	401
0	-6	1600	1622	4	1	784	803	-13	-8	296	229	-7	-17	398	223	-3	-11	953	1063	0	-10	446	465	4	13	475	485
0	-5	272	143	4	2	532	558	-13	-7	258	261	-7	-16	405	400	-3	-10	909	1088	0	-9	715	762	4	15	386	323
0	-4	2421	2389	4	4	512	514	-13	-2	256	284	-7	-14	370	302	-3	-9	700	778	0	-7	727	804	4	18	314	263
1	0	2356	2482	4	6	338	351	-12	-14	300	171	-7	-12	334	290	-3	-8	1193	1289	0	-6	998	1080	4	19	329	259
1	1	1842	1900	4	8	665	642	-12	-5	372	313	-7	-10	874	882	-3	-7	1150	1243	0	-5	544	522	5	0	370	357
1	2	1731	1666	4	9	391	342	-12	-2	265	302	-7	-9	671	723	-3	-6	1244	1274	0	-4	1544	1534	5	1	602	678
1	3	1547	1557	4	10	462	440	-11	-13	305	266	-7	-8	845	900	-3	-5	2335	2465	1	0	297	321	5	2	924	935
1	4	1647	1633	4	11	326	318	-11	-12	323	300	-7	-7	729	767	-3	-4	779	739	1	2	1149	1115	5	3	383	376
1	5	1677	1690	4	13	477	450	-11	-11	304	238	-7	-6	878	869	-3	-3	2403	2369	1	3	1128	1058	5	4	706	706
1	6	1825	1770	4	15	374	254	-11	-10	300	281	-7	-5	246	253	-3	-2	1747	1617	1	4	974	982	5	5	310	250
1	7	382	434	5	1	956	991	-11	-6	404	365	-7	-4	496	534	-3	-1	1553	1438	1	5	1193	1128	5	6	278	270
1	8	1286	1203	5	2	376	381	-11	-4	379	349	-7	-3	508	530	-2	0	1107	1023	1	6	819	795	5	7	428	476
1	10	909	881	5	3	467	464	-11	-3	270	264	-7	-2	1083	1065	-2	-18	389	274	1	7	713	711	5	8	380	352
1	11	894	828	5	4	276	289	-11	-2	358	347	-7	-1	1049	1042	-2	-14	343	400	1	8	713	682	5	9	500	497
1	12	890	830	5	5	345	309	-11	-1	267	245	-6	0	286	262	-2	-13	318	345	1	10	581	580	5	10	332	338
1	13	981	999	5	7	754	742	-10	0	661	698	-6	-17	440	316	-2	-12	839	935	1	11	491	435	5	12	455	466
1	14	831	759	5	9	802	792	-10	-16	307	270	-6	-15	409	442	-2	-11	349	433	1	12	263	333	6	1	351	308
1	15	405	337	5	10	332	310	-10	-14	330	271	-6	-14	574	524	-2	-10	957	1046	1	13	672	729	6	2	271	304
1	16	461	423	5	11	405	421	-10	-13	293	224	-6	-9	622	628	-2	-9	768	851	1	14	680	659	6	4	374	396
1	18	388	330	5	13	328	258	-10	-11	515	482	-6	-7	748	870	-2	-8	368	404	1	15	533	607	6	6	440	424
1	20	332	262	6	0	415	389	-10	-10	283	330	-6	-5	526	572	-2	-7	812	852	2	0	818	815	6	10	353	302
1	21	336	254	6	1	572	613	-10	-9	279	284	-6	-4	553	521	-2	-6	1125	1228	2	1	310	337	6	12	289	308
2	0	888	882	6	2	600	597	-10	-8	308	332	-6	-3	678	628	-2	-5	873	963	2	2	784	797	7	0	344	292
2	1	1299	1196	6	3	282	341	-10	-7	366	315	-6	-2	315	305	-2	-4	1675	1493	2	3	685	674	7	2	494	551
2	2	739	660	6	4	282	285	-10	-6	308	354	-6	-1	1195	1151	-2	-3	928	856	2	4	640	633	7	4	758	798
2	3	2109	2122	6	6	410	408	-10	-5	418	404	-5	-22	394	275	-2	-2	1194	1057	2	5	758	714	7	6	466	483
2	4	259	216	6	8	530	537	-10	-4	350	288	-5	-17	322	280	-2	-1	385	373	2	6	395	412	7	8	334	367
2	5	1882	1801	6	9	296	320	-10	-3	773	831	-5	-16	333	283	-1	0	1390	1407	2	7	236	190	7	12	319	344
2	6	468	440	6	10	397	394	-10	-2	389	416	-5	-14	484	536	-1	-14	400	432	2	8	381	441	7	14	448	416
2	7	1253	1225	6	16	298	311	-10	-1	433	454	-5	-12	763	750	-1	-12	760	860	2	11	414	339	8	0	533	544
2	8	883	811	7	1	587	577	-9	0	228	215	-5	-10	496	536	-1	-10	641	730	2	12	602	556	8	1	362	311

8	2	345	342	-8-14	348	371	-3	-8	746	808	1	3	499	466	5	6	376	385	-9-15	345	231	-3	-9	914	994
8	3	433	517	-8-12	488	459	-3	-7	407	444	1	4	328	333	5	7	295	208	-9-13	359	367	-3	-8	464	548
8	4	506	572	-8-10	1015	1031	-3	-6	801	824	1	5	682	666	5	10	407	413	-9-10	499	535	-3	-7	845	829
8	5	539	609	-8 -8	1486	1526	-3	-5	694	717	1	6	414	398	5	12	366	289	-9 -9	761	755	-3	-6	402	433
8	6	492	501	-8 -7	422	372	-3	-4	759	727	1	7	968	983	6	2	437	444	-9 -8	711	759	-3	-3	768	736
8	7	281	328	-8 -6	1024	1090	-3	-3	1618	1544	1	9	610	584	6	4	598	645	-9 -7	702	738	-3	-2	489	523
8	10	343	347	-8 -4	631	605	-3	-2	1168	1132	1	11	444	378	6	5	471	491	-9 -6	369	469	-3	-1	779	756
8	11	295	312	-8 -3	284	323	-3	-1	798	716	1	13	418	397	6	12	375	317	-9 -5	341	433	-2	0	1441	1385
9	1	279	312	-8 -2	1682	1722	-2	0	455	469	1	15	374	330	7	0	427	458	-9 -4	328	351	-2-17		427	537
9	3	484	515	-7-17	353	334	-2-17		334	374	2	0	514	500	7	1	279	295	-9 -3	803	819	-2-16		374	293
				-7-16	335	437	-2-15		384	465	2	1	790	769	7	2	502	560	-9 -2	511	513	-2-15		413	479
	L =	6		-7-15	496	479	-2-11		483	490	2	2	609	550	7	4	545	622	-9 -1	823	788	-2-14		372	374
H	K	FO	FC	-7-12	321	295	-2-10		359	406	2	3	414	428	7	6	542	569	-8-18	400	373	-2-11		766	821
-14	-1	311	402	-7-11	405	419	-2	-9	988	1044	2	4	974	948	7	7	328	309	-8-16	494	462	-2-10		613	668
-13	0	601	603	-7-10	494	456	-2	-8	406	457	2	5	356	366	7	8	324	326	-8-14	459	440	-2 -9		857	915
-13	-12	323	242	-7 -9	925	995	-2	-7	958	1016	2	6	866	895	7	9	324	318	-8-12	345	367	-2 -8		598	579
-13	-10	385	371	-7 -8	1106	1171	-2	-6	587	621	2	7	608	559	7	10	316	217	-8-10	854	900	-2 -7		726	762
-13	-6	403	337	-7 -7	859	889	-2	-5	399	357	2	9	269	287	7	12	391	378	-8 -8	871	862	-2 -6		863	942
-13	-5	267	232	-7 -6	660	691	-2	-4	933	875	2	10	552	525	8	2	360	423	-8 -7	508	425	-2 -5		695	720
-13	-4	363	312	-7 -5	506	494	-2	-3	438	416	2	11	412	440	8	5	322	384	-8 -6	930	1018	-2 -4		314	288
-12	0	261	283	-7 -4	478	459	-2	-2	682	667	2	12	607	553	8	6	330	325	-8 -4	614	591	-2 -3		740	793
-12	-13	383	366	-7 -3	618	636	-2	-1	1126	1091	2	14	547	472					-8 -3	322	335	-2 -2		996	933
-12	-11	279	232	-7 -2	1006	986	-1	0	1133	1155	2	16	304	288		L =	7		-7-17	433	361	-2 -1		1411	1480
-12	-10	328	298	-6-17	389	340	-1-16		476	571	2	20	349	187	H	K	FO	FC	-7-11	398	397	-1 0		1787	1777
-12	-9	292	240	-6-15	515	468	-1-10		891	916	3	0	607	660	-14	-7	296	283	-7 -9	594	673	-1-18		390	380
-12	-7	348	267	-6-13	514	601	-1	-8	1321	1349	3	1	1051	1066	-14	-6	287	163	-7 -8	368	368	-1-16		547	549
-12	-5	403	366	-6 -9	611	654	-1	-6	705	735	3	2	547	559	-14	-4	369	288	-7 -7	922	927	-1-14		447	474
-12	-3	627	647	-6 -7	570	521	-1	-5	593	594	3	3	1397	1435	-14	-2	420	417	-7 -6	498	462	-1-12		282	332
-12	-1	331	329	-6 -6	339	276	-1	-3	656	591	3	4	397	395	-13	0	550	551	-7 -5	369	375	-1-10		1037	1086
-11	-6	271	315	-6 -5	565	580	-1	-2	1264	1244	3	5	974	977	-13	-10	397	371	-6-13	452	447	-1 -8		1389	1454
-11	-4	467	471	-6 -4	536	621	-1	-1	235	205	3	6	320	370	-13	-8	345	373	-6-10	496	558	-1 -7		408	384
-11	-1	331	321	-5-20	333	297	0	0	920	845	3	7	1022	999	-13	-6	384	385	-6 -9	438	437	-1 -6		924	942
-10	-11	332	281	-5-16	361	294	0	1	1768	1678	3	9	834	785	-13	-5	451	446	-6 -8	465	476	-1 -5		326	268
-10	-9	664	652	-5-14	520	543	0	2	707	707	3	10	293	226	-13	-4	321	316	-6 -7	902	904	-1 -4		636	649
-10	-8	303	360	-5-13	411	385	0	3	418	368	3	11	644	601	-13	-3	553	546	-6 -5	864	903	-1 -3		251	228
-10	-7	398	422	-5-12	514	584	0	4	246	257	3	12	324	309	-13	-2	481	466	-6 -4	329	323	-1 -2		1419	1467
-10	-5	250	255	-5-10	329	325	0	5	618	611	3	13	779	716	-12	-11	411	409	-5-15	346	313	0	0	972	945
-10	-4	316	309	-5 -9	601	672	0	6	350	282	3	14	414	456	-12	-9	361	351	-5-14	516	558	0	1	971	947
-10	-3	298	308	-5 -7	700	782	0	7	582	551	3	18	291	71	-12	-7	347	345	-5-12	525	543	0	2	940	479
-10	-2	532	532	-5 -6	901	1030	0	8	378	364	4	0	956	1050	-12	-5	581	579	-5-10	400	392	0	3	633	652
-10	-1	457	506	-5 -4	1160	1290	0	9	726	729	4	1	449	494	-12	-4	324	300	-5 -6	432	488	0	4	410	335
-9	0	603	580	-4-13	649	653	0	10	723	686	4	2	790	807	-12	-3	399	423	-5 -5	381	433	0	5	339	357
-9	-17	414	386	-4-12	359	416	0	11	324	264	4	3	746	777	-12	-1	513	513	-5 -4	782	831	0	6	442	479
-9	-15	433	434	-4-11	852	1007	0	12	358	301	4	4	741	696	-11	-12	293	286	-5 -3	490	570	0	7	1082	1003
-9	-11	623	582	-4 -9	420	430	0	13	386	294	4	5	978	1001	-11	-7	396	376	-4 0	922	895	0	8	668	598
-9	-10	380	383	-4 -8	535	548	0	15	533	471	4	6	511	500	-11	-4	407	400	-4-16	321	208	0	9	664	659
-9	-9	861	872	-4 -7	796	891	0	17	368	283	4	7	427	421	-11	-3	361	328	-4-13	328	339	0	10	347	348
-9	-8	567	586	-4 -6	487	520	0-17		300	309	4	8	577	592	-11	-2	536	537	-4-10	444	555	0	15	375	274
-9	-7	899	890	-4 -5	1366	1366	0-15		430	492	4	9	289	277	-11	-1	380	383	-4 -8	523	599	0	16	335	281
-9	-6	311	292	-4 -4	790	886	0-12		295	291	4	10	557	600	-10	-17	406	316	-4 -6	510	569	0	17	358	343
-9	-5	827	883	-4 -3	1439	1514	0-11		279	225	4	11	478	465	-10	-15	361	270	-4 -5	721	801	0-15		316	294
-9	-4	349	440	-4 -2	477	459	0-10		635	691	4	13	461	395	-10	-9	474	471	-4 -4	513	542	0-10		312	333
-9	-3	404	377	-3 0	1305	1225	0	-9	649	736	4	14	350	258	-10	-8	264	226	-4 -3	829	786	0 -9		616	676
-9	-2	596	607	-3-18	367	346	0	-8	340	339	5	0	360	403	-10	-7	670	658	-4 -2	672	630	0 -8		588	620
-9	-1	1435	1465	-3-16	354	412	0	-7	605	618	5	1	261	246	-10	-5	320	268	-4 -1	405	428	0 -7		1002	1005
-8	0	1913	1919	-3-13	611	761	0	-6	366	310	5	2	304	410	-10	-3	379	309	-3 0	499	448	0 -5		330	299
-8-18		566	505	-3-12	356	423	0	-5	648	603	5	3	384	424	-10	-1	712	713	-3-17	393	382	1	1	758	767
-8-16		787	668	-3-11	599	684	0	-4	276	235	5	4	638	643	-9	0	892	877	-3-12	288	306	1	2	820	791
-8-15		407	321	-3-10	712	799	1	1	574	618	5	5	329	374	-9-18		351	207	-3-11	584	599	1	3	413	425

1	4	500	473
1	5	597	566
1	6	507	441
1	7	416	414
1	8	477	467
1	9	586	594
1	10	327	274
1	11	277	270
1	12	401	318
1	13	437	422
1	14	337	300
1	15	518	475
2	1	918	919
2	2	970	887
2	3	654	622
2	4	1123	1120
2	5	550	556
2	6	983	966
2	7	442	467
2	8	361	316
2	9	790	793
2	10	525	471
2	11	376	356
2	12	713	607
2	14	487	419
3	0	267	267
3	1	946	938
3	3	995	1033
3	5	1109	1089
3	6	430	490
3	7	644	606
3	8	364	319
3	9	662	666
3	11	724	730
3	13	513	430
3	15	410	324
3	16	328	267
4	1	506	507
4	2	621	652
4	3	563	560
4	4	328	331
4	5	448	456
4	6	391	378
4	7	263	324
4	8	414	442
4	10	417	375
4	11	285	273
4	12	303	264
4	13	339	350
5	3	249	302
5	10	359	271
5	11	317	256
6	1	330	357
6	3	465	460
6	7	424	428
7	1	347	402
7	4	337	437
7	6	359	395

L = 8

H	K	FO	FC
-14	0	399	345
-14	-6	408	336
-14	-4	404	396
-14	-2	328	330
-13	0	356	345
-13	-11	398	335
-13	-10	295	238
-13	-8	498	387
-13	-7	314	301
-13	-5	474	416
-13	-3	514	534
-13	-2	360	342
-13	-1	273	292
-12	-9	266	245
-12	-7	371	296
-12	-6	347	283
-12	-5	309	363
-12	-4	428	433
-12	-3	394	440
-12	-2	414	379
-11	-9	281	249
-11	-8	259	174
-11	-6	288	306
-11	-4	455	448
-11	-3	284	332
-10	0	289	270
-10	-13	346	213
-10	-11	302	172
-10	-9	371	333
-10	-7	350	416
-10	-6	269	154
-10	-1	647	623
-9	-18	319	233
-9	-10	302	233
-9	-9	335	322
-9	-8	522	505
-9	-6	602	595
-8	-9	472	545
-8	-8	664	741
-8	-7	397	337
-8	-6	633	598
-8	-5	434	434
-7	-16	313	185
-7	-14	396	417
-7	-12	502	466
-7	-10	427	362
-7	-9	613	554
-7	-8	732	634
-7	-6	499	505
-6	-18	361	323
-6	-15	374	316
-6	-13	503	540
-6	-12	489	521
-6	-11	522	578
-6	-10	365	442
-6	-8	568	645
-6	-6	654	736
-6	-5	830	860
-6	-4	367	370
-5	0	237	254
-5	-11	393	306
-5	-10	432	508
-5	-9	508	524
-5	-8	471	521
-5	-7	364	397
-5	-6	513	556
-5	-5	719	770
-5	-4	763	761
-5	-3	601	551
-5	-2	463	420
-5	-1	745	702
-4	0	728	722
-4	-12	376	409
-4	-10	451	466
-4	-9	456	433
-4	-8	361	295
-4	-7	421	414
-4	-6	260	326
-4	-5	306	306
-4	-4	563	543
-4	-2	670	616
-4	-1	939	916
-3	-17	419	433
-3	-15	419	515
-3	-11	460	458
-3	-10	349	355
-3	-9	1123	1242
-3	-7	1137	1231
-3	-5	412	438
-3	-3	800	802
-3	-1	1453	1405
-2	0	1639	1649
-2	-17	340	460
-2	-16	332	330
-2	-14	486	497
-2	-11	487	573
-2	-10	705	726
-2	-9	694	770
-2	-8	1367	1438
-2	-7	963	1062
-2	-6	895	893
-2	-5	344	422
-2	-4	671	634
-2	-3	672	722
-2	-2	1368	1356
-2	-1	1123	1194
-1	0	1716	1823
-1	-18	329	298
-1	-16	413	474
-1	-14	388	385
-1	-12	324	309
-1	-10	678	758
-1	-9	318	296
-1	-8	972	1017
-1	-6	1099	1138
-1	-5	558	563
-1	-4	509	516
-1	-3	252	175
-1	-2	999	1048
-1	-1	384	305
0	0	776	686
0	1	575	578
0	2	464	437
0	3	382	359
0	5	341	297
0	7	668	635
0	8	549	543
0	9	409	451
0	10	334	257
0	13	285	239
0	15	341	266
0	17	343	290
0	-13	267	248
0	-9	383	411
0	-8	459	502
0	-7	612	637
0	-5	277	292
1	0	469	444
1	1	427	384
1	2	383	347
1	3	375	355
1	4	573	554
1	5	538	495
1	6	531	473
1	7	501	495
1	10	289	295
1	12	341	284
1	13	330	277
1	15	339	347
2	1	385	407
2	2	794	805
2	3	458	464
2	4	886	873
2	6	501	495
2	7	520	505
2	8	288	315
2	9	339	313
2	10	263	250
2	12	610	531
2	14	423	336
3	0	268	265
3	1	430	430
3	2	289	338
3	3	564	566
3	4	341	327
3	5	614	584
3	8	279	303
3	10	376	366
3	11	369	389
3	12	294	279
4	1	261	319
4	3	337	364
4	5	265	263
5	0	564	558
5	2	296	307
5	5	268	273
5	6	299	301
6	0	336	350
6	3	350	362

L = 9

H	K	FO	FC
-14	0	344	321
-14	-4	307	267
-14	-3	290	234
-13	-5	497	516
-13	-3	400	386
-13	-1	311	315
-12	-12	407	350
-12	-6	486	442
-12	-4	501	460
-12	-3	268	274
-11	-9	293	194
-11	-5	611	611
-11	-4	337	310
-11	-3	508	489
-11	-1	350	378
-10	-12	364	215
-10	-7	321	321
-10	-5	339	366
-9	-13	373	309
-9	-8	348	304
-9	-5	366	293
-8	-17	322	325
-8	-14	334	316
-8	-12	364	327
-8	-11	424	393
-8	-7	611	612
-8	-6	623	596
-7	-16	382	357
-7	-14	563	577
-7	-12	531	503
-7	-10	688	699
-7	-9	324	433
-7	-8	518	629
-7	-7	338	412
-7	-6	827	972
-7	-5	431	517
-6	-16	381	256
-6	-13	567	616
-6	-11	522	649
-6	-10	431	511
-6	-9	357	389
-6	-8	437	461
-6	-7	645	656
-6	-6	398	381
-6	-5	850	891
-6	-4	347	399
-6	-3	1453	1436
-5	-12	294	257
-5	-11	295	402
-5	-10	319	369
-5	-9	339	314
-5	-7	618	682
-5	-6	299	300
-5	-5	642	658
-5	-4	599	624
-5	-3	476	438
-5	-2	306	310
-5	-1	614	572
-4	0	302	250
-4	-10	398	378
-4	-9	524	537
-4	-8	368	447
-4	-7	501	535
-4	-5	305	263
-4	-3	424	430
-4	-2	599	641
-4	-1	627	562
-3	-18	368	59
-3	-15	336	352
-3	-11	505	536
-3	-9	696	760
-3	-7	608	634
-3	-5	579	633
-3	-4	280	217
-3	-3	425	511
-3	-2	443	486
-3	-1	1325	1369
-2	0	755	811
-2	-16	383	409
-2	-14	325	300
-2	-11	270	309
-2	-10	507	525
-2	-9	542	603
-2	-8	837	911
-2	-7	320	350
-2	-6	727	755
-2	-4	422	437
-2	-3	474	490
-2	-2	809	777
-2	-1	499	548
-1	0	762	797
-1	-14	278	173
-1	-10	311	412
-1	-9	354	356
-1	-8	578	677
-1	-7	424	412
-1	-6	615	685
-1	-3	313	269
-1	-2	669	651
-1	-1	362	341
0	1	568	559
0	3	445	453
0	4	263	253
0	5	303	347
0	6	331	377
0	7	349	285
0	8	243	205
0	11	310	263
0	13	366	307
0	14	303	264
0	15	316	300
0	-13	325	309
0	-7	284	286
0	-6	297	355
0	-5	342	385
1	1	317	269
1	3	462	398
1	4	259	252
1	5	600	579
1	7	417	396
1	10	348	328
1	13	371	354
2	2	358	364
2	4	653	606
2	6	439	440
2	12	387	321
3	1	323	344
4	1	483	460
4	3	268	283
4	7	273	308
4	9	520	499
5	0	404	465
5	2	500	540
5	6	459	442

L = 10

H	K	FO	FC
-13	-6	307	229
-13	-5	316	315
-13	-4	497	392
-13	-2	262	201
-12	0	282	273
-12	-10	352	261
-12	-6	454	465
-12	-5	284	216
-12	-4	608	546
-12	-3	366	335
-12	-2	418	360
-11	-13	381	369
-11	-11	517	412
-11	-7	437	416
-11	-5	641	621
-10	-6	306	316
-9	-12	339	265
-9	-11	398	197
-9	-6	357	298
-8	-12	478	422
-8	-9	326	327
-7	-12	511	608
-7	-10	481	505
-7	-8	496	593
-7	-6	613	626
-7	-5	501	610
-7	-4	796	860
-6	-13	366	428
-6	-11	580	594
-6	-9	342	386
-6	-8	319	347
-6	-7	374	396

-6	-5	971	991
-6	-3	882	882
-6	-1	564	568
-5	0	626	606
-5	-12	439	494
-5	-6	325	345
-5	-4	665	647
-5	-2	810	786
-5	-1	421	442
-4	0	414	439
-4	-7	309	337
-4	-5	353	302
-4	-3	296	277
-4	-2	387	314
-3	-9	374	399
-3	-7	602	583
-3	-4	347	246
-3	-3	441	469
-3	-1	632	564
-2	0	903	865
-2	-7	250	285
-2	-5	239	218
-2	-4	274	246
-2	-2	461	429
-1	-12	354	337
-1	-8	295	304
-1	-6	413	444
-1	-2	378	385
-1	-1	253	315
0	0	411	321
0	2	482	448
0	3	479	485
0	4	591	555
0	5	552	529
0	6	399	371
0	7	288	248
0	8	438	407
0	10	384	301
0	11	304	279
0	12	340	278
0	14	436	355
0	-14	383	353
0	-11	339	289
0	-8	294	381
0	-6	278	354
0	-5	483	532
1	0	490	496
1	1	366	373
1	2	381	352
1	3	588	581
1	5	625	585
1	7	313	336
1	11	421	372
1	13	383	301
2	4	284	272
2	7	279	261
2	10	433	422
3	3	324	305
3	7	380	365

3	9	328	280
4	1	472	509
4	3	339	343

L = 11

H	K	FO	FC
-13	-6	332	289
-13	-4	301	310
-13	-3	252	162
-12	-7	325	319
-11	-8	466	420
-11	-7	427	324
-10	-10	379	241
-8	-6	371	387
-7	-13	340	358
-7	-5	335	365
-7	-4	319	361
-7	-3	552	582
-6	-11	345	325
-6	-6	390	390
-6	-5	346	439
-6	-4	501	552
-6	-3	353	334
-6	-2	358	289
-6	-1	291	303
-5	-14	295	224
-5	-13	346	241
-5	-11	321	284
-5	-7	452	433
-5	-6	498	522
-5	-5	360	347
-5	-4	532	524
-5	-3	274	242
-5	-1	398	404
-4	0	398	399
-4	-8	309	293
-4	-6	303	337
-4	-5	418	395
-4	-3	566	622
-4	-1	321	332
-3	-13	288	238
-3	-10	271	198
-3	-9	263	228
-3	-7	400	360
-3	-6	381	321
-3	-5	309	359
-3	-4	373	307
-3	-1	282	272
-2	-6	300	301
-2	-5	341	357
-2	-4	308	326
-1	0	334	346
-1	-12	312	339
-1	-11	325	290
-1	-8	277	276
-1	-6	448	534
-1	-4	582	622
-1	-2	431	486

-1	-1	287	391
0	0	356	333
0	2	514	503
0	3	401	420
0	4	469	461
0	5	448	447
0	6	485	464
0	8	448	367
0	10	322	262
0	11	315	270
0	12	410	315
0	-12	315	317
0	-11	285	290
0	-10	309	253
0	-8	303	379
0	-6	310	450
0	-5	372	415
1	3	449	436
1	5	370	407

L = 12

H	K	FO	FC
-9	-10	323	268
-7	-5	321	439
-7	-3	352	332
-6	0	290	283
-6	-12	361	389
-6	-8	352	359
-6	-6	341	292
-6	-4	569	614
-6	-2	365	432
-5	-13	298	261
-5	-11	295	315
-5	-9	390	420
-5	-6	356	383
-5	-5	633	628
-5	-3	518	520
-5	-1	459	506
-4	0	421	425
-4	-13	304	220
-4	-11	312	311
-4	-7	283	253
-4	-5	459	478
-4	-4	336	282
-4	-3	330	373
-3	-4	255	210
-2	-7	296	315
-2	-4	354	383
-1	0	296	261
-1	-6	339	332
-1	-4	481	555
-1	-2	327	374
0	0	371	347
0	3	336	342
0	4	341	343
0	-6	272	314

L = 13

H	K	FO	FC
-10	-7	373	322
-9	-8	398	372
-8	0	307	328
-7	-2	283	245
-6	-7	267	299
-6	-6	439	460
-6	-4	507	488
-5	0	290	328
-5	-7	370	344
-5	-5	286	331
-5	-3	590	603
-5	-2	285	311
-5	-1	314	365
-4	0	306	298
-4	-3	299	248
-3	-4	270	181

L = 14

H	K	FO	FC
-4	-1	326	286